UNIVERSITY OF OKLAHOMA
GRADUATE COLLEGE

THE STORY OF COLORS

A DISSERTATION
SUBMITTED TO THE GRADUATE FACULTY
in partial fulfillment of the requirements for the
Degree of
DOCTOR OF PHILOSOPHY

By
GOLYA SHAHROKHI
Norman, Oklahoma
2023

THE STORY OF COLORS

A DISSERTATION APPROVED FOR THE

DEPARTMENT OF BIOLOGY

BY THE COMMITTEE CONSISTING OF

Dr. Katharine A. Marske, Chair

Dr. Michael A. Patten

Dr. Cameron D. Siler

Dr. Ricardo Betancur

Dr. Brian M. Kemp

Acknowledgments

I would like to express my deepest gratitude to Dr. Katharine A. Marske and Dr. Michael A. Patten for their invaluable support and guidance throughout this project. Their advice has been instrumental in completing this project.

I would also like to thank Dr. Brian M. Kemp, Dr. Cameron D. Siler, and Dr. Ricardo Betancur-R for their advice during the different phases of this project. Their insights and feedback helped me improve my work.

I am also grateful to Dr. Cara R. Monroe, Dr. Thomas Neeson, Dr. Subir Shakaya, Dr. Krithi Sankaranaryanan, Dr. Tanvi Honap, Dr. Christopher Abin, Dr. Claire M. Curry, Brittany Bingham, Michelle Busch, Mehrnaz Afkhami, and Mehrnoush Nourbakhsh for their support to this project. Their assistance made a significant difference in the outcome.

I would like to acknowledge the American Museum of Natural History, Harvard Museum of Comparative Zoology, Yale Peabody Museum, and Western Foundation of Vertebrate Zoology for providing resources and funding that were essential to the success of this project.

Finally, I would like to thank my parents, Javad and Mary, my sister, Minoush, and my beloved husband, Bardia for their support, encouragement, and patience throughout this project. Their unwavering support and understanding helped me to stay motivated and focused.

Table of Contents

List of Tables

Chapter 1

Chapter 2

Chapter 2: Supplementary Materials

Chapter 3

Chapter 3: Supplementary Materials

List of Figures

Chapter 1

Chapter 1: Supplementary Materials

Chapter 2

Chapter 3

Chapter 3: Supplementary Materials

Abstract

Color polymorphism has long been a subject of interest among scientists seeking to comprehend and elucidate its mechanisms. Initially, the concept was defined by early scientists like Ford (1940) and Huxley (1944) as the existence of distinct colors within the same environment that did not change with age, season, or sex differences (Galeotti et al., 2003). Presently, color polymorphism is defined as the occurrence of multiple color variants within a species that can be inherited by the next generation irrespective of environmental and are expressed by individuals of the same sex and age (Buckley, 1987). In other words, each genotype or allele of a species represents a different phenotype (Roulin, 2004).

In addition to the behavioral implications of polymorphism, the evolutionary mechanisms that shape and maintain it are of great interest to evolutionary biologists. Permanent polymorphism arises from a balance of selection between two or more morphs, each with its advantages and disadvantages (Bourgeois et al., 2017; Fisher, 1930; Herrera et al., 2015). While it was previously believed that polymorphism was solely an adaptation to different habitats (Galeotti et al., 2003), recent research indicates that it may result from a combination of different selection mechanisms (Gray and McKinnon, 2007; Herrera et al., 2015).

In this study, I investigated the evolution of color dimorphism in two bird species, the Western Reef Heron (*Egretta gularis*) and Dimorphic Egret (*Egretta dimorpha*), by analyzing their color morphology, geographic distributions, and genomic variation. Both species have white and dark morphs (Hancock and Kushlan, 1984), which coexist in the same environments and share resources (Recher, 1972). The Western Reef Heron is found in coastal regions of West and East Africa, the Red Sea, the Persian Gulf, and southern India (L. H. Brown et al., 1992; Etezadifar and Amini, 2010; Mock, 1980). The Dimorphic Egret has a narrow range (Kushlan

and Hancock, 2005), from coastal Kenya and Tanzania to Madagascar and nearby islands (L. H. Brown et al., 1992; Zimmerman et al., 1996).

In the first chapter, on color morphology, I examined the reflectance of different body regions of each morph from both species to determine the pigment concentration variation in different body regions. It is possible, due to the amount of solar exposure and receiving UV radiation, that different body regions have different pigmentation concentrations. This study included a third, monomorphic species, Little Egret (*Egretta garzetta*), as a comparison for the dimorphic Western Reef Heron and Dimorphic Egret. The reflectance of five different body regions (back, tail, vent, belly, and breast) of 186 museum specimens (Wester Reef Heron: 23 dark and 11 white, Dimorphic Egret: 24 dark and 16 white, and Little Egret: 112 white) were measured with a spectrophotometer. For the statistical analysis, I adapted Kruschke's (2013) 'BEST' (Bayesian Estimation Supersedes the *t* test) to create a Bayesian analogous to the paired *t*–test for comparison among body regions within an individual. Regardless of species, the analyses indicated that the back feathers were more pigmented (darker) among dark individuals and whiter among the white ones than other body regions. This supports the hypothesis that due to the amount of sun exposure, the pigment concentration varies among different body parts of a unicolored species.

In the second chapter, I examined the geographic distributions of Western Reef Heron and Dimorphic Egret. Ecogeographical rules describe the relationship between species' traits and their geographic range and biotic factors. In particular, Gloger's rule suggests that darker individuals will be more prevalent in areas with higher temperature and humidity (Delhey, 2019). Thus, species with color dimorphism are expected to have different geographic distributions and ecological niches among color morphs. Using occurrence data from eBird

(eBird, 2022) and museum specimens, the ecological niches of morphs of Western Reef Heron and Dimorphic Egret were compared based on six climate and habitat variables (J. L. Brown and Carnaval, 2019). Surprisingly, no differentiation between the niches of morphs in both species were identified, indicating that a variety of selection pressures, rather than climate alone, may shape the distribution of morphs spatially. This suggests that the mechanism for maintaining color dimorphism must provide advantages for both morphs in the same region, which contradicts Gloger's rule. Possible mechanisms for maintaining color dimorphism include UV resistance acting on both morphs, or independent evolutionary selection on each morph.

In the third chapter, I utilized whole genome sequencing to investigate the genetic differences between the dark and white morphs of Western Reef Heron and Dimorphic Egret. Understanding the genetic basis of coloration and polymorphism can shed light on the evolutionary history of species and the underlying mechanisms of evolution. I sequenced 50 toepad samples collected from five populations (São Tomé and Príncipe, Somalia, Madagascar, Seychelles, and Tanzania) from both species, including 30 dark and 20 white morphs, resulting in 55,215 to 6,414,649 SNPs across three datasets. Despite analyzing the data for population structure, genetic differentiation, and identifying variable loci, no genomic differentiation was found between dark and white morphs for either species. Possible explanations include gene flow, a polygenic control of coloration, or limitations of toepad samples. Collecting DNA from additional populations will be necessary to resolve these questions.

References

Bourgeois, Y. X. C., Delahaie, B., Gautier, M., Lhuillier, E., Malé, P. J. G., Bertrand, J. A. M., Cornuault, J., Wakamatsu, K., Bouchez, O., Mould, C., Bruxaux, J., Holota, H., Milá, B., and Thébaud, C. (2017). A novel locus on chromosome 1 underlies the evolution of a melanic plumage polymorphism in a wild songbird. Royal Society Open Science, 4(2), 160805. https://doi.org/10.1098/rsos.160805

Brown, J. L., and Carnaval, A. C. (2019). A tale of two niches: Methods, concepts, and evolution. Frontiers of Biogeography, 11(4). https://doi.org/10.21425/F5FBG44158

Brown, L. H., Urban, E. K., and Newman, K. B. (2020). The Birds of Africa: Vol. I. Bloomsbury Publishing.

Buckley, P. A. (1987). Mendelian genes. In F. Cooke and P. A. Buckley (Eds.), In Avian Genetics, A Population and Ecological Approach (pp. 1–44). Academic Press Inc.

Delhey, K. (2019). A review of Gloger's rule, an ecogeographical rule of colour: definitions, interpretations and evidence. Biological Reviews, 94, 1294–1316. https://doi.org/10.1111/brv.12503

eBird. (2022). eBird: An online database of bird distribution and abundance. Ithaca, NY: Cornell Lab of Ornithology. http://www.ebird.org

Etezadifar, F., and Amini, H. (2010). Current status of the breeding population of the Western Reef Heron (*Egretta gularis*) along the northern coasts of the Persian Gulf and Oman Sea, and its wintering population in the south of Iran. Heron, 5(2), 71–80.

Edwards, A. W. F. (2000). The genetical theory of natural selection. Genetics, 154(4), 1419–1426. https://doi.org/https://doi.org/10.1093/genetics/154.4.1419

Ford, E. B. (1940). Polymorphism and taxonomy. In J. S. Huxley (Ed.), The New Systematics (pp. 493–513). Clarendon Press.

Galeotti, P., Rubolini, D., Dunn, P. O., and Fasola, M. (2003). Colour polymorphism in birds: Causes and functions. Journal of Evolutionary Biology, 16, 635–645. https://doi.org/10.1046/j.1420-9101.2003.00569.x

Gray, S. M., and McKinnon, J. S. (2007). Linking color polymorphism maintenance and speciation. Trends in Ecology and Evolution, 22(2), 71–79. https://doi.org/10.1016/j.tree.2006.10.005

Hancock, J., and Kushlan, J. A. (2010). The Herons Handbook. Bloomsbury Publisher.

Herrera, M. S., Kuhn, W. R., Lorenzo-carballa, M. O., Harding, K. M., Ankrom, N., Sherratt, T. N., Hoffman, J., Gossum, H. Van, Ware, J. L., Cordero-Rivera, A., and Beatty, C. D. (2015). Mixed signals? Morphological and molecular evidence suggest a color polymorphism in some neotropical polythore damselflies. PloS One, 10(4). https://doi.org/hhttps://doi.org/10.1371/journal.pone.0125074

Huxley, J. (1944). Evolution: the modern synthesis. In Allen and Unvin, London. George Alien and Unwin Ltd.

Kruschke, J. K. (2013). Bayesian estimation supersedes the t test. Journal of Experimental Psychology: General, 142(2), 573–603. https://doi.org/10.1037/a0029146

Kushlan, J. A., and Hancock, J. (2005). 14. The Herons: Ardeidea (Bird Families of the World). In Bird Families of the World (pp. xv–433). Oxford University Press.

Mock, D. W. (1980). White-dark polymorphism in herons. Proceedings of the First Welder Wildlife Foundation Symposium, 1, 145–161.

Recher, H. F. (1972). Colour dimorphism and the ecology of herons. Ibis, 114(4), 552–555. https://doi.org/10.1111/j.1474-919X.1972.tb00859.x

Roulin, A. (2004). The evolution, maintenance and adaptive function of genetic colour polymorphism in birds. Biological Reviews of the Cambridge Philosophical Society, 79(4), 815–848. http://www.ncbi.nlm.nih.gov/pubmed/15682872

Zimmerman, D. A., Turner, D. A., and Pearson, D. J. (1996). Birds of Kenya and northern Tanzania. Princeton University Press. http://agris.fao.org/agris-search/search.do?recordID=US201300075290

Chapter 1

Linking Plumage Dimorphism and Environmental Stress

Published in: *Journal of Zoology*; 22 March 2022 (https://doi:10.1111/jzo.12972)

Golya Shahrokhi[1], Michael A. Patten[2]

[1] Biology Department, University of Oklahoma, Norman, OK, USA

[2] Ecology Research Group, Faculty of Biosciences and Aquaculture, Nord University, Steinkjer, Norway

Abstract

Besides the importance of pigmentation in species recognition, pigments protect the body against different biotic and abiotic features. Melanin, the dark coloration pigments in skin, hairs, and feathers, is necessary for protecting the body from UV radiation. On the other hand, the lighter a surface is, the more solar radiation is reflected. Based on these arguments, it is possible that pigment distribution would not be the same among all body regions of a unicoloured individual due to the amount of solar exposure. Therefore, three species of the *Egretta* genus (*E. dimorpha*, *E. gularis*, and *E. garzetta*), in which all individuals are unicoloured, and two of which are dichromatic (dark grey/black and white), were selected as model studies. We hypothesized that within dark and white unicoloured Egrets, due to foraging and standing postures, body regions that are more exposed to the sun (like back and breast) would be darker and whiter compared to other body regions (vent and tail), respectively. Visual wavelength reflections of five body regions (breast, back, belly, vent, and tail) from 186 museum specimens were measured to indicate the concentration of pigments in each body region. Reflectance among body regions was compared using Kruschke's "BEST" (Bayesian Estimation Supersedes the *t* test) framework to

create Bayesian analogues for the paired *t*-test. The results show, regardless of the species, that the more exposed body regions to the sun (back followed by breast) are darker among dark individuals and whiter among white individuals in comparison to other body regions. Therefore, our hypothesis that the concentration of pigments is not similar in all body regions of unicoloured individuals was supported.

Introduction

Coloration plays a substantial role in species' ecology and evolution (Poelstra *et al*., 2014, 2015; Bourgeois *et al*., 2017; Campagna *et al*., 2017). Variation in colour, from saturation to hue to patchiness, results from a balance among evolutionary forces such as crypsis, sexual selection, and environmental response, including local adaptation. For crypsis, coloration reduces detectability by background matching (Endler, 1978, 1984). Sexual selection, by contrast, favours patches with maximal contrast (Gomez and Théry, 2007). These two forces may respond to local conditions (Gomez and Théry, 2007; Sun *et al*., 2013), such that the strength or direction of selection varies with environment. Within a given system, such as birds of the rainforest understory, these forces counterbalance; for example, small, distinctive patches, usually with maximum conspicuousness, aim to attract the opposite sex (sexual selection) (Andersson, 1994), while overall coloration is dark to avoid detection (crypsis selection) (Endler *et al*., 2005). Even if an individual is patchily coloured, another individual typically sees it as an average of all different colours (Burtt, 1986; Gomez and Théry, 2007) even though each patch is distinguishable by itself (Endler and Théry, 2002). In contrast to rainforest understory birds, animals that live in deserts are mostly dark in coloration (Ward *et al.*, 2002). Thermoregulation is one of the reasons. Dark coloration help animals to save energy by using the heat from solar radiation (Walsberg, Campbell and King, 1978). Another explanation is that dark coloration

reduces heat stress by absorbing excessive heat from solar radiation in, say, a feather layer and thus keeping skin cooler (Ward *et al.*, 2002).

Most research has been done on multicoloured or patchily coloured individuals (i.e., Margalida et al. 2008); there are few data on selective forces experienced by unicoloured individuals. Among unicoloured species, evolutionary forces may affect the concentration of pigments in different body regions in a subtle but predictable manner. It is possible that pigmentation also varies subtly in different regions of the body in response to local adaptation, such as sunlight exposure. This possibility has not been explored.

Ultraviolet radiation is part of the sun's radiation with a wavelength between 100 to 400 nm (Schuch *et al*., 2017). It contains three kinds: UVC with 100–280 nm range, UVB with 280-315 nm, and UVA with 315-400 nm range (Schuch *et al*., 2017). The UVC wavelength and most of the UVB are usually absorbed by the oxygen and ozone in the atmosphere. Therefore, the UV radiation which reaches the earth is mostly UVA and partially UVB (Schuch *et al*., 2013). Although being exposed to UV has physiological benefits, such as providing vitamin D (Holick 2007), a high dosage can be harmful. The excessive amount of UV radiation exposure, chronic or prolonged, is well-known as an environmental genotoxic driver of sunlight (Schuch *et al*., 2013). Extra UV exposure can generate DNA damage, cell death, mutagenesis, and, eventually, carcinogenesis (Hideg *et al*., 2013). Thus, the amount of received UV radiation is important for the survivorship of any terrestrial and aquatic species (McKenzie *et al*., 2011).

Different organisms have taken different evolutionary paths for protection against biotic and abiotic conditions. One of the most common protections is pigmentation, specifically melanin (Galván *et al*., 2018b). Melanin is responsible for pigmentation in many animal and plant species (Galván *et al*., 2018b). Melanin functions in signaling, as an antioxidant, free radical scavenger,

and charge transport facilitator (Herrling *et al*., 2008), but a key role is photoprotection. Individuals absorb more wavelengths of the sunlight, even those in the ultraviolet (UV) spectrum, with increasing darkness of coloration (Cuthill *et al*., 2000; Eaton and Lanyon, 2003; Hausmann *et al*., 2003).

The other approach to protect from UV radiation is absence of pigmentation, in other words, increasing albedo (Mullen and Pohland, 2008). The colour of any object is the reflection of that colour wavelength from the visual sunlight to eye receptors. A white surface means that all the visual wavelengths have been reflected, absorbing nothing. This phenomenon is valid for the UV wavelengths too. For example, in a study on 312 bird species, all-white feathers reflect considerable UV rays (Eaton and Lanyon, 2003). Many other studies on measuring UV reflection of bird feathers have indicated higher reflection of UV from white feathers compared to other colorations (Hausmann *et al*., 2003; Cuthill *et al*., 2006).

To answer the question about variation in pigmentation among different body parts of unicoloured species, we examined colour variation among different body regions within individuals of three unicoloured bird species: the Little Egret (*Egretta garzetta)*, which is entirely white, Dimorphic Egret (*E. dimorpha*), and Western Reef Heron (*E. gularis*), which are dichromatic species with completely white or dark colorations. The way that egrets perch or forage makes their back and breast more exposed to sunlight and UV. Their posture dictates that the belly, vent, and tail are tracts least exposed to the sun (Hancock and Kushlan, 1984; Kushlan and Hancock, 2006). Therefore, as a defense mechanism and as a barrier to absorb UV wavelengths, the tracts with more sunlight exposure (back and breast) will be darker and whiter among dark and white individuals, respectively (Figure 1. 1).

We hypothesized that body regions more exposed to sunlight would be darker for unicoloured individuals with dark coloration. In contrast, a uniformly pale organism may increase albedo in body parts with more sun exposure than less exposed regions to increase sunlight reflection. In short, we predicted higher and lower visual wavelength reflectance in more exposed body regions of white and dark unicoloured individuals, respectively, compared to other body regions.

Methods

Model Organism

The Little Egret is always white and is distributed year-round in most of the Old World (Mock, 1980). The Dimorphic Egret is either entirely white or completely dark grey to black, and populations of both colour morphs are roughly evenly distributed throughout its range, which extends from eastern Kenya to Madagascar and nearby islands (Zimmerman et al., 1996). The Western Reef Heron is typically dark grey, yet there are a few populations of completely white individuals in west and northeast of Africa; these birds are distributed coastally in the northern half of Africa and around the Red Sea and Persian Gulf (Mock, 1980; Etezadifar and Amini, 2010).

Data Collection

All measurements for this study were collected from specimens in the American Museum of Natural History in New York City, NY, USA. Five body regions (back, tail, vent, belly, and breast) of 186 museum specimens (*E. garzetta*: 112 white morphs; *E. gularis*: 23 dark and 11 white morphs; *E. dimorpha*: 24 dark and 16 white morphs; in total 139 white unicoloured individuals and 47 unicolour dark individuals). We did not measure head feathers because they include ornamental plumes in the breeding season, which complicates assessment. Each of the body regions of each specimen was measured three times with a Konica-Minolta CR-400

Spectrophotometer. The mean of the three measurements was used for subsequent analyses. The spectrophotometer was standardized between each measurement. The wavelength reflection was recorded in Commission International d'Edairage LAB (CIELAB, also known as LAB) measurement system (Schanda, 2007; Hunter Associates Laboratory, 2008). In this method, the colour of the measured area is expressed in three dimensions, L*, a*, and b*. L* ranges from 0 (black) to 100 (white) and shows how dark a scanned surface is. Whereas a* and b* range from -100 to +100 and represent how green/red and blue/yellow, the scanned surface is, respectively. Because the egrets are either white or dark grey, a* was excluded from analyses, and b* (the blueness) was used solely for dark-morph individuals as a second criterion for dark pigmentation (Shahrokhi and Patten, 2022).

Chemicals used to preserve museum specimens or failure to remove subcutaneous fat discolored feathers of many of our samples; they had turned yellow or brownish. To avoid discoloration bias, we fitted a linear regression to mean yellowness (b*) and mean whiteness (L*) for a given feather tract and used resultant residuals as a new response variable (i.e., the tract with discoloration regressed out). For all tracts observed data and bias-corrected data gave similar results (S 1. 1). Therefore, hereafter we present the observed data.

Statistical Analyses

We adopted Kruschke's (2013) "BEST" (Bayesian Estimation Supersedes the *t* test) framework to create a Bayesian analogue to the paired *t*-test for comparison among tracts within individuals of a species. The reasons for choosing this method are: first, the distribution of data is flexible (we modeled with a *t*-distribution but could have used alternatives, such as Ί); second, output is a distribution of estimates rather than a single point estimate; and, third, pairing controlled for multiple tracts being measured within the same individual specimen. Comparisons of a given

feather tract among species were analyzed similarly but with a Bayesian analogue to the two-sample *t*-test. Both models were built in JAGS and run via R 4.0 using the package 'rjags' (Plummer, 2016). We estimated these parameters via three chains in standard Markov chain Monte Carlo ran for 10,000 iterations with a 1,000 burn-in. Priors were flat, and no thinning was required. Model convergence was checked with standard trace plots. Differences are marked if > 0.90 of the posterior distribution of the parameter of interest was positive or negative; anything less is too uncertain. Moreover, meaningful differences are those for which magnitude of mean effect size (η)—essentially a Cohen's *d*—exceeded 0.40, the low end of a moderate effect.

Results

Regardless of species, the back feathers were the darkest tract on dark morphs and whitest tract on white morphs (Figure 1. 2). Among all pairwise comparisons between every two body tracts, most differences were relative to back feathers. This pattern held between back and any other tracts in all measurements for both morphs (Figure 1. 3, for *E. gularis*). Since the patterns for the two other species (*E. garzetta* and *E. dimorpha*) were similar; the graphs for those species can be found in the Supplementary Information (S 1. 2, and S 1. 3).

Variation among different body regions was remarkably consistent within white-morph individuals of each of the three species. As predicted, the back was always the whitest part of the body, with the highest difference between back and belly and between back and breast (Table 1. 1). On the ventral side, the breast was noticeably whiter than either the belly or the vent, with the highest difference between breast and belly and the lowest between breast and vent (Table 1. 1).

For darkness and blueness measurements, a similar pattern was detected at the intra-individual level among the dark morphs of two species (*E. gularis* and *E. dimorpha*). The back was always the darkest (L values) and bluest (b values) part of the body, with the highest difference between

back and belly and the lowest difference between back and breast (Figure 1. 1; Table 1. 1). Ventrally, the breast was bluer than other body regions, with the highest difference between breast and belly and the lowest between breast and vent (Table 1. 2).

Discussion

Most previous studies on coloration compare either different species that live in similar environments or individuals within a species whose colour patterns and hues vary (e.g., Campagna *et al*., 2017). Our study is the first to focus on variation among feather tracts within unicoloured individuals across three egret species. For dark individuals, we predicted that the feather tracts that are more exposed to the sun (back and breast) would be darker or more pigmented compared to other tracts (belly, tail, and vent). The feather tracts most exposed to the sun (back and breast) for white morph individuals will be whiter or less pigmented than other tracts (tail, vent, and belly). To test our hypotheses, we measured visual wavelength colour reflection to measure how dark or white each of the body tracts is compared to other body regions. The back feathers were indeed the darkest, which indicates the highest relative eumelanin concentration in this area of the body, among the dark individuals, and indeed whiter than other tracts among the white individuals. The patterns held within each species, which means of neither whiteness nor darkness differed.

In other birds, as with egrets, the head feathers of Golden Eagles (*Aquila chrysaetos*) from all around Europe have different melanin concentrations as a response to photodamage (Galván *et al*., 2018a). The variation was not based on isolation, or structure but resulted from local adaptation. Melanin concentration correlated with altitude and UV exposure. As the elevation increases, the UV intensity increases, and as a result feathers contained more melanin. As with

Golden Eagles and egrets, more thrushes with dark plumage occur in highlands where the UV intensity is higher (Sandoval and Barrantes, 2019).

Other studies, such as Nicolaï et al. (2020), Jablonski and Chaplin (2010), Hansson et al. (2007), and D'Orazio et al. (2006), reported a positive correlation between melanin concentration in skin and hair and UV exposure. All these local adjustments are considered a defense mechanism against photodamage, which means that more exposed body regions to sunlight are darker than other body tracts (Choudhary *et al*., 2020; Markiewicz and Idowu, 2020). Our results, also, for the dark individuals are consistent with the common defense system.

Another hypothesis that could account for darker back feathers would be if dark-morph birds preferentially applied oil from their uropygial gland to those feathers. These oils darken feathers and thus would achieve a photoprotective effect (López-Rull *et al*., 2010). A preen oil hypothesis could not be generalized to white morphs, though, unless white birds preferentially avoided applying preen oil to their back feathers, an unlikely situation given the role these oils appear to play in maintaining feather integrity (Shawkey *et al*., 2003) and avoiding ectoparasites (Proctor and Owens, 2000).

Most studies on UV have measured reflectance to answer questions about mate choice and avian vision. A protection hypothesis implies that white feathers are not for mate attraction but because they reflect UV radiation. Morph is genetically hardwired, so there is no room for adaptive plasticity—regardless of environment, a white morph cannot become dark or vice versa. It may be that white and dark morphs will segregate via "matching habitat choice" (Edelaar et al., 2017), and any habitat matching may increase with environmental harshness, such as UV reflectance (Stella et al., 2018). Future research ought to investigate feather structure, mate choice, and molecular development of white feathers.

It may be that solar radiation in general, and not just UV radiation in particular, shapes some of aspects of dichromatism. Birds, like mammals, are endothermic. Regulating core body temperature may pose a challenge in hot environments or seasons (Lovegrove, 2019). The role played by dark or light plumage is debated. It may be that darker feathers absorb solar radiation to prevent transmitting heat to the skin (Wolf and Walsberg, 2000). Conversely, paler feathers reflect more light and thus reduce body temperature (Arai *et al*., 2017; Fargallo *et al*., 2018). A thermoregulation hypothesis would seem to lead to the same predictions as the UV hypothesis. However, it may be more difficult to acquire stable dimorphism on purely thermoregulatory grounds because physiological effects of both the UV hypothesis and thermoregulation hypothesis are expected to be more proximate (relative to a more ultimate response to UV radiation).

Besides environmental factors, such as UV exposure, producing melanin is under genetic control too. So far, more than 150 genes have been identified that affect skin and feather colour either directly or indirectly (Brenner and Berking, 2010). When an individual faces UV stress, the stress activates melanogenesis (Ducrest *et al.*, 2008). It activates DNA repair, antioxidant responses, and survival pathways essential for genomic stability and the prevention of harmful transformation or apoptosis (Abdel-Malek *et al*., 2010). Although some studies, e.g., Golden Eagles (Galván *et al*., 2018a), have shown no evidence of genetic differences among colour variations, we cannot confirm that the environment solely causes the colour differentiation among egrets' tracts. Therefore, molecular and developmental studies are needed.

If the underlying causal mechanisms for the back feathers being darkest on dark morphs (photoprotection) and whitest on white morphs (albedo) hold, then it is plausible that dichromatism in both *E. dimorpha* and *E. gularis* have evolved via disruptive selection. This

possibility is in response to the same environmental conditions but different melanin deposition or expression. Disruptive selection is when intermediate phenotypes have reduced fitness while the two phenotypic extremes have a fitness advantage (Rueffler *et al*., 2006; Planqué *et al*., 2016). Disruptive selection is considered as one of morphological diversification's main drivers (Rueffler *et al*., 2006). Under this view, it is possible that the intermediate individuals could not resist UV stress and be selected against through time. On the other hand, the unicolour individuals could manage to resist the UV exposure by local adaptation: dark morphs resist UV stress and protect the body from excess UV exposure by increased melanin concentration in the back and breast feathers, while in white morphs those regions are whiter. Our results are consistent with predictions of a model of disruptive selection, yet more morphological, molecular, and mate choice studies need to be done to support this hypothesis.

Acknowledgments

We want to thank the American Museum of Natural History, New York, NY, US., for giving us an opportunity to conduct our research on their collections. Funding was provided through the American Museum of Natural History collection study grant and the University of Oklahoma Graduate College Roberson research grant.

Data Availability

The measurements can be found through the doi: 10.17632/jf4ffbnyc9.1.

References

Abdel-Malek, Z.A., Kadekaro, A.L. and Swope, V.B. (2010). Stepping up melanocytes to the challenge of UV exposure. *Pigment Cell Melanoma Res.* **23**, 171–186.

Andersson, M. and Iwasa, Y. (1996). Sexual Selection. *Trends Ecol. Evol.* **11**, 53–58.

Bourgeois, Y.X.C., Delahaie, B., Gautier, M., Lhuillier, E., Malé, P.J.G., Bertrand, J.A.M., Cornuault, J., Wakamatsu, K., Bouchez, O., Mould, C., Bruxaux, J., Holota, H., Milá, B. and Thébaud, C. (2017). A novel locus on chromosome 1 underlies the evolution of a melanic plumage polymorphism in a wild songbird. *R. Soc. Open Sci.* **4**, 1–14.

Brenner, M. and Berking, C. (2010). Grundlagen der hautpigmentierung. *Der Hautarzt* **61**, 554–560.

Burtt, E.H. (1986). An analysis of physical, physiological, and optical aspects of avian coloration with emphasis on Wood-Warblers. *Ornithol. Monogr.* **38**, iii–126.

Campagna, L., Repenning, M., Silveira, L.F., Fontana, C.S., Tubaro, P.L. and Lovette, I.J. (2017). Repeated divergent selection on pigmentation genes in a rapid finch radiation. *Sci. Adv.* **3**, 1–12.

Choudhary, R., Sharma, A., Kumar, S., Upadhyay, R.C., Singh, S.V. and Mohanty, A. (2020). Role of alpha-melanocyte stimulating hormone (α-MSH) in modulating the molecular mechanism adopted by melanocytes of Bos indicus under UVR stress. *Mol. Cell. Biochem.* **465**, 141–153.

Cuthill, I.C. (2006). Perception and measurements. In *Bird Coloration. Volume I: Mechanisms And Measurements*: 3–40. Hill, G.E. and McGraw, Kevin, J. (Eds.). Harvard University Press.

Cuthill, I.C., Partridge, J.C., Bennett, A.T.D., Church, S.C., Hart, N.S. and Hunt, S. (2000). Ultraviolet vision in birds. *Adv. Study Behav.* **29**, 159–214.

D'Orazio, J.A., Nobuhisa, T., Cui, R., Arya, M., Spry, M., Wakamatsu, K., Igras, V., Kunisada, T., Granter, S.R., Nishimura, E.K., Ito, S. and Fisher, D.E. (2006). Topical drug rescue strategy and skin protection based on the role of Mc1r in UV-induced tanning. *Nature* **443**,

340–344.

Ducrest, A.L., Keller, L. and Roulin, A. (2008). Pleiotropy in the melanocortin system, coloration and behavioural syndromes. *Trends Ecol. Evol.* **23**, 502–510.

Eaton, M.D. and Lanyon, S.M. (2003). The ubiquity of avian ultraviolet plumage reflectance. *Proc. R. Soc. B Biol. Sci.* **270**, 1721–1726.

Edelaar, P., Jovani, R. and Gomez-Mestre, I. (2017). Should I change or should I go? Phenotypic plasticity and matching habitat choice in the adaptation to environmental heterogeneity. *Am. Nat.* **190**, 506–520.

Endler, J.A. (1978). A predator's view of animal color patterns. *Evol. Biol.* **11**, 319–364.

Endler, J.A. (1984). Progressive background in moths, and a quantitative measure of crypsis. *Biol. J. Linn. Soc.* **22**, 187–231.

Endler, J.A. and Thery, M. (1996). Interacting effects of lek placement, display behavior, ambient light, and color patterns in three neotropical forest-dwelling Birds. *Am. Nat.* **148**, 421–452.

Endler, J.A., Westcott, D.A., Madden, J.R. and Robson, T. (2005). Animal visual systems and the evolution of color patterns: Sensory processing illuminates signal evolution. *Evolution (N. Y).* **59**, 1795–1818.

Etezadifar, F. and Amini, H. (2010). Current status of the breeding population of the Western Reef Heron (*Egretta gularis*) along the northern coasts of the Persian gulf and Oman sea , and its wintering population in the south of Iran. *Heron* **5**, 71–80.

Galván, I., Jorge, A., Pacheco, C., Spencer, D., Halley, D.J., Itty, C., Kornan, J., Nielsen, J.T., Ollila, T., Sein, G., Stój, M. and Negro, J.J. (2018a). Solar and terrestrial radiations explain continental-scale variation in bird pigmentation. *Oecologia* **188**, 683–693.

Galván, I., Rodríguez-Martínez, S. and Carrascal, L.M. (2018b). Dark pigmentation limits thermal niche position in birds. *Funct. Ecol.* **32**, 1531–1540.

Gomez, D. and Théry, M. (2007). Simultaneous crypsis and conspicuousness in color patterns: Comparative analysis of a neotropical rainforest bird community. *Am. Nat.* **169**, S42–S61.

Hancock, J. and Kushlan, J.A. (1984). *The Herons Handbook*. London: Croom and Helm.

Hansson, L.A., Hylander, S. and Sommaruga, R. (2007). Escape from UV threats in zooplankton: A cocktail of behavior and protective pigmentation. *Ecology* **88**, 1932–1939.

Hausmann, F., Arnold, K.E., Marshall, N.J. and Owens, I.P.F. (2003). Ultraviolet signals in birds are special. *Proc. R. Soc. B Biol. Sci.* **270**, 61–67.

Hideg, É., Jansen, M.A.K. and Strid, Å. (2013). UV-B exposure, ROS, and stress: Inseparable companions or loosely linked associates? *Trends Plant Sci.* **18**, 107–115.

Hunter Associates Laboratory, I. (2008). CIE L* a* b* Color Scale. *Vol. 8*.

Jablonski, N.G. and Chaplin, G. (2010). Human skin pigmentation as an adaptation to UV radiation. *Proc. Natl. Acad. Sci. U. S. A.* **107**, 8962–8968.

Kruschke, J.K. (2013). Bayesian estimation supersedes the t test. *J. Exp. Psychol. Gen.* **142**, 573–603.

Kushlan, J.A. and Hancock, J. (2005). 14. The Herons: Ardeidea (Bird Families of the World). *Bird Families of the World*: xv–433. New York: Oxford University Press.

Margalida, A., Negro, J.J. and Galván, I. (2008). Melanin-based color variation in the Bearded Vulture suggests a thermoregulatory function. *Comp. Biochem. Physiol. - A Mol. Integr. Physiol.* **149**, 87–91.

Markiewicz, E. and Idowu, O.C. (2020). Melanogenic difference consideration in ethnic skin type: A balance approach between skin brightening applications and beneficial sun exposure. *Clin. Cosmet. Investig. Dermatol.* **13**, 215–232.

McKenzie, R.L., Aucamp, P.J., Bais, A.F., Björn, L.O., Ilyas, M. and Madronich, S. (2011). Ozone depletion and climate change: Impacts on UV radiation. *Photochem. Photobiol. Sci.* **10**, 182–198.

Mock, D.W. (1980). White-dark polymorphism in herons. *Proc. First Weld. Wildl. Found. Symp.* **1**, 145–161.

Mullen, P. and Pohland, G. (2008). Studies on UV reflection in feathers of some 1000 bird species: Are UV peaks in feathers correlated with violet-sensitive and ultraviolet-sensitive

cones? *Ibis (Lond. 1859).* **150**, 59–68.

Nicolaï, M.P.J., Shawkey, M.D., Porchetta, S., Claus, R. and D'Alba, L. (2020). Exposure to UV radiance predicts repeated evolution of concealed black skin in birds. *Nat. Commun.* **11**, 1–8.

Planqué, R., Powell, S., Franks, N.R. and van den Berg, J.B. (2016). Disruptive selection as a driver of evolutionary branching and caste evolution in social insects. *J. Evol. Biol.* **29**, 2111–2128.

Plummer, M. (2016). rjags: Bayesian graphical models using MCMC. *R Packag. version 3-13*.

Poelstra, J.W., Vijay, N., Bossu, C.M., Lantz, H., Ryll, B., Müller, I., Baglione, V., Unneberg, P., Wikelski, M., Grabherr, M.G., Wolf, J.B.W., Muller, I., Baglione, V., Unneberg, P., Wikelski, M., Grabherr, M.G., Wolf, J.B.W., Müller, I., Baglione, V., Unneberg, P., Wikelski, M., Grabherr, M.G. and Wolf, J.B.W. (2014). The genomic landscape underlying phenotypic integrity in the face of gene flow in crows. *Science (80-.).* **344**, 1410–1414.

Poelstra, J.W., Vijay, N., Hoeppner, M.P. and Wolf, J.B.W. (2015). Transcriptomics of colour patterning and coloration shifts in crows. *Mol. Ecol.* **24**, 4617–4628.

Rueffler, C., Van Dooren, T.J.M., Leimar, O. and Abrams, P.A. (2006). Disruptive selection and then what? *Trends Ecol. Evol.* **21**, 238–245.

Sandoval, L. and Barrantes, G. (2019). Is black plumage an adaptation to high elevations in a cosmopolitan bird genus? *J. Avian Biol.* **50**, 1–8.

Schanda, J. (2007). Colorimetry: Understanding the CIE System. *John Wiley Sons*.

Schuch, A.P., Garcia, C.C.M., Makita, K. and Menck, C.F.M. (2013). DNA damage as a biological sensor for environmental sunlight. *Photochem. Photobiol. Sci.* **12**, 1259–1272.

Schuch, A.P., Moreno, N.C., Schuch, N.J., Menck, C.F.M. and Garcia, C.C.M. (2017). Sunlight damage to cellular DNA: Focus on oxidatively generated lesions. *Free Radic. Biol. Med.* **107**, 110–124.

Shahrokhi, G. and Patten, M.A. (2022), Linking plumage dimorphism and environmental stress, Mendeley Data, V1, doi: 10.17632/jf4ffbnyc9.1

Stella, D., Pecháček, P., Meyer-Rochow, V.B. and Kleisner, K. (2018) UV reflectance is associated with environmental conditions in Palaearctic *Pieris napi* (Lepidoptera: Pieridae). *Insect Sci.* **25**, 508–518.

Sun, Y., Li, J., Zhang, W. and Wang, T.J. (2013). Local stress evolution in thermal barrier coating system during isothermal growth of irregular oxide layer. *Surf. Coatings Technol.* **216**, 237–250.

Walsberg, G.E., Campbell, G.S. and King, J.R. (1978). Animal coat color and radiative heat gain: A re-evaluation. *J. Comp. Physiol.* □ *B* **126**, 211–222.

Ward, J.M., Blount, J.D., Ruxton, G.D. and Houston, D.C. (2002). The adaptive significance of dark plumage for birds in desert environments. *Ardea* **90**, 311–323.

Zimmerman, D.A., Turner, D.A. and Pearson, D.J. (1996). Birds of Kenya and northern Tanzania. Princeton University Press.

Figures and Tables

Table 1. 1. The relative whiteness (L*) body tracts within *Egretta* species, assessed using the BEST approach. The ">" or "<" means the posterior probability distribution was between 90.0% and 97.5% with absolute corresponding effect size, |η|, between 0.4 and 0.5. The ">>" or "<<" means more than 97.5% of the posterior probability distribution of estimated difference score was greater than zero with |η| greater than 0.55. The ">>>" or "<<<" means the |η| is equal or greater than 1.0.

	Little Egret (*E. garzetta*) N = 112				Wester Reef Heron (*E. gularis*) N = 11				Dimorphic Egret (*E. dimorpha*) N = 16			
	Belly	Vent	Tail	Back	Belly	Vent	Tail	Back	Belly	Vent	Tail	Back
Breast	>>	>	>	=	>	=	>>	=	>>	>>	=	<<
Belly		<<	<<	<<		=	>>	=		=	<<	<<<
Vent			<<	=			>>	=			<	<<<
Tail				=				<				=

Table 1. 2. The relative darkness (L*) and blueness (b*) body tracts within *Egretta* species, assessed using the BEST approach. The ">" or "<" means the posterior probability distribution was between 90.0% and 97.5% with absolute corresponding effect size, |η|, between 0.4 and 0.5. The ">>" or "<<" means more than 97.5% of the posterior probability distribution of estimated difference score was greater than zero with |η| greater than 0.55. The ">>>" or "<<<" means the |η| is equal or greater than 1.0.

	Wester Reef Heron *E. gularis* (L*) N = 23				Dimorphic Egret *E. dimorpha* (L*) N = 24				Western Reef Heron *E. gularis* (b*) N = 23				Dimorphic Egret *E. dimorpha* (b*) N = 24			
	Belly	Vent	Tail	Back	Belly	Vent	Tail	Back	Belly	Vent	Tail	Back	Belly	vent	tail	back
Breast	=	=	=	<<<	=	>	=	<<	>	>>	>>	<<<	>>	>>	>	<<<
Belly		=	=	<<		=	=	<<		>>	>	<<<		=	=	<<<
Vent			=	<<			=	<<			=	<<<			<<	<<<
Tail				<<				<<				<<<				<<<

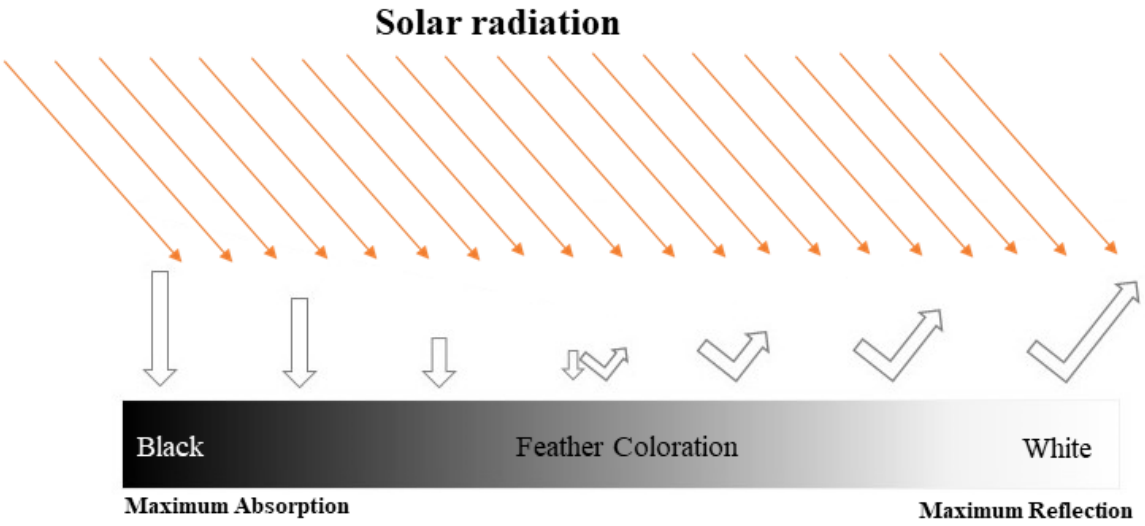

Figure 1. 1. An illustration of solar radiation absorption and reflection for the range of black to white feather coloration.

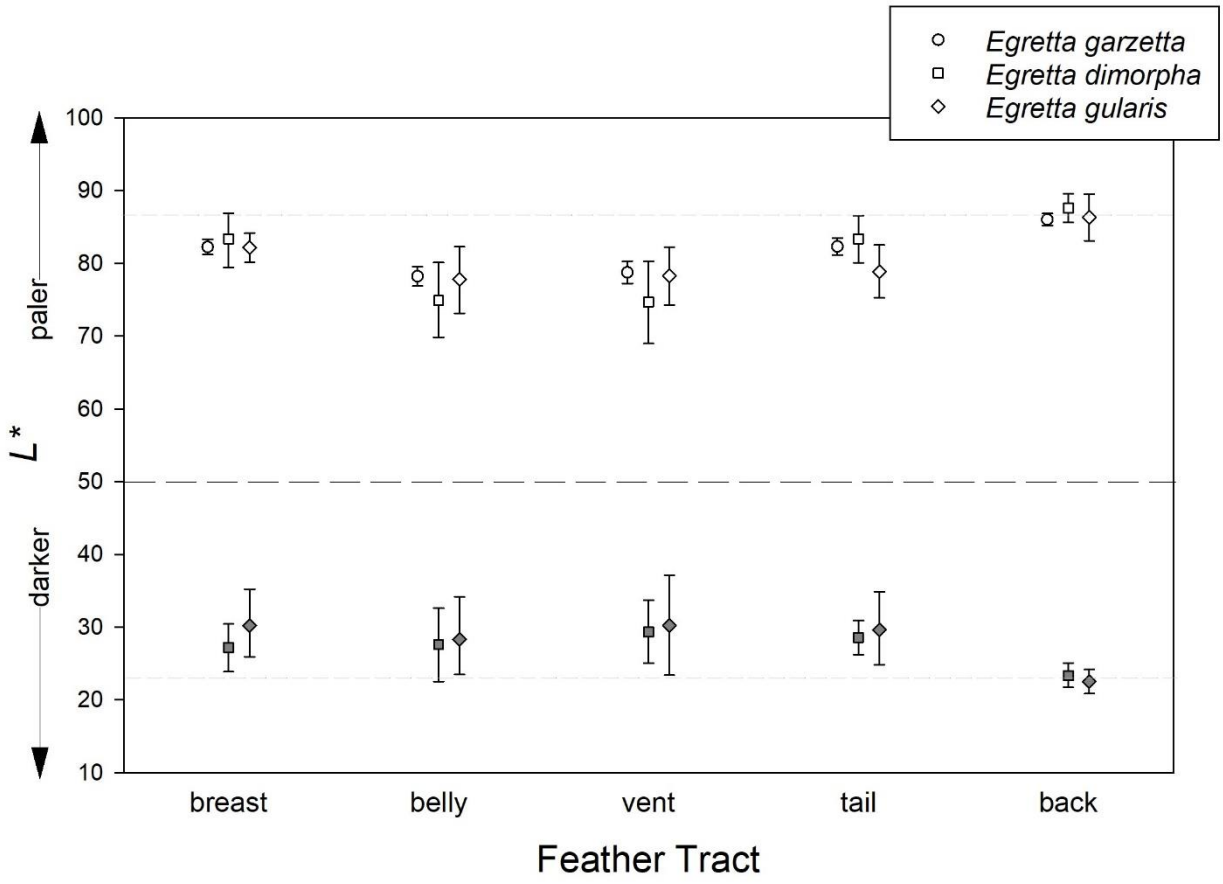

Figure 1. 2. Plumage darkness (L* values) of five feather tracts of three species *Egretta egrets*. Values shown are estimated means and associated 95% highest density Bayesian credible intervals. Note that back feathers are whiter that other tracts across all three species yet darker than other tracts in dark morphs of two species.

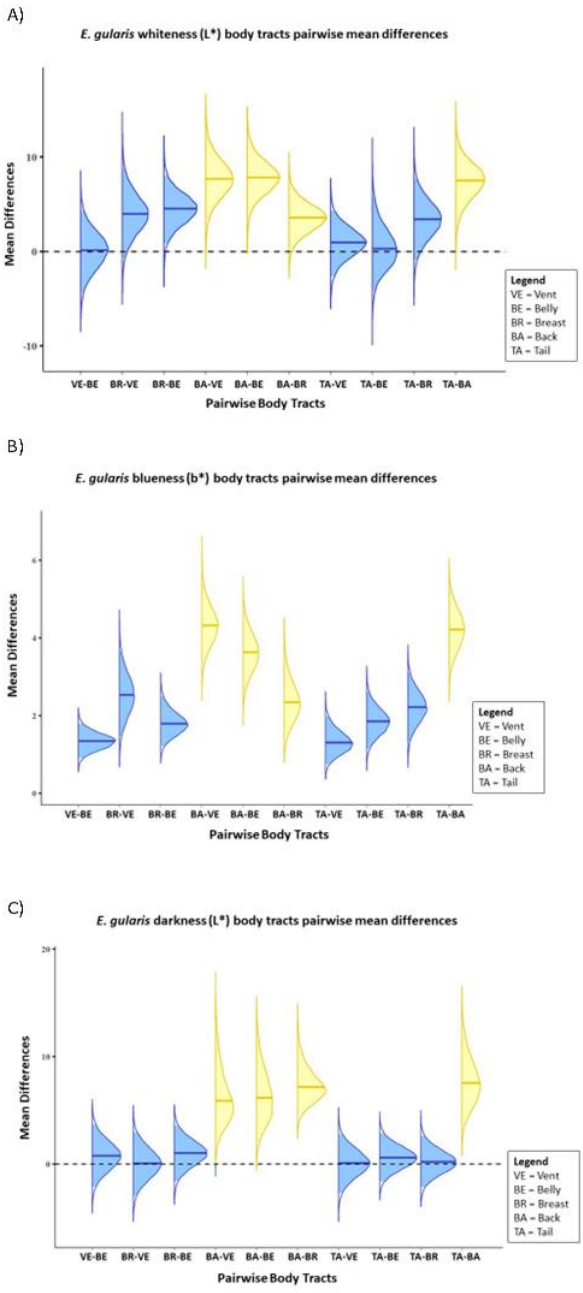

Figure 1. 3. Pairwise differences between body regions of *Egretta gularis* within each color morph (white = 11, dark = 23). A) The difference of whiteness (L*) among white morphs. B) The difference of blueness (b*) among dark morphs. C) The difference of darkness (L*) among dark morphs. The yellow graphs represent pairwise differences between back, which we expect to be under the strongest selection, and other body regions, as indicated. The blue graphs indicate pairwise differences between other body regions. The dotted line indicated no difference.

Supplementary Materials

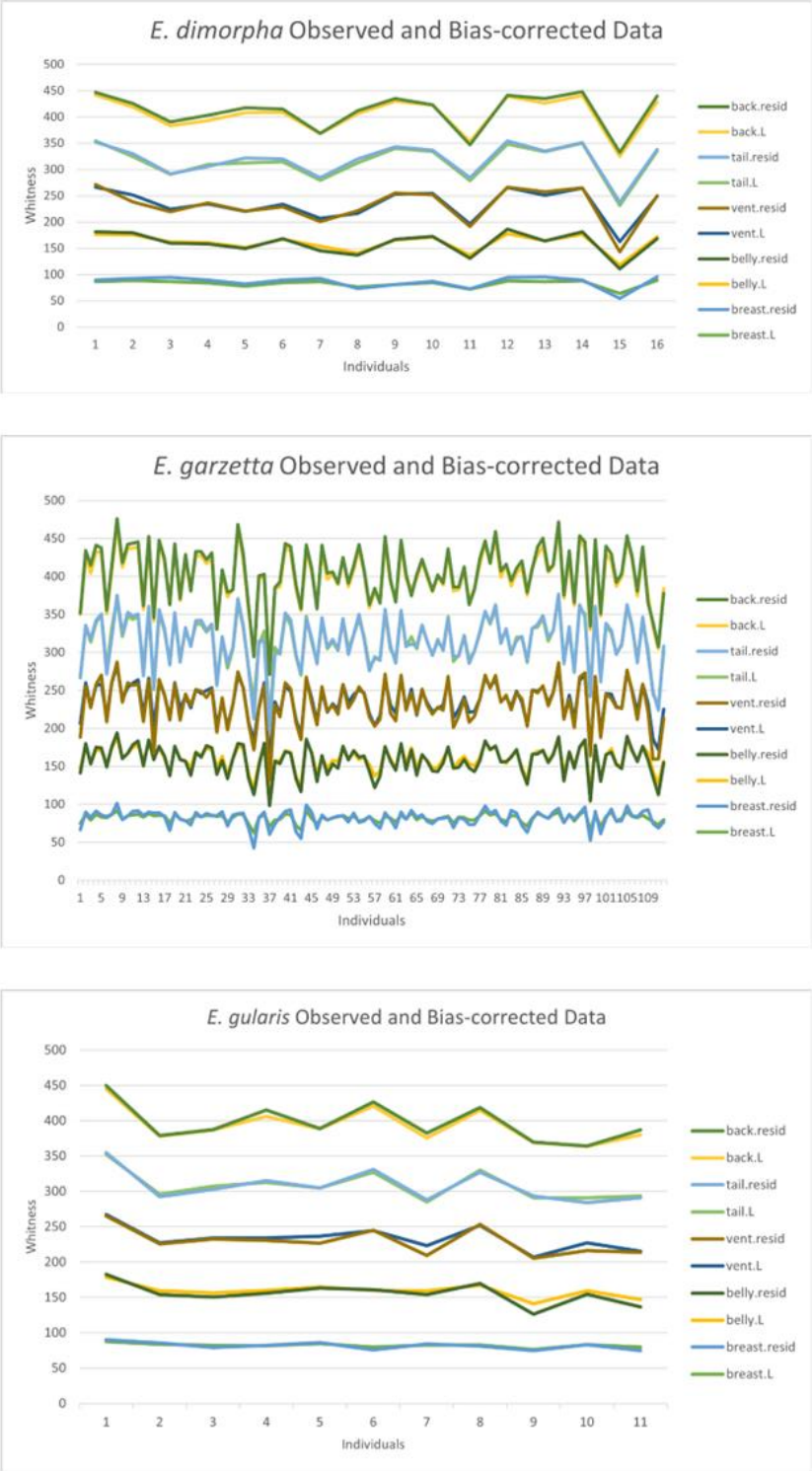

Figure S 1. 1. Comparison between the observed data and bias-correlated data (residuals) between whiteness of tracts of three species. For each tract, the differences between the bias-correlated data (residuals) and observed data are not statistically significant (p-value > 0.05).

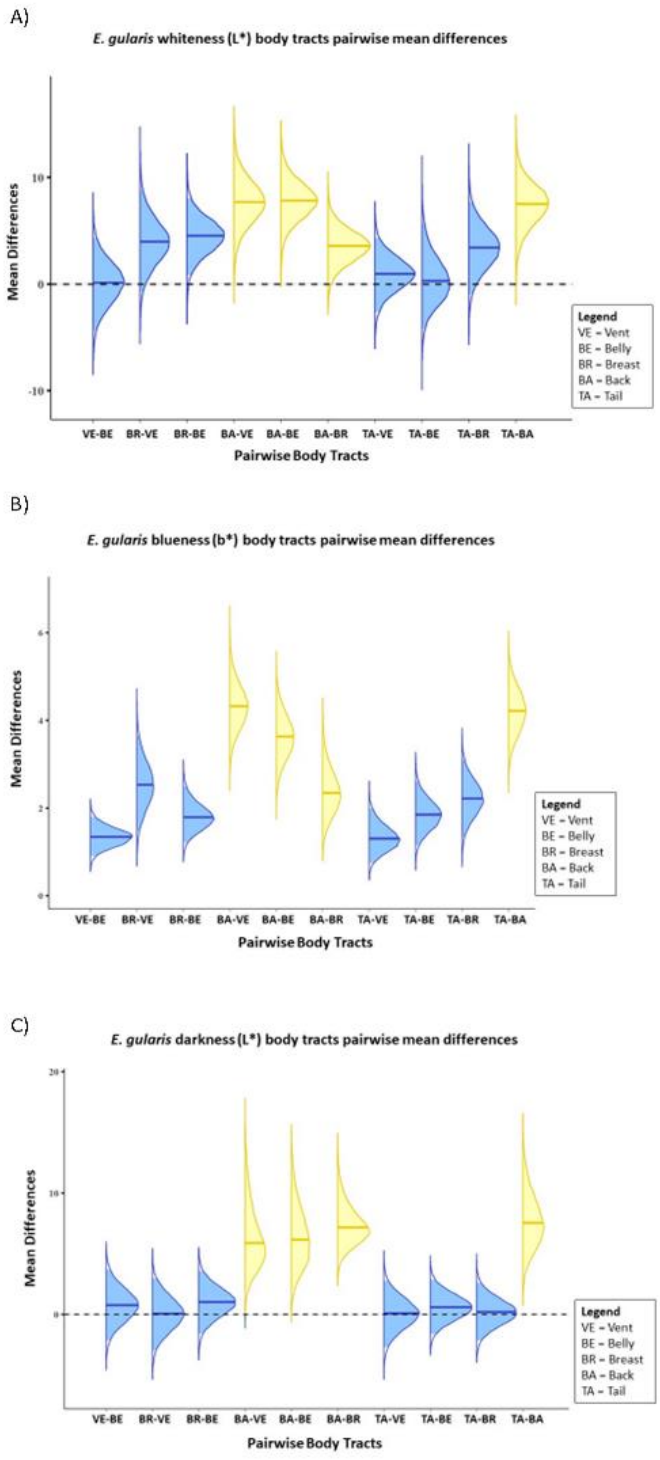

Figure S 1. 2. Pairwise differences between body regions of *Egretta dimorpha* within each color morph (white= 16, dark=24). A) The difference of whiteness (L*) among white morphs. B) The difference of blueness (b*) among dark morphs. C) The difference of darkness (L*) among dark morphs. The yellow graphs represent pairwise differences between back, which we expect to be under the strongest selection, and other body regions, as indicated. The blue graphs indicate pairwise differences between other body regions. The dotted line indicated no difference.

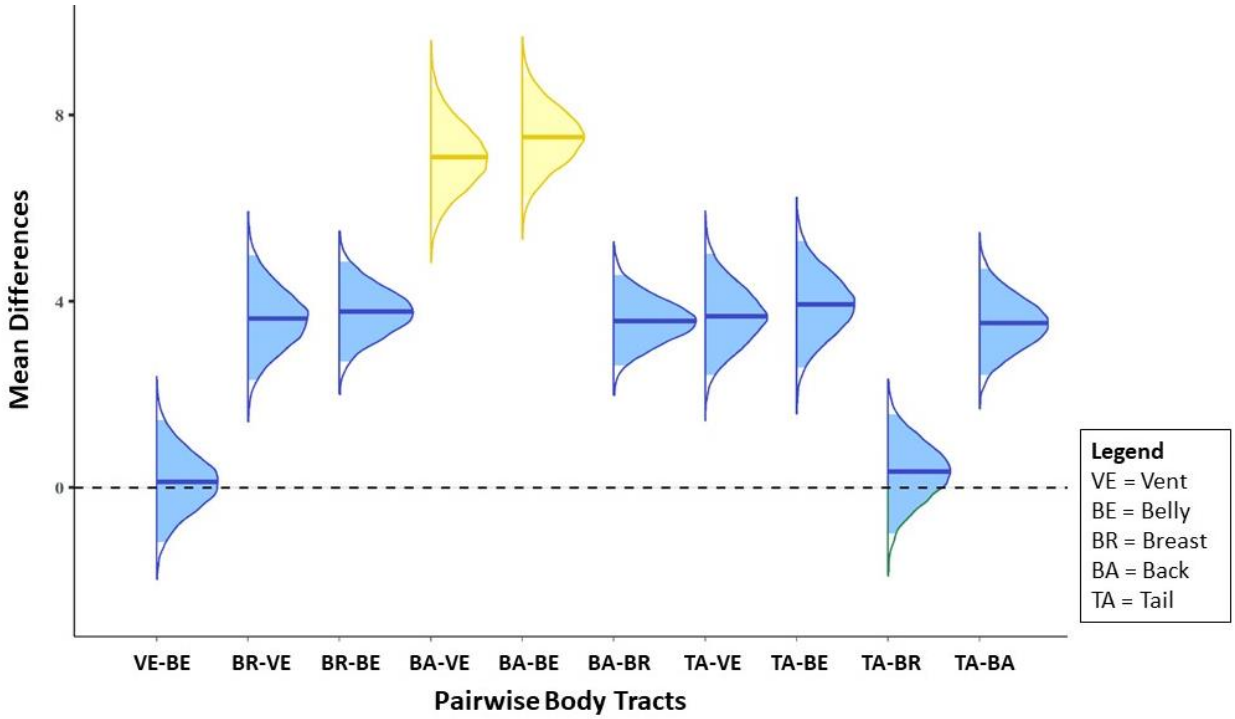

Figure S 1. 3. Pairwise differences between body regions of *Egretta garzetta* (white= 112). The difference of whiteness (L*) among white morphs. The yellow graphs represent pairwise differences between back, which we expect to be under the strongest selection, and other body regions, as indicated. The blue graphs indicate pairwise differences between other body regions. The dotted line indicated no difference.

Chapter 2

Contradicting Gloger's Rule: The Maintenance of Color Dimorphism in Herons and Egrets

Submitted at: *Ornithology*

Golya Shahrokhi[1], Michael A. Patten[2], Katharine A. Marske[1]

[1] Biology Department, University of Oklahoma, Norman, OK, USA

[2] Ecology Research Group, Faculty of Biosciences and Aquaculture, Nord University, Steinkjer, Norway

Abstract

Geographic variation in species' traits along regular environmental gradients are often described as ecogeographical rules. Gloger's rule describes variation in pelage coloration, which is typically related temperature and humidity, with darker individuals more prevalent in areas with high temperature and humidity. This predicts that for species with color dimorphism, different color morphs may have different geographic distributions and ecological niches. In contrast, if the ecological niches between the morphs do not differ, it suggests that factors other than response to a regular environmental gradient may be shaping the distribution of color variation. To test this hypothesis, the ecological niches of morphs in Western Reef Heron and Dimorphic Egret were compared using occurrence data from eBird and museum specimens and by quantifying their ecological niches using six climate and habitat variables. Ecological niches did not differ between color morphs of either species, suggesting that the mechanism for maintaining color dimorphism must provide advantages for both morphs in the same region, in contrast to Gloger's rule. Possible mechanisms include selection for UV resistance in both color morphs, or independent evolutionary selection in each morph in response to different environmental factors.

Introduction

Biogeography aims to understand how and why biodiversity is distributed across geographic space (Lomolino et al. 2006; Marcondes et al. 2021). One pattern of interest to evolutionary biologists is intraspecific variation in species' traits, such as body size or coloration, across space and in particular, along environmental gradients (Gaston et al. 2008; Goldenberg et al. 2022). When the pattern is widely replicated across different species, it suggests shared responses to environmental gradients or ecogeographical rules (Gaston et al. 2008). To the extent that trait variation can be explained by particular environmental drivers (e.g., heat or humidity), ecogeographical rules can help to predict species' distributions and detect responses to changing environmental conditions (Gaston et al. 2008; Marcondes et al. 2021).

Two ecogeographic rules describe geographic variation in species coloration. Bogert's rule, also known as the thermal melanism hypothesis, has been proposed for ectotherms in which those living in cooler regions have darker colors that help them absorb more energy and get warm from solar radiation (Bogert 1949; Delhey 2018). Gloger's rule, proposed for endothermic animals (Gloger 1833; Gaston et al. 2008), proposes that darker-coated endotherms should be more common in warmer and humid regions (Gloger 1833; Gaston et al. 2008; Delhey 2018).

Although Gloger (Gloger 1833) emphasized the combined effects of temperature and humidity in driving color variation, several researchers have identified different biological explanations which might drive this relationship. One of the explanations is crypsis, or background-matching—one of the most common functions of disruptive evolutionary mechanisms for a species that lives in a heterogeneous environment (Galeotti et al. 2003). Low contrast with the background makes it harder for predators to detect prey (Gomez and Théry 2007) or vice versa (Ferguson-Lees and Christie 2001). For instance, understory rainforest bird species usually have

an overall dark coloration, which decreases detectability (Endler et al. 2005). Since warm and humid conditions develop dense vegetation and dark environments, darker animals have the advantage of matching to the background and being less detectable (Zink and Remsen Jr 1986; McNaught and Owens 2002; Caro 2005; Roulin and Randin 2015; Friedman and Remeš 2017).

Another explanation for darker feathers, skin, or hair is the higher level of hardness (Bonser and Witter, 1993) due to melanization (McGraw 2006; Delhey 2015). As a result, bacteria degrade dark coats slower than pale coats (Goldstein et al. 2004; Gunderson et al. 2008). Therefore, darker-colored coated vertebrates have more advantages than lighter ones in warm and humid regions, which are more suitable environments for bacterial growth (Burtt et al. 2004). Dark pigmentation also imparts higher resistance to UV solar radiation (Galván et al. 2018), which provides an additional advantage in warm regions.

These hypothesized explanations for Gloger's rule all predict that individuals of different color morphs should be found in different regions (or different habitats within the same region). However, like other ecogeographical rules, Gloger's rule has some exceptions. For instance, Barn Owl (*Tyto alba*) populations living in areas with dry, cool winters in the southern regions of North America have more black spots than those living in cold wetter regions further north (Roulin and Randin 2015). The authors concluded that factors other than climate may be driving the selection of plumage coloration or that genes related to plumage traits may impact physiological or behavioral processes beyond coloration. Another example is our previous study. We found that both light and dark morphs of two dimorphic egret species have different mechanisms of handling excessive UV, which let them live next to each other (Shahrokhi and Patten 2022). The contrasting spatial distributions predicted by different mechanisms suggest

that comparing the ecological niches inhabited by different color morphs may yield insights into the drivers of color polymorphism within species.

Herons (Order Ardeidae), together with owls (Order Strigiformes), landfowls (Order Galliformes), and cuckoos (Order Cuculiformes), are among the four avian orders with the highest percentage of species showing color polymorphism (Galeotti et al. 2003). Within herons, all color polymorph species express white and dark morphs, and most studies on color polymorphism of Ardeidae show no differences in nest success, foraging, survivorship, and fitness between morphs (e.g., Green et al. 2011; Bates and Ballard 2014). Therefore, this group, which includes many dimorph species (rather than polymorph) distributed across different regions, can be a great model for examining species' ecological drivers of color polymorphism.

To investigate the mechanisms contributing to color dimorphism in the Ardeiformes, we compare the ecological niches of light and dark morphs of the Western Reef Heron (*Egretta gularis*) and Dimorphic Egret (*Egretta dimorpha*). The Western Reef Heron occurs along coasts in West Africa, East Africa, around the Red Sea and the Persian Gulf, and in southern India (Mock 1980; Brown et al. 1992; Etezadifar and Amini 2010) (Figure 2. 1a). The Dimorphic Egret has the narrowest geographic range among all species in family Ardeidae (Kushlan and Hancock 2005), ranging from coastal Kenya and Tanzania south to Madagascar and nearby islands (Brown et al. 1992; Zimmerman et al. 1996) (Figure 2. 1b). Both species have individuals that are either white or dark gray (Hancock and Kushlan 1984). Dark and light morphs of both species have been reported to occur in the same environments, live in the same groups, and share the same food resources (Recher 1972). In the same region, occurrences contrast to expectations under Gloger's rule, suggesting that different mechanisms maintain color polymorphism in these species by acting independently on each morph. To test this, we estimate niche similarity and

equivalence between two color morphs of each species. If Gloger's role applies to Western Reef Heron and Dimorphic Egret, suggesting that dimorphism is related to heat, humidity, or crypsis, we would expect to detect low niche similarity among color morphs. In contrast, if Gloger's rule does not apply, we would not expect to detect a significant difference in ecological niches between the morphs. No differentiation might suggest that the same mechanism maintains both morphs in sympatry, consistent with our previous findings for UV tolerance, or where different mechanisms contribute to the success of the dark and white morphs. This study can be considered as a new way to evaluate evolution mechanisms.

Methods

Occurrence Data and Study Area

We compiled species occurrences data from eBird (eBird 2022) and specimens in the American Museum of Natural History in New York City, NY, US, to cover most of the ranges of morphs of each species. From the eBird dataset, out of 1173 occurrences of *Egretta gularis* and 521 occurrences of *Egretta dimorpha,* we retained 80 and 46 records, respectively, for which the color morphs were determined (Table S 2. 1). For each color morph, we removed duplicate localities. If more than one color was recorded, the locality was considered for each morph independently. Due to the high similarity between the white morphs of the Western Reef Heron and the Little Egrets and to reduce the false identification data points, we used only the occurrence points of the white morphs of the Western Reef Heron for which the specific characters leading to identification were listed (i.e., amount of yellowness in the tarsus). Therefore, a high portion of white morphs of Western Reef Heron was excluded from the eBird data set. From the museum collection, 34 and 42 specimens of *E. gularis* and *E. dimorpha* were georeferenced for the data points. In total, 113 (71 dark morphs and 42 white morphs) for *E.*

gularis and 86 (48 dark morphs and 38 white morphs) for *E. dimorpha* were used for subsequent analyses (Table S 2. 1 and Figure 2. 1).

Environmental Data

We quantified ecological niches of morphs using six climate and habitat variables addressed by the suggested hypotheses for the Gloger's rule. To test the effects of temperature, solar radiation, and humidity, the average annual temperature (°C), elevation (m), solar radiation (KJ m-2 day-1), total annual precipitation (mm) and water vapor pressure (kPa) were obtained at 2.5 arc-min (~5 km^2) resolution from WorldClim version 2.1 climate data for 1970-2000 (released in January 2020) (Fick and Hijmans 2017). All layers were cropped to between -20 to 80 degrees (latitude) and -30 to 60 degrees (longitude), and 25 to 50 degrees (latitude) and -35 to -5 degrees (longitude), for the Dimorphic Egret and Western Reef Heron, respectively. The Global Habitat Dissimilarity (vegetation) dataset (Tuanmu and Jetz 2015) with 2.5 arc-min (~5 km2) resolution was included to test the hypothesis related to crypsis and background matching. This dataset has been selected because it covers all habitat heterogeneities among land-cover types (e.g., forests, grasslands, wetlands, etc.) due to its high resolution (Tuanmu and Jetz 2015).

Estimates of Climatic Niche Similarity and Equivalence

To compare ecological niches between white and dark morphs, we quantified niche overlap between color morphs of each species in environmental space (E-space). We used density kernel smoothing based on the abundance of observations to transfer occurrence points into E-space. Since both species are not considered as a long-distance migratory species (Hancock and Kushlan 1984), all niche comparison tests were estimated using four different defined buffers (50 km, 100 km, 250 km, and 500 km) around each data point to find the best coverage of the dispersal range of each of these nonmigratory birds. The results obtained using each test buffer

were compared via a *t-test*. All analyses were conducted in R (Rstudio 2020; R Core Team 2022) using the package *Humboldt* (Brown and Carnaval 2019). In the following, we explain what each niche comparison test estimates.

For each defined buffer around occurrence points, we plotted environments within the buffer on a two-dimensional PCA space to visualize all environments that are accessible to each morph in each cell. This analysis shows how the environmental layers are correlated; and how well each environmental variable can explain data distribution.

To compare niches between color morphs of a species, we ran the Niche Overlap Test and the Niche Divergence Test (Brown and Carnaval 2019). These tests show whether the differences between the morphs are actual because of the niche divergence by comparing analogous and non-analogous environmental space, or E-space. The analogous E-space is the area of E-space in common between the two morphs. The non-analogous E-space is the area of E-space for one morph that is not shared with the other. In the Niche Overlap Test, we compare the realized niches of both morphs in E-space by considering both analogous and non-analogous E-space for both morphs. However, for the Niche Divergence Test, we consider only the analogous E-space between the morphs and ignore the non-shared E-space. In both tests, the comparison between morphs' realized niches is estimated by calculating Schoener's *D* similarity index (Schoener 1968). The scale of this index is between 0, which means wholly dissimilar, to 1, completely similar.

The other statistic we ran is the Niche Equivalency Test, which has three steps (Brown and Carnaval 2019). The first step is calculating the similarity between the realized niches of morphs by using Shoenor's *D* (Schoener 1968) and Warren's *I* (Warren et al. 2008) indices. The Warren's *I* index ranges between 0 and 1 and is scaled the same as the Schoener's *D* index (0,

niches are completely dissimilar, and one, niches are entirely identical). In the second step, a null distribution was created based on all occurrence points. To create a null distribution, we randomly selected an equal number of occurrence points to the real dataset for each morph out of the pool of mixed occurrence points. Then Schoener's *D* and Warren's *I* were calculated for each resampling between the reshuffled groups. To generate the null distribution, this reshuffling was performed 500 times. In the final step, the Schoener's *D* and Warren's *I* indices of the experimental data occurrence points are compared to the values of the null distribution. If $p > 0.05$, then values of the real data points and the null distribution do not differ. In other word, there is no difference between the niches of the two morphs.

The other test we ran was the Background Statistic Test (Brown and Carnaval 2019), which tests whether the differences between niches are the consequence of differences in the environments different color morphs can access (i.e., the environments available in the background space). This test also uses the values of Schoener's *D* and Warren's *I* indices as indicators. Unlike the Niche Equivalency test, in the Background Statistic test, the occurrence points of one morph were reshuffled and resampled in geographic space. This step aims to see how the E-space for that morph would be changed due to shifting the occurrence points. Randomization was performed 500 times, as above, and the Schoener's *D* and Warren's *I* values for each resampling were calculated to generate the null distribution. Then, the generated values for the null distribution for each morph were compared to the Schoener's *D* and Warren's *I* values of the other morph. Here, $p > 0.05$ indicates that the differences in morphs' niches *are* due to accessibility to different environments. If $p < 0.05$, the differences between the morphs' niches are not because of differences in environments that morphs have access to. This test was performed for each morph independently.

Based on the combined results of the Niche Equivalency and the Background Statistics tests, we can conclude whether the two compared niches are equivalent or not. If the Niche Equivalency shows a non-significant result and the Background Statistic test estimates the significant result, we can conclude that the niches of morphs are equivalent and identical (Brown and Carnaval 2019). However, the significant Niche Equivalency, regardless of the result of the Background Statistic test, means that the morphs' niches are different. Meanwhile, if both tests show non-significant results, it shows that the total E-space of one (or both) of the defined morph landscapes are identical to one (or both) morphs' realized niches. In other words, it means the niches are equivalent. but this may be due to limited E-space availability in both distributions.

Finally, we estimated Potential Niche Truncation Index (PNTI) for each morph to determine how the predicted niche is close to the fundamental niche. This index estimates how much of a morph's predicted niche falls outside the study region's E-space (Brown and Carnaval 2019). The lower PNTI value means the predicted niche is a good representation of the fundamental niche (PNTI < 0.15). Conversely, the high (PNTI > 0.3) or moderate (PNTI = 0.15–0.3) index value indicates that the estimated niche poorly represents the fundamental niche (i.e., that much of the species' fundamental niche falls outside of the conditions sampled by our occurrence points).

Results

Western Reef Heron (*Egretta gularis*)

A comparison of four different buffer tests to determine which buffer can cover the individuals' movements did not indicate a significant difference (Table 2. 1). In a report of dark morphs of the Western Reef Heron, the longest movement distance was recorded at 500 km (Ashkenazi 1993). Therefore, we present the results of the 500km buffer.

Based on Principal Components Analysis (PCA), about 70% (PCI = 40.07%, PCII = 29.66%) of the variance in environmental data input was captured in a two-dimensional space (Figure 2. 2a). The six variables are projected inside a two-dimensional circle E-space. The average annual temperature, elevation, solar radiation, and average annual precipitation are best represented by both PCs. The vapor pressure and habitat dissimilarity are best presented by PCI. The length of each arrow of each variable represents how well that parameter explains the distribution of the data. The habitat dissimilarity has the shortest length, which means it does not explain the data distribution very well. Other variables' lengths are similar, which means they all contribute similarly to how the data are distributed. The habitat dissimilarity and vapor pressure are pointed in one direction, which means they are highly correlated. In contrast, the average annual temperature, elevation, solar radiation, and average annual precipitation point opposite each other. This means they are negatively correlated. Other pairwise combinations of variables are unrelated.

The Schoener's *D* index value for both Niche Overlap and Niche Divergence tests are similar (*D* = 0.661). The Niche Equivalency test indices show high similarity (*D* = 0.66). The comparison test between the observed niche similarity of two morphs and the null distribution failed to reject the null hypothesis (*P* = 0.95). The similarity indices for the Background Statistic Test show high similarity (*D* = 0.66). The p-value shows that the test is statistically significant (*P* = 0.01). This means that the similarity between two morphs is too high to be explained by chance. The combination of these two statistical tests shows that the realized niches between the morphs are identical, and their niches can be called equivalent.

The Potential Niche Truncation Index (PNTI) value for the dark morph was low (PNTI < 0.15), meaning the predicted realized niche is a robust representation of the morph's fundamental

niche. In contrast, the PNTI for the white morph is high (PNTI > 0.3), which shows that the occurrence points of white morphs are less effective at characterizing the fundamental niche. However, the overlap map of both morphs, which shows the morphs' niches as Kernel Density Isopleths (Figure 2. 3a), indicates that the most suitable environments for both morphs entirely overlap.

Dimorphic Egret (*Egretta dimorpha*)

Similar to the Western Reef Heron, the size of the geographical buffer around occurrence points for the Dimorphic Egret did not affect the outcome of the analyses (Table 2. 1). Therefore, we also present the results of the 500km buffer for the Dimorphic Egret.

The principal component analyses recovered a two-dimensional space, which captured 67.41% of the variance in environmental data input (PCI = 48.93%, PCII = 18.48%) (Figure 2. 2b). The vapor pressure, average annual temperature, and elevation are best represented by PCI. PCII best represents the average annual precipitation. Based on the arrow length, the habitat dissimilarity and solar radiation cannot explain the data distribution very well. However, the vapor pressure, average annual temperature, elevation, and average annual precipitation are the well-explanatory variables of the data distribution. There is a positive correlation between the average annual temperature and vapor pressure, and they both have a high negative correlation with the elevation. The average annual precipitation is uncorrelated with other well-explanatory variables.

The Niche Overlap Test and Niche Divergence Test show high similarity between the predicted niches of morphs (D = 0.662). These results are in line with the results of the Niche Equivalency test and Background Statistics Test. The Scheoner's D index for the Niche Equivalency Test indicates a high similarity (D = 0.662) compared to the null distribution, emphasizing that the similarity is true (P = 0.91). In support of this result, the Background Statistic Test was

statistically significant ($D = 0.662$, $P = 0.00$). It suggests that the similarity between the morphs' predicted niches is real and not due to chance.

The dark and white morphs' PNTI values are similar (PNTI = 0.16). This value is in the moderate range of the PNTI categories, which means the predicted niches do not completely reflect the fundamental niches of either morph. However, the overlap map of both morphs shows the morphs' niches as Kernel Density Isopleths (Figure 2. 3b) and the highest density, which indicates the most suitable environments, are mostly overlapped between the two morphs.

Discussion

Ecogeographical rules describe patterns of geographic variation in species' phenotypes. Gloger's rule, which describes variation in pelage coloration based on temperature and humidity, predicts that darker-colored individuals should be more prevalent in areas with higher temperature and humidity than lighter-colored individuals. For color-dimorphic species, this predicts that dark and light-colored individuals should have different geographic distributions, resulting in different ecological niches. In this study, we compared the ecological niches of white and dark color morphs of dimorphic species, Western Reef Heron and Dimorphic Egret, and detected no differentiation between the niches. This suggests that dimorphism in these species is maintained by processes other than those typically associated with Gloger's rule, which includes variation in heat, humidity, and crypsis.

Our results indicate strong niche overlap among color morphs for both species. However, the Potential Niche Truncation Index (PNTI) value for the white morph of the Western Reef Heron and both morphs of the Dimorphic Egret fall into a moderate to high range of risk that the realized ecological niche is underestimated compared to the fundamental niche. This means that our results should be interpreted with caution. One factor contributing to a high PNTI may be a

small sample size. Most data points collected from eBird did not specify the plumage coloration, which meant we could not include them in our study, and the limited number of white Western Reef Heron occurrences with definitive identifications further reduced the available data for modeling. Although the PNTI value shows that the occurrence points do not fully represent the fundamental niches of all morphs, the niche overlap map for both species shows a high overlap in the densest regions of niche space for each morph. Thus, even if additional sampling were to fill in regions of niche space that are under-sampled in our analyses, it is unlikely that it would yield an inference of strongly differentiated niches. Therefore, we conclude that the ecological niches between the morphs of either dimorph species are more similar than expected by chance, indicating no niche differentiation among morphs for either species.

A lack of niche differentiation between morphs indicates that the mechanism maintaining color polymorphism should confer advantages to both morphs in the same region, in contrast to the mechanisms associated with Gloger's rule. Our previous work suggests that this mechanism may be UV resistance (Shahrokhi and Patten 2022). All terrestrial species need to manage the amount of UV they receive to increase their survivorship (McKenzie et al. 2011). The Western Reef Heron and Dimorphic Egret are mostly distributed in the equatorial region and receive a high dosage of solar radiation, including UV. Pigmentation, specifically melanin, is the most common evolutionary solution for managing UV radiation (Galván et al. 2018). Another evolutionary response to UV among species is albinism (Mullen and Pohland 2008; Shahrokhi and Patten 2022); as feathers get whiter, more sunlight, including UV, is reflected away from the body (Eaton and Lanyon 2003; Hausmann et al. 2003; Cuthill 2006). Our previous work has shown that in dark morphs of dimorph unicolored egret species, the body regions with the highest sun exposure (the back and chest) have a higher concentration of pigments, while the light morphs

are lightest in those same regions (Shahrokhi and Patten 2022). Dark individuals are able to withstand an excessive amount of UV radiation by absorbing it in their feathers, while white individuals protect their bodies by reflecting UV radiation (Hausmann et al. 2003; Tickell 2003; Cuthill 2006). Therefore, despite different evolutionary responses to UV radiation among color morphs, they can occur in the same geographic area (Shahrokhi and Patten 2022) and may occupy similar ecological niches.

UV resistance is one potential explanation for the similarity between ecological niches of morphs of Western Reef Herons and Dimorphic Egrets. The other possibility is that independent selective processes maintain each color morph. The Western Reef Heron and Dimorphic Egret are mostly distributed in the coastal region of the equator. Most coastal birds, such as egrets, are piscivores which mostly have white ventral coloration. The white plumage coloration makes it easier for birds to be undetected against the sky (Ashmole and Ashmole 1969; Tickell 2003). Thus, crypsis may be the driver of selective pressure maintaining the light individuals in this region and habitat. On the other hand, in this region, water evaporation and humidity are high, which is suitable for feather-degrading bacteria (*Bacillus lichentiformis*) growth (Delhey 2019). Here, because of melanin which increases the hardness (Burtt et al. 2004; Delhey 2019), the dark morphs have less plumage degradation compared to lighter individuals. Therefore, having feathers with more resistance against degradation may be the driver of selective pressure for dark individuals.

Under either potential explanation, the morphs of Western Reef Heron and Dimorphic Egrets have similar ecological niches. The similarity shows that the distribution of color morphs cannot be predicted by Gloger's rule for either species. Our results highlight the complexity of determining the drivers of color variation, where dimorphism may not be easily attributed to a

single environmental mechanism. Other studies have shown similar complexity, even for species that show patterns consistent with Gloger's rule. For instance, in a study on two families of Australian birds (Meliphagidae and Acanthizidae), the species' plumage coloration showed geographical variation consistent with Gloger's rule, but because of precipitation and vegetation (Friedman and Remeš 2017). The researchers found that humidity does not have a significant negative relationship with plumage brightness in Meliphagidae, but precipitation does. In Acanthizidae, the correlation between humidity and brightness has just been observed on the ventral side. Temperature and latitude are not correlated with coloration in either group.

Another study on the Dark-eyed Junco (*Junco hyemalis*) in Canada (de Zwaan et al. 2017) noticed the complexity of morphs' distribution. Based on the study's findings, the number of individuals with the lighter coloration is greater in higher elevations, with a lower temperature and higher amount of UV radiation. Interestingly, the UV reflection was not different among individuals at higher and lower elevations. However, the authors hypothesized that the reason for the higher numbers of lighter individuals in higher elevations is the hardness level of feathers. They suggested that because of higher habitat suitability for feather mites in lower elevation regions, the darker individuals may have advantages in handling them against feather degradation. Still, this hypothesis has not been tested and needs to be examined scientifically.

In conclusion, similar ecological niches between the white and dark color morphs of Western Reef Heron and Dimorphic Egret suggest that the selective pressures which maintain dimorphism within these species are not in line with Gloger's Rule. In other words, the results indicate that dimorphism is likely maintained by a selective pressure that benefits both morphs within the same region, allowing for the high niche similarity we detected. One possible selective pressure is the UV resistance which lets both morphs live next to each other. The other

possibility is independent selections for each morph, resulting in similar living habitats and ecological niches. Although the UV resistance hypothesis has been tested and supported by other studies (Shahrokhi and Patten 2022), other selective pressures (crypsis, feather hardness, etc.) have not been examined on these species. This study is a good example of using ecological niche comparison to investigate ecological rules. Most of the species in the genus *Egretta* are dimorphs with varying degrees of spatial overlap among color morphs. Therefore, comparing the ecological niches may help to identify potential ecological drivers of color variation, which can be confirmed with physiological, behavioral, and molecular studies.

Acknowledgments

We would like to express our gratitude to everyone who contributed to this research, including our colleagues in the American Museum of Natural History, New York, NY, USA, who assisted with data collection. We are extremely grateful for the invaluable help provided by Dr. Clair M. Curry and Melissa Sadir.

Funding statement

This research was supported by the American Museum of Natural History collection study grant and the University of Oklahoma Graduate College Roberson research grant.

Ethics Statement

This research adhered to ethical guidelines for the use of museum specimens and eBird dataset.

Authors contribution

The authors declare no conflict of interest related to this research. Golya Shahrokhi and Michael A. Patten conceived and designed the study. Golya Shahrokhi collected the data. Golya Shahrokhi and Katharine A. Marske analyzed the data and wrote the manuscript.

References

Ashkenazi, S. (1993). Dark-morph individuals of Egretta spp. in Israel. Colonial Waterbirds, 16(2), 202–207.

Ashmole, N. P., and Ashmole, M. J. (1969). Comparative feeding ecology of sea birds of a tropical oceanic island. Bulletin American Museum of Natural History, 40(1), 1–31. https://doi.org/10.2307/4511544

Bates, E. M., and Ballard, B. M. (2014). Factors influencing behavior and success of foraging Reddish Egrets (Egretta rufescens). Waterbirds, 37(2), 191–202. https://doi.org/10.1675/063.037.0213

Bogert, C. M. (1949). Thermoregulation in reptiles; a factor in evolution. Evolution, 3(3), 195–211. https://doi.org/10.1111/j.1558-5646.1949.tb00021.x

Brown, J. L., and Carnaval, A. C. (2019). A tale of two niches: Methods, concepts, and evolution. Frontiers of Biogeography, 11(4). https://doi.org/10.21425/F5FBG44158

Brown, L. H., Urban, E. K., and Newman, K. B. (2020). The Birds of Africa: Vol. I. Bloomsbury Publishing.

Burtt, E. R., Ichida, J. M., Burtt, E. H., and Burtt, E.R et Ichida, J. M. (2004). Gloger's rule, feather-degrading bacteria, and color variation among song sparrows. The Condor, 106, 681–686.

Caro, T. (2005). The adaptive significance of coloration in mammals. BioScience, 55(2), 125–136. https://doi.org/10.1641/0006-3568(2005)055[0125:TASOCI]2.0.CO;2

Cuthill, I. C. (2006). Perception and measurements. In G. E. Hill and J. McGraw, Kevin (Eds.), Bird Coloration. Volume I: Mechanisms And Measurements (pp. 3–40). Harvard University Press. https://doi.org/10.1650/0010-5422(2007)109[482:bcvmam]2.0.co;2

Delhey, K. (2015). The colour of an avifauna: A quantitative analysis of the colour of Australian birds. Scientific Reports, 5(December), 1–12. https://doi.org/10.1038/srep18514

Delhey, K. (2018). Darker where cold and wet: Australian birds follow their own version of Gloger's rule. Ecography, 41(4), 673–683. https://doi.org/10.1111/ecog.03040

Delhey, K. (2019). A review of Gloger's rule, an ecogeographical rule of colour: definitions, interpretations and evidence. Biological Reviews, 94, 1294–1316. https://doi.org/10.1111/brv.12503

Eaton, M. D., and Lanyon, S. M. (2003). The ubiquity of avian ultraviolet plumage reflectance. Proceedings of the Royal Society B: Biological Sciences, 270(1525), 1721–1726. https://doi.org/10.1098/rspb.2003.2431

eBird. (2022). eBird: An online database of bird distribution and abundance. Ithaca, NY: Cornell Lab of Ornithology. http://www.ebird.org

Endler, J. A., Westcott, D. A., Madden, J. R., and Robson, T. (2005). Animal visual systems and the evolution of color patterns: Sensory processing illuminates signal evolution. Evolution, 59(8), 1795–1818. https://doi.org/10.1111/j.0014-3820.2005.tb01827.x

Etezadifar, F., and Amini, H. (2010). Current Status of the Breeding Population of the Western Reef Heron Egretta gularis along the Northern Coasts of the Persian Gulf and Oman Sea, and its Wintering Population in the South of Iran. Heron, 5(2), 71–80.

Ferguson-Lees, J., and Christie, D. A. (2001). Raptors of the world (C. Helm, Ed.). Houghton Mifflin Harcourt.

Fick, S. E., and Hijmans, R. J. (2017). WorldClim 2: new 1-km spatial resolution climate surfaces for global land areas. International Journal of Climatology, 37(12), 4302–4315. https://doi.org/10.1002/joc.5086

Friedman, N. R., and Remeš, V. (2017). Ecogeographical gradients in plumage coloration among Australasian songbird clades. Global Ecology and Biogeography, 26(3), 261–274. https://doi.org/10.1111/geb.12522

Galeotti, P., Rubolini, D., Dunn, P. O., and Fasola, M. (2003). Colour polymorphism in birds: Causes and functions. Journal of Evolutionary Biology, 16, 635–645. https://doi.org/10.1046/j.1420-9101.2003.00569.x

Galván, I., Rodríguez-Martínez, S., and Carrascal, L. M. (2018). Dark pigmentation limits thermal niche position in birds. Functional Ecology, 32(6), 1531–1540. https://doi.org/10.1111/1365-2435.13094

Gaston, K. J., Chown, S. L., and Evans, K. L. (2008). Ecogeographical rules: Elements of a synthesis. Journal of Biogeography, 35(3), 483–500. https://doi.org/10.1111/j.1365-2699.2007.01772.x

Gloger, C. L. (1833). Das Abandern der Vogel durch Einfluss des Klimas. August Schulz, Breslau, Germany.

Goldenberg, J., Bisschop, K., D'Alba, L., and Shawkey, M. D. (2022). The link between body size, colouration and thermoregulation and their integration into ecogeographical rules: a critical appraisal in light of climate change. Oikos, 2022(6). https://doi.org/10.1111/oik.09152

Goldstein, G., Flory, K. R., Browne, B. A., Majid, S., Ichida, J. M., and Burtt, E. H. (2004). Bacterial degradation of black and white feathers. Auk, 121(3), 656–659. https://doi.org/10.2307/4090304

Gomez, D., and Théry, M. (2007). Simultaneous crypsis and conspicuousness in color patterns: Comparative analysis of a neotropical rainforest bird community. American Naturalist, 169(S1), S42–S61. https://doi.org/10.1086/510138

Green, M. C., Hill, A., Troy, J. R., Holderby, Z., and Geary, B. (2011). Status of breeding Reddish Egrets on Great Inagua, Bahamas with comments on breeding Territoriality and the effects of hurricanes. Waterbirds, 34(2), 213–217.

Gunderson, A. R., Frame, A. M., Swaddle, J. P., and Forsyth, M. H. (2008). Resistance of melanized feathers to bacterial degradation: Is it really so black and white? Journal of Avian, 39(5), 539–545. https://doi.org/10.1111/j.2008.0908-8857.04413.x

Hancock, J., and Kushlan, J. A. (2010). The Herons Handbook. Bloomsbury Publisher.

Hausmann, F., Arnold, K. E., Marshall, N. J., and Owens, I. P. F. (2003). Ultraviolet signals in birds are special. Proceedings of the Royal Society B: Biological Sciences, 270(1510), 61–67. https://doi.org/10.1098/rspb.2002.2200

IUCN. (2022). The IUCN red list of threatened species. http://www.iucnredlist.org/

Kushlan, J. A., and Hancock, J. (2005). 14. The Herons: Ardeidea (Bird Families of the World). In Bird Families of the World (pp. xv–433). Oxford University Press.

Lomolino, M. V., Riddle, B. R., and Brown, J. H. (2006). Biogeography (3rd ed.). Sinauer Associates Inc.

Marcondes, R. S., Nations, J. A., Seeholzer, G. F., and Brum, R. T. (2021). Rethinking Gloger's rule: climate, light environments, and color in a large family of tropical birds (Furnariidae). The American Naturalist, 197(5), 592–606. https://doi.org/10.1086/713386

McGraw, K. J. (2006). Mechanics of melanin-based coloration. In G. E. Hill and K. J. McGraw (Eds.), Bird Coloration (pp. 243–294). Harvard University Press.

McKenzie, R. L., Aucamp, P. J., Bais, A. F., Björn, L. O., Ilyas, M., and Madronich, S. (2011). Ozone depletion and climate change: Impacts on UV radiation. Photochemical and Photobiological Sciences, 10(2), 182–198. https://doi.org/10.1039/c0pp90034f

McNaught, M. K., and Owens, I. P. F. (2002). Interspecific variation in plumage colour among birds: Species recognition or light environment? Journal of Evolutionary Biology, 15(4), 505–514. https://doi.org/10.1046/j.1420-9101.2002.00431.x

Mock, D. W. (1980). White-dark polymorphism in herons. Proceedings of the First Welder Wildlife Foundation Symposium, 1, 145–161.

Mullen, P., and Pohland, G. (2008). Studies on UV reflection in feathers of some 1000 bird species: Are UV peaks in feathers correlated with violet-sensitive and ultraviolet-sensitive cones? Ibis, 150(1), 59–68. https://doi.org/10.1111/j.1474-919X.2007.00736.x

R Core Team. (2022). R: A language and environment for statistical computing. In R: A language and environment for statistical computing. R Foundation for Statistical Computing, Vienna, Austria. URL http://www. R-project. org (4.2.2). R Foundation for Statistical Computing. https://www.r-project.org/.

Recher, H. F. (1972). Colour dimorphism and the ecology of herons. Ibis, 114(4), 552–555. https://doi.org/10.1111/j.1474-919X.1972.tb00859.x

Roulin, A., and Randin, C. (2015). Gloger's rule in North American Barn Owls. Auk, 132(2), 321–332. https://doi.org/10.1642/AUK-14-167.1

Rstudio, T. (2020). RStudio: Integrated Development for R. In Rstudio Team, PBC, Boston, MA URL http://www.rstudio.com/. https://doi.org/10.1145/3132847.3132886

Schoener, T. W. (1968). The anolis lizards of bimini: resource partitioning in a complex fauna. Ecology, 49(4). https://doi.org/10.2307/1935534

Shahrokhi, G., and Patten, M. A. (2022). Linking plumage dimorphism and environmental stress. Journal of Zoology, 1–9. https://doi.org/10.1111/jzo.12972

Tickell, WL. L. N. (2003). White Plumage. Journal of Waterbird Society, 26(1), 1–12.

Tuanmu, M. N., and Jetz, W. (2015). A global, remote sensing-based characterization of terrestrial habitat heterogeneity for biodiversity and ecosystem modelling. Global Ecology and Biogeography, 24(11), 1329–1339. https://doi.org/10.1111/geb.12365

Warren, D. L., Glor, R. E., and Turelli, M. (2008). Environmental niche equivalency versus conservatism: Quantitative approaches to niche evolution. Evolution, 62(11), 2868–2883. https://doi.org/10.1111/j.1558-5646.2008.00482.x

Zimmerman, D. A., Turner, D. A., and Pearson, D. J. (1996). Birds of Kenya and northern Tanzania. Princeton University Press. http://agris.fao.org/agris-search/search.do?recordID=US201300075290

Zink, R. M., and Remsen Jr, J. V. (1986). Evolutionary processes and patterns of geographic variation in birds. Curr. Ornithol, 4, 1–69.

Figures and Tables

Table 2. 1. Principal components analysis (PCA1 and PCA2) and how the first two axes can explain the variability between the morphs. The Schoener's D index, the p-value for Niche Equivalency, and Background Statistical tests. The non-significant p-value for the Niche Equivalency test and significant p-value for the Background Statistic test mean identical ecological niches between the morphs.

	Western Reef Heron	**Dimorphic Egret**
500 km	PC1: 40.7 % PC2: 29.66 % Schoener's D index: 0.661 Niche Equivalency p-value: 0.95 Background Statistic test p-value: 0.01	PC1: 48.93 % PC2: 18.48 % Schoener's D index: 0.662 Niche Equivalency p-value: 0.91 Background Statistic test p-value: 0.00

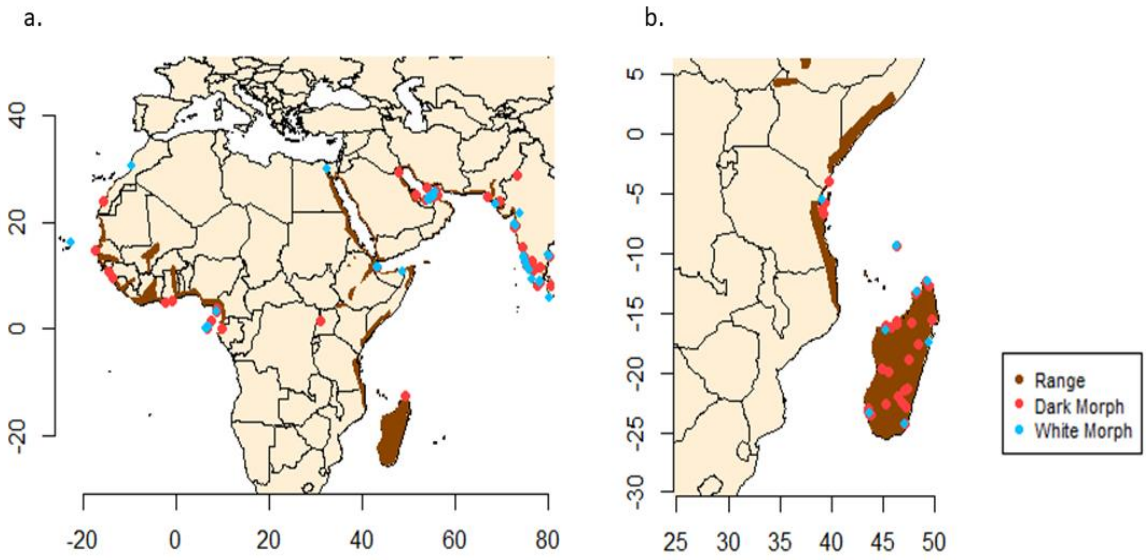

Figure 2. 1. Global distribution (2016) and occurrence points of dark and white morphs of (a) Western Reef Heron *(Egretta gularis)* and (b) Dimorphic Egret *(E. dimorpha)*

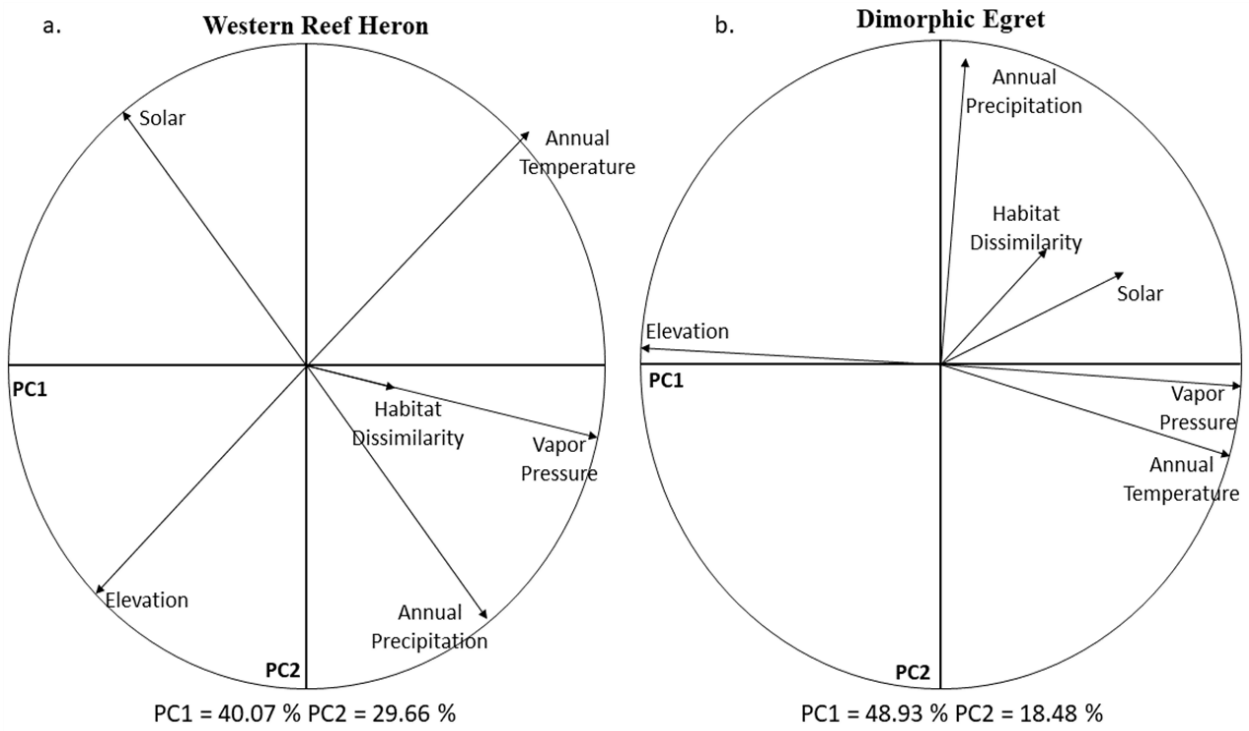

Figure 2. 2. Correlation circle and important principal components of environmental variation for (a) Western Reef Heron and (b) Dimorphic Egret. About 70% and 67.41% of the variances in environmental data were captured in two-dimensional for the Western Reef Heron and Dimorphic Egret, respectively. For each environmental variable, the length of the arrow represents how well that parameter explains the data distribution. (a) For Western Reef Heron, solar radiation, annual temperature, elevation, and average annual precipitation are best represented by both PCs, while vapor pressure and habitat dissimilarity are best presented by PC1. (b) For Dimorphic Egret, vapor pressure and mean annual temperature are best presented by PC1 and are negatively correlated with elevation. The mean annual precipitation is best presented by PC2. The habitat dissimilarity and solar radiation are presented by both PCs but explain less variation than the other variables.

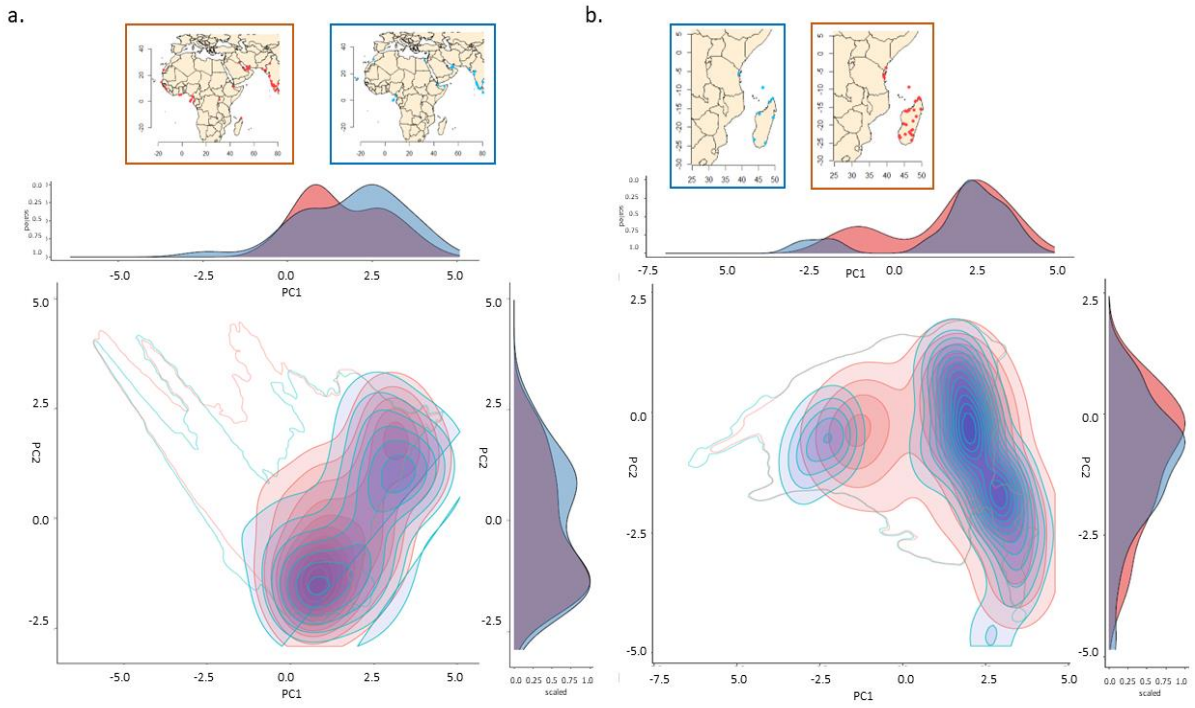

Figure 2. 3. Plots of Niche Overlap between dark (red) and white (blue) morphs of (a) Western Reef Heron (*Egretta gularis*) and (b) Dimorphic Egret (*Egretta dimropha*). Climate niche of each morph has been shown as filled kernel density isopleths. The empty, outlined areas shows accessible E-space to each morph. Regions with higher density represent higher occupied regions of the Niche. The density of each morphs' niches for each PC has been shown as a density histogram. The map of occurrence points of each morph with representative of similar color of kernel density border are added to correspond kernel color on overlap plot.

Supplementary Materials

Table S 2. 1. Summary of occurrence data points of Western Reef Heron (*Egretta gularis*) and Dimorphic Egret (*Egretta dimorpha*) from eBird dataset and American Museum of Natural History specimens that were used in niche comparisons.

Data Source	Species	Accession Number/ID	Color morph	Country	Latitude	Longitude
eBird	*Egretta gularis*	OBS245057021	White	United Arab Emirates	24.422718	54.482695
	Egretta gularis	OBS245318442	Dark	United Arab Emirates	24.423337	54.409597
	Egretta gularis	OBS330011950	White	United Arab Emirates	24.725917	54.638373
	Egretta gularis	OBS330011950	Dark	United Arab Emirates	24.725917	54.638373
	Egretta gularis	OBS237453341	Dark	United Arab Emirates	24.4065126	54.2985535
	Egretta gularis	OBS238424095	White	United Arab Emirates	24.1824628	54.0712738
	Egretta gularis	OBS238543710	Dark	United Arab Emirates	24.0714066	53.5581779
	Egretta gularis	OBS238683728	Dark	United Arab Emirates	24.4596506	54.4396591
	Egretta gularis	OBS239616423	Dark	United Arab Emirates	24.294145	54.129971
	Egretta gularis	OBS493759023	White	United Arab Emirates	24.602621	54.6090245
	Egretta gularis	OBS385374620	Dark	United Arab Emirates	24.567915	54.540234
	Egretta gularis	OBS385374620	White	United Arab Emirates	24.567915	54.540234
	Egretta gularis	OBS245282037	Dark	United Arab Emirates	24.577764	54.633904
	Egretta gularis	OBS245338801	Dark	United Arab Emirates	24.446745	54.436983
	Egretta gularis	OBS298177628	White	United Arab Emirates	24.281	54.4253
	Egretta gularis	OBS298177095	Dark	United Arab Emirates	24.443992	54.224924
	Egretta gularis	OBS282074562	White	United Arab Emirates	24.84491	55.35159
	Egretta gularis	OBS282074562	Dark	United Arab Emirates	24.84491	55.35159
	Egretta gularis	OBS237844704	Dark	United Arab Emirates	25.03335	56.348877

	Egretta gularis	OBS238416122	Dark	United Arab Emirates	25.101572	56.359112
	Egretta gularis	OBS563424765	Dark	United Arab Emirates	25.774054	55.9461379
	Egretta gularis	OBS330012447	Dark	United Arab Emirates	25.533105	55.602454
	Egretta gularis	OBS330012447	White	United Arab Emirates	25.533105	55.602454
	Egretta gularis	OBS331418681	Dark	United Arab Emirates	25.612587	55.633074
	Egretta gularis	OBS461088147	Dark	Canada	46.1725796	-59.937973
	Egretta gularis	OBS456010063	White	Cape Verde	16.0187429	-22.741624
	Egretta gularis	OBS529724609	White	Djibouti	11.587507	43.131775
	Egretta gularis	OBS529724609	Dark	Djibouti	11.587507	43.131775
	Egretta gularis	OBS376458090	Dark	Western Sahara	23.8285349	-15.735468
	Egretta gularis	OBS564413775	Dark	Ghana	5.262146	-1.020651
	Egretta gularis	OBS193110246	Dark	Ghana	5.0116026	-2.4142456
	Egretta gularis	OBS206624849	Dark	Guinea	10.6648542	-14.610024
	Egretta gularis	OBS206510147	Dark	Guinea	9.5244219	-13.693192
	Egretta gularis	OBS206510724	Dark	Guinea	9.5319121	-13.692403
	Egretta gularis	OBS558336719	White	India	13.7197078	80.1262093
	Egretta gularis	OBS566774230	White	India	23.1785543	68.6559677
	Egretta gularis	OBS570101516	Dark	India	23.801798	69.5041466
	Egretta gularis	OBS301318914	White	India	21.6722749	73.7930793
	Egretta gularis	OBS301617334	Dark	India	12.668801	76.64444
	Egretta gularis	OBS571524323	Dark	India	12.1495037	76.4734101
	Egretta gularis	OBS274917964	White	India	13.2779588	74.7247553
	Egretta gularis	OBS438182116	White	India	13.2707381	74.7312737

	Egretta gularis	OBS483107462	White	India	13.633329	74.674682
	Egretta gularis	OBS483107462	Dark	India	13.633329	74.674682
	Egretta gularis	OBS353470456	Dark	India	15.2592125	74.6238399
	Egretta gularis	OBS564928763	White	India	9.340145	76.385179
	Egretta gularis	OBS566805867	Dark	India	11.7819938	75.4481061
	Egretta gularis	OBS566805867	White	India	11.7819938	75.4481061
	Egretta gularis	OBS480299822	Dark	India	12.5772246	74.945426
	Egretta gularis	OBS480299822	White	India	12.5772246	74.945426
	Egretta gularis	OBS352423510	White	India	11.0206903	75.8569264
	Egretta gularis	OBS368566440	Dark	India	18.9956148	72.8613456
	Egretta gularis	OBS375615562	Dark	India	19.4760601	72.759726
	Egretta gularis	OBS375615562	White	India	19.4760601	72.759726
	Egretta gularis	OBS541843415	Dark	India	19.2021592	72.9785007
	Egretta gularis	OBS541843415	White	India	19.2021592	72.9785007
	Egretta gularis	OBS523735804	Dark	India	28.8001566	73.2336187
	Egretta gularis	OBS303180187	Dark	India	10.9701261	76.9286299
	Egretta gularis	OBS553313355	Dark	India	8.0782268	77.5510794
	Egretta gularis	OBS439607466	Dark	India	11.6875401	78.1803417
	Egretta gularis	OBS340633329	White	India	8.9272661	78.1870794
	Egretta gularis	OBS472096545	White	India	8.7833815	78.1940746
	Egretta gularis	OBS472096545	Dark	India	8.7833815	78.1940746
	Egretta gularis	OBS548233531	Dark	India	8.8067716	78.1379048
	Egretta gularis	OBS548233531	White	India	8.8067716	78.1379048

	Egretta gularis	OBS346178694	White	India	13.4296116	80.3099513
	Egretta gularis	OBS346178694	Dark	India	13.4296116	80.3099513
	Egretta gularis	OBS371764900	Dark	Iran	26.5441406	54.0233132
	Egretta gularis	OBS572648233	White	Sri Lanka	5.967653	80.374123
	Egretta gularis	OBS215274035	Dark	Sri Lanka	8.1457802	80.5303192
	Egretta gularis	OBS446980165	Dark	Qatar	25.1445076	51.6192198
	Egretta gularis	OBS370713597	Dark	Equatorial Guinea	3.715386	8.747914
	Egretta gularis	OBS370387515	Dark	Equatorial Guinea	3.271453	8.580999
	Egretta gularis	OBS370387515	White	Equatorial Guinea	3.271453	8.580999
	Egretta gularis	OBS291386803	White	Morocco	30.3623594	-9.5867729
	Egretta gularis	OBS164581548	Dark	Senegal	14.729373	-17.432963
	Egretta gularis	OBS286664807	Dark	United Arab Emirates	24.840055	55.344334
	Egretta gularis	OBS286664807	White	United Arab Emirates	24.840055	55.344334
	Egretta gularis	OBS341645084	White	Egypt	29.956877	32.548028
	Egretta gularis	OBS564596788	Dark	Kuwait	29.257349	47.7546501
	Egretta dimorpha	OBS219247007	White	Madagascar	-20.2106562	47.109375
	Egretta dimorpha	OBS219249087	Dark	Madagascar	-23.4963104	43.761463
	Egretta dimorpha	OBS236661307	White	Madagascar	-15.4953707	49.76964
	Egretta dimorpha	OBS236661307	Dark	Madagascar	-15.4953707	49.76964
	Egretta dimorpha	OBS259613869	White	Madagascar	-23.354352	43.653144
	Egretta dimorpha	OBS584128444	Dark	Madagascar	-15.4961667	49.769166
	Egretta dimorpha	OBS584128932	Dark	Madagascar	-15.7188333	46.313
	Egretta dimorpha	OBS584128706	White	Madagascar	-16.3065	46.816666

	Egretta dimorpha	OBS584128754	White	Madagascar	-15.6606667	47.9075
	Egretta dimorpha	OBS584128505	White	Madagascar	-18.867	47.518333
	Egretta dimorpha	OBS367936682	Dark	Madagascar	-21.9677864	46.52915
	Egretta dimorpha	OBS367936727	Dark	Madagascar	-23.1316615	43.606443
	Egretta dimorpha	OBS367952925	White	Madagascar	-18.9139022	47.519292
	Egretta dimorpha	OBS584128746	Dark	Madagascar	-15.763	47.8135
	Egretta dimorpha	OBS308954377	White	Madagascar	-24.8123038	46.156679
	Egretta dimorpha	OBS190600634	White	Madagascar	-23.443212	43.756286
	Egretta dimorpha	OBS202524331	Dark	Madagascar	-16.1342197	45.845260
	Egretta dimorpha	OBS232081404	Dark	Madagascar	-23.2828847	43.642879
	Egretta dimorpha	OBS273285011	Dark	Madagascar	-21.440849	47.102783
	Egretta dimorpha	OBS273285011	White	Madagascar	-21.440849	47.102783
	Egretta dimorpha	OBS298398537	Dark	Madagascar	-12.6485457	49.522891
	Egretta dimorpha	OBS298398537	White	Madagascar	-12.6485457	49.522891
	Egretta dimorpha	OBS334213522	White	Madagascar	-19.9026677	45.505971
	Egretta dimorpha	OBS334213522	Dark	Madagascar	-19.9026677	45.505971
	Egretta dimorpha	OBS346541299	Dark	Madagascar	-15.859554	46.353678
	Egretta dimorpha	OBS346541299	White	Madagascar	-15.859554	46.353678
	Egretta dimorpha	OBS370888416	White	Madagascar	-15.5698897	46.422626
	Egretta dimorpha	OBS370910210	Dark	Madagascar	-23.466603	43.809914
	Egretta dimorpha	OBS334444960	White	Madagascar	-19.1471953	44.796752
	Egretta dimorpha	OBS443482074	White	Madagascar	-21.7073167	46.968934
	Egretta dimorpha	OBS446973592	White	Madagascar	-15.871341	46.352934

	Egretta dimorpha	OBS446973592	Dark	Madagascar	-15.871341	46.352934
	Egretta dimorpha	OBS462997205	Dark	Madagascar	-18.891725	47.526566
	Egretta dimorpha	OBS549567621	Dark	Madagascar	-21.259198	47.422071
	Egretta dimorpha	OBS535125063	Dark	Madagascar	-22.6431545	45.329255
	Egretta dimorpha	OBS267879639	Dark	Kenya	-4.0139322	39.726090
	Egretta dimorpha	OBS267879639	White	Kenya	-4.0139322	39.726090
	Egretta dimorpha	OBS325597603	Dark	Tanzania	-5.8210823	39.383325
	Egretta dimorpha	OBS325597603	White	Tanzania	-5.8210823	39.383325
	Egretta dimorpha	OBS452286825	Dark	Tanzania	-6.6818323	39.224415
	Egretta dimorpha	OBS452286825	White	Tanzania	-6.6818323	39.224415
	Egretta dimorpha	OBS403036557	White	Kenya	-3.908	39.786
	Egretta dimorpha	OBS403036557	Dark	Kenya	-3.908	39.786
	Egretta dimorpha	OBS427801155	Dark	Tanzania	-6.2791046	39.177471
	Egretta dimorpha	OBS560255199	White	Kenya	-3.3202196	39.970842
	Egretta dimorpha	OBS521562484	White	Kenya	-4.418884	39.525013
American Museum of Natural History	*Egretta gularis*	AMNH648714	Dark	Pakistan	-24.8333333	66.983333
	Egretta gularis	AMNH530005	White	Somaliland	-10.8333333	48.583333
	Egretta gularis	AMNH265280	Dark	Uganda	-1.48333333	30.916666
	Egretta gularis	AMNH529999	White	Somaliland	-11.4333333	43.45
	Egretta gularis	AMNH529998	Dark	Somaliland	-12.3	49.3
	Egretta gularis	AMNH268413	White	Sao Thome	-0.36666666	6.7166666
	Egretta gularis	AMNH264841	White	Sao Thome	-0.28333333	6.75
	Egretta gularis	AMNH268410	White	Sao Thome	-0.33333333	6.7333333

	Egretta gularis	AMNH264842	White	Sao Thome	-0.31666666	6.7333333
	Egretta gularis	AMNH268406	Dark	Sao Thome	-0.31666666	6.7333333
	Egretta gularis	AMNH264839	Dark	Sao Thome	-0.33333333	6.7333333
	Egretta gularis	AMNH268408	Dark	Sao Thome	-0.35	6.7
	Egretta gularis	AMNH268404	Dark	Sao Thome	-0.31666666	6.7333333
	Egretta gularis	AMNH268407	Dark	Sao Thome	-0.26666666	6.75
	Egretta gularis	AMNH264840	White	Sao Thome	-0.31666666	6.7333333
	Egretta gularis	AMNH268402	Dark	Sao Thome	-0.33333333	6.7166666
	Egretta gularis	AMNH530004	Dark	Sao Thome	-0.26666666	6.7333333
	Egretta gularis	AMNH268409	Dark	Sao Thome	-0.3	6.4833333
	Egretta gularis	AMNH268412	White	Sao Thome	-0.18333333	6.45
	Egretta gularis	AMNH264843	White	Sao Thome	-0.1	6.65
	Egretta gularis	AMNH268411	White	Sao Thome	-0.21666666	6.75
	Egretta gularis	AMNH530005	White	Sao Thome	-0.11666666	6.65
	Egretta gularis	AMNH265985	Dark	San Thome	-0.1	6.4666666
	Egretta gularis	AMNH297264	Dark	Gabon	-1.6	7.4166666
	Egretta gularis	AMNH344768	Dark	Sao Thome	-0.35	6.7166666
	Egretta gularis	AMNH349761	Dark	Goban	0	9.8
	Egretta gularis	AMNH297265	Dark	Sao Thome	-0.33333333	6.7333333
	Egretta gularis	AMNH265986	Dark	Sao Thome	-0.38333333	6.6833333
	Egretta gularis	AMNH268405	Dark	Gabon	-1.6	7.4166666
	Egretta gularis	AMNH265989	Dark	Sao Thome	-0.26666666	6.75
	Egretta gularis	AMNH344769	Dark	Gabon	-1.6	7.4166666

	Egretta gularis	AMNH265988	Dark	Gabon	-0.01666666	9.8
	Egretta gularis	AMNH265987	Dark	Sao Thome	-0.23333333	6.7333333
	Egretta dimorpha	AMNH793528	Dark	Seychelles	-9.36666666	46.333333
	Egretta dimorpha	AMNH410725	White	Madagascar	-23.35	43.666666
	Egretta dimorpha	AMNH410733	White	Madagascar	-23.35	43.666666
	Egretta dimorpha	AMNH410724	White	Madagascar	-24.3	47.2
	Egretta dimorpha	AMNH529992	Dark	Madagascar	-13.3166666	48.166666
	Egretta dimorpha	AMNH410726	Dark	Madagascar	-16.1	45.333333
	Egretta dimorpha	AMNH410730	Dark	Madagasar	-13.25	48.316666
	Egretta dimorpha	AMNH410729	White	Madagascar	-17.4833333	49.466666
	Egretta dimorpha	AMNH410717	Dark	Madagascar	-22.4666666	46.883333
	Egretta dimorpha	AMNH410727	Dark	Madagascar	-17.6166666	48.466666
	Egretta dimorpha	AMNH529991	Dark	Madagascar	-13.3166666	48.166666
	Egretta dimorpha	AMNH529995	Dark	Madagascar	-23.0166666	43.533333
	Egretta dimorpha	AMNH530000	Dark	Tanzanina	-6.65	39.216666
	Egretta dimorpha	AMNH410715	Dark	Madagascar	-13.2833333	48.166666
	Egretta dimorpha	AMNH410731	White	Madagascar	-12.2666666	49.383333
	Egretta dimorpha	AMNH410718	White	Madagascar	-23.35	43.666666
	Egretta dimorpha	AMNH529996	Dark	Madagascar	-12.3	49.3
	Egretta dimorpha	AMNH410723	Dark	Madagascar	-24.3	47.2
	Egretta dimorpha	AMNH530001	White	Tanzania	-5.5	39.066666
	Egretta dimorpha	AMNH410722	White	Madagascar	-16.4	45.316666
	Egretta dimorpha	AMNH410716	Dark	Madagascar	-22.4666666	46.883333

	Egretta dimorpha	AMNH529993	White	Madagascar	-13.2666666	48.3
	Egretta dimorpha	AMNH410720	Dark	Madagascar	-23.5333333	43.733333
	Egretta dimorpha	AMNH410719	Dark	Madagascar	-23.55	43.75
	Egretta dimorpha	AMNH410714	Dark	Madagascar	-22.8333333	47.266666
	Egretta dimorpha	AMNH410721	Dark	Madagascar	-19.65	44.966666
	Egretta dimorpha	AMNH529979	White	Seychelles	-9.38333333	46.316666
	Egretta dimorpha	AMNH529986	Dark	Seychelles	-9.36666666	46.333333
	Egretta dimorpha	AMNH529997	Dark	Madagascar	-12.2833333	49.25
	Egretta dimorpha	AMNH529988	White	Seychelles	-9.36666666	46.333333
	Egretta dimorpha	AMNH529978	Dark	Seychelles	-9.36666666	46.333333
	Egretta dimorpha	AMNH529977	White	Seychelles	-9.38333333	46.316666
	Egretta dimorpha	AMNH529924	White	Seychelles	-9.36666666	46.316666
	Egretta dimorpha	AMNH529989	Dark	Seychelles	-9.36666666	46.316666
	Egretta dimorpha	AMNH529984	Dark	Seychelles	-9.38333333	46.316666
	Egretta dimorpha	AMNH529980	Dark	Seychelles	-9.36666666	46.333333
	Egretta dimorpha	AMNH529985	White	Seychelles	-9.36666666	46.333333
	Egretta dimorpha	AMNH529987	Dark	Seychelles	-9.36666666	46.316666
	Egretta dimorpha	AMNH529976	Dark	Seychelles	-9.36666666	46.333333
	Egretta dimorpha	AMNH529983	White	Seychelles	-9.36666666	46.333333
	Egretta dimorpha	AMNH529981	White	Seychelles	-9.36666666	46.316666
	Egretta dimorpha	AMNH529982	Dark	Seychelles	-9.36666666	46.333333

Chapter 3

From Dark to White: Investigating the Genetics of Plumage Coloration in Two Dimorphic Bird Species using Whole Genome Sequencing

Manuscript in preparation

Golya Shahrokhi[1], Subir Shakaya[2], Cara Monroe[3], Brian M. Kemp[3]

[1] Biology Department, University of Oklahoma, Norman, OK, USA

[2] Museum of Comparative Zoology Labs, Harvard University, Cambridge, MA, USA

[3] Department of Anthropology, University of Oklahoma, Norman, OK, USA

Abstract

Coloration plays a critical role in species recognition, social signaling, camouflage, and mate choice, and genetic mutations that affect color variation can be maintained by evolution. Thus, identifying the genes responsible for coloration and polymorphism can enhance our understanding of the evolution and history of species. In this study, we analyzed the whole genomes of two dimorphic bird species, the Western Reef Heron (*Egretta gularis*) and the Dimorphic Egret (*Egretta dimorpha*), to identify the genes underlying color variation among morphs. We generated shotgun sequencing data from 50 toepad samples collected from five populations, including 30 dark and 20 white morphs, resulting in 55,215 to 6,414,649 SNPs across three datasets. We compared the sequences of dark and white morphs using Weir and Cockerham's F_{ST} index. Loci with F_{ST} higher than 0.5 were considered highly differentiated loci. The closest genes to these loci of interest have been identified from the reference (*Egretta gazetta*). The population structure of each morph was compared and generated by applying principal components, STRUCTURE, and F_{ST} per population. We did not find any genomic

differentiation between the two morphs in either species or among populations within species. Our findings suggest two possibilities: hybridization and gene flow between the dark and white morphs or a polygenic control of coloration. We recommend collecting modern DNA samples from both color morphs from previous and in-between populations to determine which of these possibilities applies to the Western Reef Heron and Dimorphic Egret.

Introduction

Color can be vital in species recognition and signaling functions such as camouflage, social signals, and mating choice (Bortolotti, 2006; Hill and McGraw, 2006a; Poelstra *et al.*, 2014; Bourgeois *et al.*, 2017; Campagna *et al.*, 2017). Among different phenotype traits, coloration is a characteristic that can drive natural selection, sexual selection, and, eventually, the process of speciation (Hill and McGraw, 2006b; Orteu and Jiggins, 2020). Due to its rapidly evolving nature, color is one of the most dynamic phenotypes (Hubbard *et al.*, 2010). It is often used to gauge evolutionary flexibility, adaptation, or stability (Friedman and Remeš, 2017) in animals and plants. Recently, there has been growing interest among scientists in linking coloration underlying phenotypes to genotypes, particularly genes that have a significant impact on overall coloration (Mundy, 2005; Poelstra *et al.*, 2015; Lopes *et al.*, 2016; San-Jose and Roulin, 2017) and evolution (Aguillon, Walsh and Lovette, 2021). As a result, identifying the specific genes linked to color variation can be a fruitful line of research for evolutionary biologists and others (Aguillon *et al.*, 2021).

The coloration of a species is altered by the mutation of genes related to color (Herrera *et al.*, 2015), leading to a color polymorphism. The existence of color variation within a species is the result of a delicate balance between various evolutionary forces (Herrera *et al.*, 2015; Bourgeois *et al.*, 2017) that affect their aspects such as morphology, behavior, physiology, or life history

(Sinervo and Svensson, 2002; Calsbeek and Sinervo, 2007; McKinnon and Pierotti, 2010). As a result, the study of coloration in species with color polymorphism has been a subject of great interest, as it provides valuable insights into the complex forces that drive the evolution of species (Rankin *et al.*, 2016). Researchers can gain a deeper understanding of these evolutionary forces by identifying the relevant genes and examining genomic changes within a color polymorph species.

It is hypothesized that the coloration of discrete morphs is controlled by a small number of highly influential genes, regardless of any variation within each color (Rankin *et al.*, 2016). However, the genes responsible for coloration can differ depending on the type of pigmentation (Aguillon *et al.*, 2021), and the genetic basis for color variation remains poorly understood (Rankin *et al.*, 2016). Among vertebrates, melanin-based pigmentation is one of the most well-studied pigments, as it is under strong genetic control (Roulin, 2004; Hill and McGraw, 2006a). For example, over 150 genes were involved in the production and breakdown of melanin pigment in mice (Bennett and Lamoreux, 2003). The *melanocortin-1 receptor* (*MC1R*) is the most extensively studied color gene and has been shown to account for color variation in various animals (Theron *et al.*, 2001; Mundy *et al.*, 2004; Rogers *et al.*, 2004; Rosenblum, Hoekstra and Nachman, 2004; Mullen and Hoekstra, 2008; Haas *et al.*, 2009; Uy *et al.*, 2009). In addition to MC1R, other genes have been identified as contributors to melanin-based coloration patterns in both mammals and birds (Bourgeois *et al.*, 2016), including agouti-signaling protein (*ASIP*) (Minvielle *et al.*, 2007; Hiragaki *et al.*, 2008; Nadeau *et al.*, 2008; Kingsley *et al.*, 2009); *Corin* (Yan *et al.*, 1999; Enshell-Seijffers, Lindon and Morgan, 2008; Manceau *et al.*, 2010), Dopachrome tautomerase (*DCT*) (Jackson *et al.*, 1992), Pro-opiomelanocortin (*POMC*) (Yaswen *et al.*, 1999; Roulin *et al.*, 2011), Solute carrier family 24 member 5 (*SLC24A5*) (Lamason *et al.*,

2005; Nadeau *et al.*, 2008), Tyrosinase (*TYR*) (Sato *et al.*, 2007); and Tyrosinase related protein 1 (*TYRP1* (Nadeau *et al.*, 2007; Laaksonen *et al.*, 2015). On the other hand, other studies suggest that instead of a few genes with high effectiveness, the interaction of multiple genes plays a significant role in shaping phenotypic variation (Mackay, 2014). Thus, studying the entire genome may be essential in understanding color polymorphism since the genes responsible for color variation may vary across species, highlighting the need for a broader approach.

Although color polymorphism is not a widespread phenomenon among birds, occurring in only 3.5% of species (Roulin, 2004), avian species are often chosen as model organisms for study due to their well-established phylogeny (Cracraft *et al.*, 2004); additionally, they can be found in a variety of habitats (Prum *et al.*, 2015). There are some bird families that have a high proportion of color polymorph species (Strigiformes, Galliformes, Cuculiformes, and Pelecaniformes: Ardeidae) (Galeotti *et al.*, 2003). Among these, Ardeidae, the heron species, typically are dimorphic- they have two completely distinct morph colors in most color polymorph species (Hancock, 1999)- and are broadly geographically distributed (Hancock and Kushlan, 1984), making them a model system for investigating the evolution of color polymorphism (Green, 2006; Hill and Green, 2011; Shahrokhi and Patten, 2022). The different morphs of heron species have been compared in terms of their life history attributes (e.g., foraging), survivorship, and fitness (e.g., Green et al., 2011; Holderby et al., 2012; Bates and Ballard, 2014). However, a genetic comparison of avian color morphs has yet to be conducted.

In this study, we investigated the genomic differentiation between the morphs of two dimorphic herons, the Western Reef Heron (*Egretta gularis*) and Dimorphic Egret (*Egretta dimorpha*). Since Chapin (1932) deemed them as distinct species, controversy among ornithologists has arisen as to whether these birds should be considered as single species (and, thus, represent

subspecies) or separate species (Hancock and Kushlan, 1984; Dowsett and Dowset-Lemaire, 1993; Dickinson, 2003). However, following Dickinson (2003), in this study the two are considered as distinct species.

Western Reef Herons have a broad geographic distribution, found in the coasts of East and West Africa, the Red Sea, the Persian Gulf, and Southern India (Mock, 1980; Brown, Urban and Newman, 1992; Etezadifar and Amini, 2010). The Dimorphic Egret has a narrower range (Kushlan and Hancock, 2005), distributed along the coasts of Kenya and Tanzania to Madagascar, and nearby islands (Brown *et al.*, 1992; Zimmerman, Turner and Pearson, 1996). Both species are color dimorph, either completely white or completely dark grey (Hancock and Kushlan, 1984). Whereas the morphs of both species have been observed in all regions of their distribution in the same groups (Recher, 1972), they occur in different proportions (Etezadifar and Amini, 2010). Thus, these two species are excellent model organisms for investigating the genes responsible for maintaining color polymorphism.

The aim of our study was to identify differences, if they exist, across the genomes of different color morphs of Western Reef Heron and Dimorphic Egret from different populations. We hypothesized that variation is homologous and predates morph divergence in both species. Specifically, we expected to observe high variation among morphs near loci that contribute to melanin pigmentation, and low differentiation across the genome between populations of each species. We also compared population structure within each named species and across species complexes, to understand how variation in gene flow might contribute to persistence of two color morphs in both species.

Methods

Sample Collection

We sampled toepad tissues (10-15 g) from 52 museum specimens of Western Reef Heron (*Egretta gularis*) and Dimorphic Egret (*Egretta dimorpha*) from American Museum Natural History that were collected between the years 1870 - 1910. Geographic sampling focused on birds preserved from localities where both color morphs of a species were present (Figure 3. 1). In total, 11 samples of Western Reef Heron (8 samples from São Tomé and Príncipe: 5 dark and 3 white; and 3 samples from Somalia: 1 dark and 2 white) and 41 samples of Dimorphic Egret (26 samples from Madagascar: 15 dark and 11 white; 14 samples from Aldabra Island of Seychelles: 8 dark and 6 white; 2 samples from Tanzania: 1 dark and 1 white) (Table 3. 1 and Table S 3. 1).

Laboratory Facility

DNA extraction and library preparation were performed in the ancient DNA (aDNA) laboratory at the University of Oklahoma's Laboratories of Molecular Anthropology and Microbiome Research (LMAMR). This laboratory is designed for processing aged and highly degraded DNA samples, including historical or ancient DNA and samples expected to yield low copy number. Precautions are taken in this workspace to minimize contamination.

DNA Extraction

We followed the protocol of Kemp et al. (2014) to extract DNA from each sample. Approximately 3-4 g of dried samples were removed from the whole and transferred to 1.5 mL tubes filled with 500 µL 0.5 M EDTA (pH 8.0) and rocked gently at room temperature for 48 hours. A negative extraction control was included with each batch of extractions at a ratio of 1:7 with the samples. To each tube, 90 µL of proteinase K (BIOBASIC cat # 32,181) at a

concentration of 1 mg/30 µl (or >20 units/30 µl) were added to each sample following EDTA incubation, and the tubes were incubated at 64-65°C for 3 hours. After proteinase K digestion, the tubes were centrifuged at 15,000 rpm for 1 minute to pellet any undigested tissue and/or non-tissue contaminants from specimen storage. The liquid volumes were then transferred to new 1.5 mL tubes to which 750 µL of 2.5% "resin" (i.e., 2.5% celite in 6 M guanidine HCl) and 250 µL of 6 M guanidine HCl were added. The tubes were vortexed multiple times over approximately 2 minutes.

Next Promega Wizard minicolumns were connected to 3-mL Luer-Lok syringe barrels without plungers and placed on a vacuum manifold. Initially, 3 mL of DNA-free water was drawn across the columns to wash away any potential contaminating DNA. The DNA/resin mixture was then pulled across the columns. The minicolumns with silica on the filter were rinsed by pulling 3 mL of 80% isopropanol across them. After this, excess isopropanol was removed by centrifuging the minicolumns at 10,000 rpm for 2 min in new 1.5 mL tubes. Subsequently, the minicolumns were transferred to new tubes, and 50 µL of DNA-free water, heated to 64-65 °C, was added. The tubes were left for 3 minutes before centrifugation at 10,000 rpm for 30 seconds. This step was repeated one more time, resulting in 100 µL of extracted DNA.

Inhibition Test and Repeat Silica Extraction

The extracted DNA was assessed for PCR inhibitors using the method described by Kemp et al. (2014), with a "turkey collective" used as a positive control. This collective consisted of DNA extracted from multiple archaeological turkey bones (Kemp et al., 2017), which were pooled together to reduce variability in mtDNA copy number and potential inhibitors. The turkey collective was previously shown to consistently amplify in PCR, serving as a reliable control prior to use in experiments (Kemp et al., 2017).

PCR inhibition tests were performed on full-concentration DNA eluates using a 15 µl PCR reaction that amplified a 186 bp section of turkey D-loop with T15709F and T15894R primers (Kemp et al., 2017). These reactions contained 1.5 µL of turkey collective DNA and 1.5 µL of potentially inhibited DNA eluates from the toepads. PCR negative controls and turkey collective DNA-only reactions were included to monitor for contamination and to ensure successful PCR amplification. After 60 cycles of PCR, amplification failure of turkey collective DNA in the presence of any ancient toepad DNA eluate indicated inhibition. Successful amplification of the turkey collective DNA in the presence of an ancient DNA eluate was considered inhibitor-free.

Eluates found to be inhibited were subjected to a repeat silica extraction procedure (Kemp et al., 2014), which involved adding 2.5% resin and 6 M guanidine HCl to the eluate and vortexing the mixture. The same DNA extraction procedure was followed, except that the elution volume matched the extracted volume. The resulting eluates were tested for inhibition, and any eluates still found to be inhibited were subjected to another round of repeat silica extraction and testing until no inhibition was detected in any of the eluates.

Library Construction and Sequencing

The DNA extracts were used to create shotgun libraries with blunt-end dual-indexed Illumina libraries using the BEST (i.e., blunt-end single-tube library building) protocol following Caroe et al. (2017). The BEST method is a widely utilized approach with high efficiency in preparing DNA libraries from highly degraded samples. Initially, the fragmented DNA is repaired using a combination of enzymes to fill in missing nucleotides and remove damaged ones, resulting in longer and higher-quality DNA fragments. Next, the repaired DNA is converted into blunt ends using enzymes that remove any overhanging nucleotides or damaged regions. Blunt ends are

crucial for ligation of adapters to DNA fragments, which is necessary for amplification and sequencing.

In the next step, adapters containing sequences that allow the fragments to be amplified and sequenced were added to the ends of the repaired DNA fragments. Each sample was given a unique index acting as a barcode that enabled multiple samples to be sequenced in a single run while being identified individually. A PCR reaction was then used to amplify the DNA fragments to enrich the library for shorter fragments. The thermocycling conditions began with a single cycle which had a 45 second denaturation at 96°C, followed by 35 cycles consisting of 10 seconds of 98° C, 15 seconds of 60° C, and 30 seconds of 72°C; and a final extension at 72° C for 5 minutes. After a successful amplification, the amplified libraries were purified by using elute in 30 µL of Elution Buffer (EB). The size distribution and concentration of the libraries were assessed through qPCR using 6Kapa Biosystems SYBR® FAST qPCR Master Mix and an Agilent Fragment Analyzer. The dual-indexed shotgun libraries were then pooled in equimolar concentrations and sequenced on an Illumina Hiseq (2X150) at Admera Health, LLC.

Bioinformatics Processing and Data Analyses

Trimmomatic (V 0.39) (Bolger, Lohse and Usadel, 2014) was used to process the raw reads. Trimmomatic performed the following tasks: (1) removal of Illumina adapters from the reads; (2) removal of leading low quality or N bases below a quality score of 25; (3) removal of trailing low quality or N bases below a quality score of 25; (4) scanning the reads with a 4-base window, removing windows when the average quality score dropped below 20; and (5) dropping reads below 50 bp in length. The resulting reads were then mapped against the *Egretta garzetta* genome (GCA_000687185.1_ASM68718v1) using Burrows-Wheeler Aligner (BWA V 0.7.17) (Li and Durbin, 2009). The reads were then cleaned, readgroups were added, and PCR duplicates

were marked and removed using Picard (V 3.0.0) ("Picard ToolKit," 2018) and SAMtools (V 1.13) (Li et al., 2009). Next, single nucleotide polymorphism (SNP) calling was conducted using GATK (V 4.3.0.0) (Depristo et al., 2011) following the GATK Best Practices Workflow. Finally, the data were output in variant call format (VCF) file where vcftools (V 0.1.16) (Danecek et al., 2011) was used to filter data for quality control. The genotype filtering criteria were: (a) minor allele frequency (MAF) of 0.05; (b) maximum missing of 0.5; (c) removal of indels; (d) minimum quality threshold of 30; and (e) minimum and maximum number of alleles per site set to 2.

To ensure the reliability of the sequences and sequence coverage, each sequence file was subset into three separate files to compare the results of the entire data coverage with that of one-third coverage. The entire process of mapping against the reference genome, cleaning, calling the SNPs, and converting to a VCF file was applied independently to each of the data splits. All three resulting VCF files were filtered in two ways. The first method was the same as the original data, while the second was more lenient, including the removal of indels, a minimum quality threshold of 30, and the minimum and maximum number of alleles per site set to 2. This step was applied only to the subsets for the combined dataset (i.e., including both species; see below).

Statistical Analyses

The VCF files generated above were separated into 6 new files by species, color morphs, and locations. These include: (1) both species with mixed location and color morphs, (2) Dimorphic Egret with all locations and color morphs, (3) Dimorphic Egret from Madagascar with mixed color morphs, (4) Dimorphic Egret from Seychelles with mixed color morphs, (5) Western Reef Heron with all locations and mixed color morphs, and (6) Western Reef Heron from Sao Tome with mixed color morphs. All statistical analyses were conducted on all data files.

Identifying Candidate Genes

We tested the degree of genetic differentiation between dark and light morphs of a population using the Weir and Cockerham's F_{ST} index, which ranges from 0 (no differentiation) to 1 (completely different). In this study, values above 0.5 were considered to be indicative of possible fixed loci for populations with a specific coloration. The F_{ST} was calculated from each VCF file using vcftools (Danecek et al., 2011), using a sliding windows approach between each color morph, a window size of 10,000 bp, and a step size of 2,500 bp. The genetic differentiation between SNPs was visualized in R (V 4.2.2) (R Core Team, 2022) in RStudio (RStudio Team, 2020) to generate a Manhattan plot with the *qqman* R package (Turner, n.d.). Loci within high differentiation windows (> 0.5) were identified as candidates, with their corresponding genes and protein products identified from the reference genome (*Egretta garzetta*).

Populations Structure and Comparisons

We performed a principal component analysis (PCA) to visualize population structure by identifying genetic variation across individuals or groups of individuals. PCA identifies the dimensions or axes in the data that explain the most variation among the individuals, ranked according to the amount of variation they explain. First, we pruned our datasets of linked variants to meet the assumption of independently measured variables. To do the linkage pruning, we used PLINK 1.9 (Purcell and Chang, n.d.; Chang et al., 2015) with the following criteria: 50 Kb for the window, 10 bp steps in the window to calculate the linkage, and 0.1 as the r^2 threshold. After pruning the data, we performed PCA using PLINK 1.90 (Purcell and Chang, 2023; Chang et al., 2015) and generated eigenvalues and eigenvector files. To visualize the PCA, we used the *tidyverse* (Wickham et al., 2019) and *plotly* (Plotly Technologies Inc., 2015) R packages. The *tidyverse* package was used for data manipulation and visualization, while the

plotly package was used to create an interactive plot of the PCA results. The interactive plot allows for easy visualization of the relationship between individuals and groups along the principal components.

We used the STRUCTURE version 2.3.4 (Pritchard, Stephens and Donnelly, 2000) program based on the Markov Chain Monte Carlo (MCMC) algorithm to identify both genetic cluster membership and admixture of individuals from the independent-SNPs data. We specified the number of genetic clusters (K) from 1 to 10 and used the admixture model with correlated allele frequencies for each dataset. We conducted 3 independent runs for each K value, with a burn-in of 5,000 and a number of MCMC steps set to 50,000 each. To determine the best K value for each dataset, we used the ΔK method developed by Evanno et al. (2005) and applied it using the Structure Harvester web server (v. 0.6.94) developed by Earl and vonHoldt (2012). After obtaining the optimal K value, we used the program CLUMPP (V 1.1.2b) (Jakobsson and Rosenberg, 2007) to obtain cluster membership coefficients for each individual, which were averaged across the 10 runs.

Weir and Cockerham's (1984) pairwise F_{ST} was also calculated between each geographic population within the larger population. The resulting value ranges between 0 and 1, with 0 indicating no differentiation and 1 indicating complete differentiation. The intermediate values can be useful for assessing the genetic structure of populations and identifying potential barriers to gene flow. To calculate the F_{ST} per population, we performed the analysis in R (V 4.2.2) (R Core Team, 2022) using the *vcfR* (Knaus and Grünwald, 2017), *adegenet* (Jombart, 2008; Jombart and Ahmed, 2011), and *hierfstat* (Goudet, 2005) R packages.

Results

After the first series of filtering, two individual samples (AMNH529988 and AMNH529977: both white morphs of Dimorphic Egret from Seychelles) were excluded due to low quality, resulting in a total of data from 50 samples for analysis with average coverage depth of 6X. In the second series of filtering, we created three datasets: (1) both morphs of Western Reef Heron and Dimorphic Egret combined (referred to below as "dataset 1"); (2) both morphs of both populations of Western Reef Heron (referred to below as "dataset 2"); and (3) all populations of both morphs of Dimorphic Egret (referred to below as "dataset 3") (Table 3. 1).

For the subset files with one-third coverage (2x), the candidate genes and principal components analyses and compared to the original dataset. The graphs of analyses for both filtration methods can be found in the supplementary material (Figure S 3. 1 – Figure S 3. 4).

Identifying Candidate Genes

We calculated Weir and Cockerham F_{ST} between the three datasets described above and used a cutoff of 0.5 to identify nucleotide differences of importance between morphs. In dataset 1, we found a locus with F_{ST} differentiation of 0.55 (Figure 3. 2a), but no genes were present within the assigned window, based on the annotation of the *Egretta garzetta* genome (NCBI: GCA_000687185.1_ASM68718v1). The downstream gene to this window encodes for FCH and double SH3 domains protein 2 (*FCHSD2*), which is involved in various cellular processes, such as endocytosis, and cytoskeleton organization (Salzer, Kostan and Djinović-Carugo, 2017; Carman and Dominguez, 2018; Zhai et al., 2022). The gene upstream of the window encodes for a hypothetical protein (gene ID: gene-Z169_05120) with an unknown function. Similarly, a comparison between morphs in dataset 2 displayed a locus with a higher F_{ST} of approximately 0.7, indicating greater genetic differentiation (Figure 3. 2b). The nearest gene to that window was

Epithelial discoidin domain-containing receptor 1 (*DDR1*), which plays a significant role in cellular processes such as adhesion, migration, and proliferation (Vogel, 1999; Wang et al., 2006; Rammal et al., 2016). Finally, in dataset 3 no differentiation between color morphs was observed, and all scaffolds differentiation fell below the 0.5 threshold (Figure 3. 2c). For the subset datasets, no loci were detected above the 0.5 F_{ST} threshold under either filtration method (Figure S 3. 1 and Figure S 3. 2).

Populations Structure and Comparisons

The PCA plot of the combined dataset of Dimorphic Egret and Western Reef Heron populations, dataset 1, showed that the first two axes accounted for approximately 27% of the variation among populations (Figure 3. 3a). The populations of Madagascar, Seychelles, São Tomé and Príncipe, Tanzania, and Somalia were clustered into three groups, with individuals from the latter two in between. Notably, no differentiation between white and dark morphs was observed in any of the populations. Conversely, the Western Reef Heron dataset, dataset 2, did not exhibit any clustering differentiation between populations or color morphs (Figure 3. 3b). Regarding Dimorphic Egret, dataset 3, the PCA analysis revealed two clusters, with Madagascar displaying most of its variation defined by PC1, and Seychelles with most of its variation defined by PC2. However, no differentiation between dark and white morphs of either species was detected (Figure 3. 3c). In the subset datasets, no differences between the dark and white morphs was detected under either filtration scheme. Population structuring was only detected in the subsets with the relaxed filtering, in which the Western Reef Heron and Dimorphic Egret formed distinct clusters (Figure S 3. 3 and Figure S 3. 4).

To estimate the number of distinct genetic groups and individual admixture, we performed STRUCTURE analysis twice for each dataset, once for the separated color morphs and once for

the mixed morphs. The optimal number of genetic clusters (K) for both versions of the combined dataset was 3, indicating that the individuals could be partitioned into 3 distinct genetic structures (Figure 3. 4a). Specifically, the three demes corresponded to populations from (1) Madagascar, (2) Seychelles and Tanzania, and (3) São Tomé and Príncipe and Somalia. For both the Western Reef Heron and Dimorphic Egret datasets (dataset 2 and 3, respectively), for both separated and mixed morphs, the best K value was 2. However, clear genetic structure was not detected in either dataset (Figure 3. 4b and c).

The comparisons between every two populations indicate the genetic differentiation between populations using F_{ST} estimates. Populations with F_{ST} values < 0.05 or negative were considered to have no genetic differentiation, while values falling between 0.05 and 0.15 were regarded as having moderate genetic differentiation (Cocca et al., 2020). Values > 0.15 indicated high genetic differentiation between populations. The datasets were analyzed in two ways: one with separated morphs and one with mixed morphs.

When analyzing the morphs separately in the combined dataset 1, the genetic differentiation between both morphs of São Tomé and Príncipe and both morphs of Dimorphic Egret in Madagascar and Seychelles is high. The population in Somalia shows moderate genetic variation from Madagascar and Seychelles but low to no variation with Tanzania and São Tomé and Príncipe (Table 3. 2a). However, when analyzing the morphs together, there is significant genetic differentiation between the Western Reef Heron populations (São Tomé and Príncipe and Somalia) and the Dimorphic Egret populations (Madagascar and Seychelles). In both analyses, genetic differentiation between Madagascar and Seychelles populations is low (Table 3. 2b). When Western Reef Heron (São Tomé and Príncipe and Somalia) and Dimorphic Egret (Madagascar, Seychelles, and Tanzania) are considered independently (dataset 2 and dataset 3,

respectively), we detect moderate variation between populations of Western Reef Heron (Table 3. 3a and 3b), and no substantial differentiation between populations of Dimorphic Egret (Table 3. 4a and 4b).

Discussion

In this study, we examined the variation between the genomes of two color morphs within two species belonging to the family Ardeidae, the Western Reef Heron and Dimorphic Egret, to determine the gene(s) responsible, if any, for color variation within these species. We obtained 52 toepad samples of black and white morphs from both species from five populations (São Tomé and Príncipe, Somalia, Madagascar, Seychelles, and Tanzania). From these, DNA from 50 samples yield high quality comparative data with an average sequence depth coverage of 6X, which is comparable to that found in other historical DNA studies for birds (e.g., Wu et al., 2022; Wu et al., 2023). Although two loci showed a high differentiation between the dark and white morphs, we could not find any significant genome-wise differences between the dark and white morph of either species or among any of the five populations, and these two loci were not detected using subsets of the data, even under a more relaxed filtering scheme.

We generated subsets of data to test the reliability of our sequences and the coverage of the original data. Similar to the complete dataset, the subsets did not reveal any differences between the dark and white morphs for either of the species, regardless of the filtration method used. However, under the relaxed filtration, we observed shaped clusters between the Western Reef Heron and Dimorphic Egret, which were not detected under the original filtration. This difference between the filtering methods was due to data and SNP loss under the more restricted filtration. The failure to detect the two outlier loci in any of the subset data may have been due to the fragmented nature of the short-read genomes generated, which can suffer from low genome

coverage or low sequencing depth, resulting in increased sequencing error. Nevertheless, even if the coverage of the original data was insufficient to detect the differences between the dark and white morphs, we were able to detect 50,000 species-specific SNPs, which were lower than the thresholds, and each sequenced spot was detected with the most likelihood in the total of 50 individuals.

In the combined dataset of both species, and in the Western Reef Heron dataset, we identified one 10,000 bp genomic window in each that had a higher F_{ST} than 0.5. In the combined dataset, the FCH and double SH3 domains protein 2 (*FCHSD2*) gene was the closest gene to the selected locus. In humans, this gene regulates clathrin-mediated endocytosis, a process by which cells take up molecules and other substances from the extracellular environment (Katoh and Katoh, 2004). In addition to its role in endocytosis, *FCHSD2* has been implicated in regulating the actin cytoskeleton, a network of protein fibers that provides structural support to cells and is involved in cell movement and shape changes (Carman and Dominguez, 2018). *FCHSD2* is primarily expressed in muscle tissue and has been implicated in several cellular processes related to muscle development and maintenance (Vogel, 1999; Katoh and Katoh, 2004). While *FCHSD2* does not appear to play a direct role in pigmentation or coloration, it is important to note that many genetic and environmental factors can interact to influence this aspect of the phenotype.

In the Western Reef Heron dataset, the nearest gene to the selected locus was Epithelial discoidin domain-containing receptor 1 (*DDR1*). The gene is mainly expressed in epithelial cells and plays a crucial role in regulating various cellular processes such as cell adhesion, migration, differentiation, and proliferation (Vogel, 1999; Chung et al., 2017). *DDR1* has also been shown to regulate the expression of tight junction proteins in epithelial cells and to be involved in wound healing and tissue repair (Olaso et al., 2011; Cario, 2018). Although *DDR1* may be

important in regulating cellular processes in epithelial tissues, there is currently no known function for *DDR1* in plumage formation or in the production or regulation of bird coloration. Despite the likelihood that cell adhesion, migration, differentiation, and proliferation are involved in feather and plumage structure development, there is currently no evidence to suggest that *DDR1* plays a specific role in these processes (Chuong, 1993).

The loci close to *FCHSD2* and *DDR1* genes showed higher differentiation between the dark and white morphs than other loci in the two datasets. However, their functional involvement in plumage structure or coloration is unknown to the best of our knowledge. This uncertainty is evident in the principal component analysis (PCA), pairwise F_{ST} comparison between populations, and STRUCTURE analysis, which show no genomic differentiation between the dark and white morphs in any datasets or populations. In the PCA, no distinct clusters are detected between the dark and white morphs in any datasets. However, the combined dataset reveals some population clustering, with two clusters for the Dimorphic Egret (Madagascar and Seychelles) and one for the Western Reef Heron. The two clusters of the Dimorphic Egret can also be seen in the PCA of the Dimorphic Egret dataset. The clusters suggest population differentiation between both species and among populations of Dimorphic Egret.

The STRUCTURE results align with the findings from PCA, which show geographic structure between species but no differences between the dark and white morphs in any of the datasets. In the combined dataset, three distinct structures are evident, corresponding to Madagascar, Seychelles, and a combined group of São Tomé and Príncipe, as well as Somalia. However, there is no structural differentiation between populations in the Dimorphic Egret dataset. Interestingly, the individuals from Tanzania show a Western Reef Heron-like clustering in the STRUCTURE analyses, which is inconsistent with the PCA results. This inconsistency could be due to the

small sample size or potential misidentification of the bird species. Dimorphic Egrets and Western Reef Herons are morphologically similar, with slight differences in body size and tarsus color, and their ranges overlap in some locations along the coast of East Africa. Therefore, collecting more samples from Tanzania would help to resolve these conflicting results.

The pairwise F_{ST} analyses revealed no significant differences between the dark and white morphs in any datasets. However, within the combined dataset, there was a high level of genetic differentiation between São Tomé and Príncipe and Madagascar and Seychelles, which is consistent with the results of the PCA and STRUCTURE analyses. The genetic variation observed between Tanzania and Somalia, and other populations may be due to the small sample size. It is worth noting that the pairwise F_{ST} analyses are sensitive to sample size, whereas the STRUCTURE analysis, which is based on a Bayesian approach, is less so (Qu et al., 2020). Therefore, more samples would potentially help to resolve the relationships between these populations.

The genetic differentiation between Western Reef Heron and Dimorphic Egret in the different analyses is consistent with the scenario of low level of gene flow. This pattern supports their treatment as an independent and separate species. However, the lack of genetic variation between populations of each species in the species-specific datasets (Western Reef Heron and Dimorphic Egret) indicates sufficient gene flow among populations within each species' range to result in homogeneity. Such gene flow could result from either long-distance migration or stepping-stone movement via unsampled populations. Although these species are not considered long-distance migratory species, some reports of long-distance movement exist. Individual dark morphs of Western Reef Heron have been identified in North and South America in various locations, including the eastern coast of Trinidad, Nantucket Island in Massachusetts, and Brazil, during the

last 20 years (ANONYMOUS, 1983; Murphy and Nanan, 1987; Elisa Fedrizzi, Vaske Júnior and Bugoni, 2007). Thus, it is possible that individuals of the Western Reef Heron dispersed from western Africa (São Tomé and Príncipe) to the east side of the continent (Somalia) or vice versa. However, gene flow may also occur via a stepping-stone movement between east and west via unsampled populations, potentially via coastal areas of North Africa. The third potential explanation for the lack of differentiation may be high gene flow between the color morphs, with individuals of different plumage color interbreeding often enough to swamp tendencies toward fixation. Pure plumage coloration is more common within both species. However, intermediate individuals with varying degrees of white and gray coloration have been recorded in both species (Hancock and Kushlan, 1984). More comprehensive geographic sampling will be needed to differentiate among these gene flow scenarios.

Our failure to detect differentiation among color morphs in genes expected to be involved in plumage coloration is harder to explain. The plumage coloration trait among these species is likely polygenic, with many genes contributing to the final phenotype (Mackay, 2014), resulting in lack of fixation of a few focal genes. In Korean domestic chickens (*Gallus gallus domesticus*), plumage coloration is a polygenic trait that is not related to well-known pigmentation genes, such as MC1R, TYR, PMEL, MLPH, ASIP, etc. (Park et al., 2013). Plumage coloration in Swainson's thrush (*Catharus ustulatus*) may also be polygenic, with strong associations of related genes on the Z sex chromosome, including SNPS linked to TYRP1 (Delmore et al., 2016). These examples support the possibility that plumage coloration may be a polygenic trait in Western Reef Heron and Dimorphic Egret.

In conclusion, although our results support the continued treatment of Western Reef Heron and Dimorphic Egret as distinct taxa, we were unable to detect significant genomic differentiation

between dark and white morphs for either species. Possible explanations for this finding include high gene flow between color morphs within each species, or that plumage coloration may be a polygenic trait in both Western Reef Heron and Dimorphic Egret. The white plumage coloration is typical among Egrets and has emerged multiple times through independent events (Sibley and Ahlquist, 1990; Sheldon, Mccracken and Stuebing, 1995; Hruska *et al.*, 2023). This plumage history supports the possibility of polygenic control of plumage coloration as a driver of our results, rather than gene flow among the morphs. However, analyzing fresh and modern samples from both studied and new populations, for both color morphs and species, will help to clarify these species' complex mechanisms of pigmentation and coloration, gene flow, and genomic structure.

References

Aguillon, S. M., Walsh, J., and Lovette, I. J. (2021). Extensive hybridization reveals multiple coloration genes underlying a complex plumage phenotype. Proceedings of the Royal Society B: Biological Sciences, 288(1943). https://doi.org/10.1098/rspb.2020.1805

ANONYMOUS. (1983). An intriguing footnote to sightings of a Western Reef Heron on Nantucket Island, Massachusetts. Birds, 5, 1032.

Bates, E. M., and Ballard, B. M. (2014). Factors influencing behavior and success of foraging Reddish Egrets (Egretta rufescens). Waterbirds, 37(2), 191–202. https://doi.org/10.1675/063.037.0213

Bennett, D. C., and Lamoreux, M. L. (2003). The color loci of mice - A genetic century. Pigment Cell Research, 16(4), 333–344. https://doi.org/10.1034/j.1600-0749.2003.00067.x

Bolger, A. M., Lohse, M., and Usadel, B. (2014). Trimmomatic: A flexible trimmer for Illumina sequence data. Bioinformatics, 30(15), 2114–2120. https://doi.org/10.1093/bioinformatics/btu170

Bortolotti, G. R. (2006). Natural selection and coloration: Protection, concealment, advertisement, or deception? In G. E. Hill and K. J. McGraw (Eds.), Bird coloration (Vol. 2, pp. 3–35). Harvard University Press.

Bourgeois, Y. X. C., Bertrand, J. A. M., Delahaie, B., Cornuault, J., Duval, T., Milá, B., and Thébaud, C. (2016). Candidate gene analysis suggests untapped genetic complexity in melanin-based pigmentation in birds. Journal of Heredity, 107(4), 327–335. https://doi.org/10.1093/jhered/esw017

Bourgeois, Y. X. C., Delahaie, B., Gautier, M., Lhuillier, E., Malé, P. J. G., Bertrand, J. A. M., Cornuault, J., Wakamatsu, K., Bouchez, O., Mould, C., Bruxaux, J., Holota, H., Milá, B., and Thébaud, C. (2017). A novel locus on chromosome 1 underlies the evolution of a melanic plumage polymorphism in a wild songbird. Royal Society Open Science, 4(2), 160805. https://doi.org/10.1098/rsos.160805

Brown, L. H., Urban, E. K., and Newman, K. B. (2020). The Birds of Africa: Vol. I. Bloomsbury Publishing.

Calsbeek, R., and Sinervo, B. (2007). Correlational selection on lay date and life-history traits: Experimental manipulations of territory and nest site quality. Evolution, 61(5), 1071–1083. https://doi.org/10.1111/j.1558-5646.2007.00098.x

Campagna, L., Repenning, M., Silveira, L. F., Fontana, C. S., Tubaro, P. L., and Lovette, I. J. (2017). Repeated divergent selection on pigmentation genes in a rapid finch radiation. Science Advances, 3(5), 1–12. https://doi.org/10.1126/sciadv.1602404

Cario, M. (2018). DDR1 and DDR2 in skin. Cell Adhesion and Migration, 12(4), 386–393. https://doi.org/10.1080/19336918.2018.1485618

Carman, P. J., and Dominguez, R. (2018). BAR domain proteins—a linkage between cellular membranes, signaling pathways, and the actin cytoskeleton. In Biophysical Reviews (Vol. 10, Issue 6, pp. 1587–1604). Springer Verlag. https://doi.org/10.1007/s12551-018-0467-7

Carøe, C., Gopalakrishnan, S., Vinner, L., Mak, S. S. T., Sinding, M. H. S., Samaniego, J. A., Wales, N., Sicheritz-Pontén, T., and Gilbert, M. T. P. (2017). Single-tube library preparation for degraded DNA. Methods in Ecology and Evolution, 9(2), 410–419. https://doi.org/10.1111/2041-210X.12871

Chang, C. C., Chow, C. C., Tellier, L. C. A. M., Vattikuti, S., Purcell, S. M., and Lee, J. J. (2015). Second-generation PLINK: Rising to the challenge of larger and richer datasets. GigaScience, 4(1). https://doi.org/10.1186/s13742-015-0047-8

Chapin, J. P. (1932). The birds of the Belgian Congo. Part I. Bulletin American Museum of Natural History, 415–417.

Chung, V. Y., Tan, T. Z., Huang, R. L., Lai, H. C., and Huang, R. Y. J. (2017). Loss of discoidin domain receptor 1 (DDR1) via CpG methylation during EMT in epithelial ovarian cancer. Gene, 635, 9–15. https://doi.org/10.1016/j.gene.2017.09.001

Chuong, C. -M. (1993). The making of a feather: Homeoproteins, retinoids and adhesion molecules. In BioEssays (Vol. 15, Issue 8, pp. 513–521). https://doi.org/10.1002/bies.950150804

Cocca, M., Barbieri, C., Concas, M. P., Robino, A., Brumat, M., Gandin, I., Trudu, M., Sala, C. F., Vuckovic, D., Girotto, G., Matullo, G., Polasek, O., Kolčić, I., Gasparini, P., Soranzo,

N., Toniolo, D., and Mezzavilla, M. (2020). A bird's-eye view of Italian genomic variation through whole-genome sequencing. European Journal of Human Genetics, 28(4), 435–444. https://doi.org/10.1038/s41431-019-0551-x

Cracraft, J., Barker, F. K., Braun, M., Harshman, J., Dyke, G., Feinstein, J., Stanley, S., Cibois, A., Schikler, P., Beresford, P., García-moreno, J., Sorenson, M. D., Yuri, T., and Mindell, D. P. (2004). Phylogenetic relationships among modern birds (Neornithes): toward an avian tree of life. Assembling the Tree of Life, August, 468–489.

Danecek, P., Auton, A., Abecasis, G., Albers, C. A., Banks, E., DePristo, M. A., Handsaker, R. E., Lunter, G., Marth, G. T., Sherry, S. T., McVean, G., and Durbin, R. (2011). The variant call format and VCFtools. Bioinformatics, 27(15), 2156–2158. https://doi.org/10.1093/bioinformatics/btr330

Delmore, K. E., Toews, D. P. L., Germain, R. R., Owens, G. L., and Irwin, D. E. (2016). The genetics of seasonal migration and plumage color. Current Biology, 26(16), 2167–2173. https://doi.org/10.1016/j.cub.2016.06.015

Depristo, M. A., Banks, E., Poplin, R., Garimella, K. v., Maguire, J. R., Hartl, C., Philippakis, A. A., del Angel, G., Rivas, M. A., Hanna, M., McKenna, A., Fennell, T. J., Kernytsky, A. M., Sivachenko, A. Y., Cibulskis, K., Gabriel, S. B., Altshuler, D., and Daly, M. J. (2011). A framework for variation discovery and genotyping using next-generation DNA sequencing data. Nature Genetics, 43(5), 491–501. https://doi.org/10.1038/ng.806

Dickinson, E. C. (2003). The Howard and Moore Complete Checklist of the Birds of the World (Third). Christopher Helm.

Dowsett, R. J., and Dowset-Lemaire, F. (1993). Comments on the taxonomy of some Afrotopical bird species. Tauraco Research Report, 5, 323–389.

Earl, D. A., and vonHoldt, B. M. (2012). STRUCTURE HARVESTER: A website and program for visualizing STRUCTURE output and implementing the Evanno method. Conservation Genetics Resources, 4(2), 359–361. https://doi.org/10.1007/s12686-011-9548-7

Elisa Fedrizzi, C., Vaske Júnior, T., and Bugoni, L. (2007). Western Reef-Heron Egretta gularis in Brazil (Ciconiiformes: Ardeidae) Arrebentação View project ATUNA-Projeto de

Implantação de Atratores de Tunídeos e Afins em Meia água na Plataforma Externa do Litoral de Pernambuco View project. Revista Brasileira de Ornitologia, 15(3), 481–483. https://www.researchgate.net/publication/228978327

Enshell-Seijffers, D., Lindon, C., and Morgan, B. A. (2008). The serine protease Corin is a novel modifier of the agouti pathway. Development, 135(2), 217–225. https://doi.org/10.1242/dev.011031

Etezadifar, F., and Amini, H. (2010). Current status of the breeding population of the Western Reef Heron (Egretta gularis) along the northern coasts of the Persian Gulf and Oman Sea, and its wintering population in the south of Iran. Heron, 5(2), 71–80.

Evanno, G., Regnaut, S., and Goudet, J. (2005). Detecting the number of clusters of individuals using the software STRUCTURE: A simulation study. Molecular Ecology, 14(8), 2611–2620. https://doi.org/10.1111/j.1365-294X.2005.02553.x

Friedman, N. R., and Remeš, V. (2017). Ecogeographical gradients in plumage coloration among Australasian songbird clades. Global Ecology and Biogeography, 26(3), 261–274. https://doi.org/10.1111/geb.12522

Galeotti, P., Rubolini, D., Dunn, P. O., and Fasola, M. (2003). Colour polymorphism in birds: Causes and functions. Journal of Evolutionary Biology, 16, 635–645. https://doi.org/10.1046/j.1420-9101.2003.00569.x

Goudet, J. (2005). HIERFSTAT, a package for R to compute and test hierarchical F-statistics. Molecular Ecology Notes, 5, 184–186. https://doi.org/10.1111/j.1471-8278

Green, M. C. (2006). Status Report and survey recommendations on the Reddish Egret (Egretta rufescens). U.S. Fish and Wildlife Service, Atlanta, GA., 37pp.

Green, M. C., Hill, A., Troy, J. R., Holderby, Z., and Geary, B. (2011). Status of breeding Reddish Egrets on Great Inagua, Bahamas with comments on breeding Territoriality and the effects of hurricanes. Waterbirds, 34(2), 213–217.

Haas, F., Pointer, M. A., Saino, N., Brodin, A., Mundy, N. I., and Hansson, B. (2009). An analysis of population genetic differentiation and genotype-phenotype association across

the hybrid zone of carrion and hooded crows using microsatellites and MC1R. Molecular Ecology, 18(2). https://doi.org/10.1111/j.1365-294X.2008.04017.x

Hancock, J. (1999). Herons and Egrets of the World. Academic Press.

Hancock, J., and Kushlan, J. A. (2010). The Herons Handbook. Bloomsbury Publisher.

Herrera, M. S., Kuhn, W. R., Lorenzo-carballa, M. O., Harding, K. M., Ankrom, N., Sherratt, T. N., Hoffman, J., Gossum, H. Van, Ware, J. L., Cordero-Rivera, A., and Beatty, C. D. (2015). Mixed signals? Morphological and molecular evidence suggest a color polymorphism in some neotropical polythore damselflies. PloS One, 10(4). https://doi.org/hhttps://doi.org/10.1371/journal.pone.0125074

Hill, A., and Green, M. C. (2011). Characterization of 12 polymorphic microsatellites for the Reddish Egret, (Egretta rufescens). Conservation Genetics Resources, 3(1), 13–15. https://doi.org/10.1007/s12686-010-9267-5

Hill, G. E., and McGraw, K. J. (2006a). Bird Coloration. Vol. 1. Mechanisms and Measurement. Harvard University Press.

Hill, G. E., and McGraw, K. J. (2006b). Bird Coloration. Vol. 2. Function and Evolution. Harvard University Press.

Hiragaki, T., Inoue-Murayama, M., Miwa, M., Fujiwara, A., Mizutani, M., Minvielle, F., and Ito, S. (2008). Recessive black is allelic to the yellow plumage locus in Japanese quail and associated with a frameshift deletion in the ASIP gene. Genetics, 178(2), 771–775. https://doi.org/10.1534/genetics.107.077040

Holderby, Z., Simper, W., Geary, B., and Clay, M. (2012). Potential factors affecting nest initiation date, clutch size and nest success in the plumage dimorphic Reddish Egret potential factors. Waterbirds, 35(3), 437–442.

Hruska, J. P., Holmes, J., Oliveros, C., Shakya, S., Lavretsky, P., McCracken, K. G., Sheldon, F. H., and Moyle, R. G. (2023). Ultraconserved elements resolve the phylogeny and corroborate patterns of molecular rate variation in herons (Aves: Ardeidae). Ornithology, 1–41. https://doi.org/10.1093/ornithology/ukad005

Hubbard, J. K., Uy, J. A. C., Hauber, M. E., Hoekstra, H. E., and Safran, R. J. (2010). Vertebrate pigmentation: from underlying genes to adaptive function. Trends in Genetics, 26(5). https://doi.org/10.1016/j.tig.2010.02.002

Jackson, I. J., Chambers, D. M., Tsukamoto, K., Copeland, N. G., Gilbert, D. J., Jenkins, N. A., and Hearing, V. (1992). A second tyrosinase-related protein, TRP-2, maps to and is mutated at the mouse slaty locus. EMBO Journal, 11(2), 527–535. https://doi.org/10.1002/j.1460-2075.1992.tb05083.x

Jakobsson, M., and Rosenberg, N. A. (2007). CLUMPP: A cluster matching and permutation program for dealing with label switching and multimodality in analysis of population structure. Bioinformatics, 23(14), 1801–1806. https://doi.org/10.1093/bioinformatics/btm233

Jombart, T. (2008). Adegenet: A R package for the multivariate analysis of genetic markers. Bioinformatics, 24(11), 1403–1405. https://doi.org/10.1093/bioinformatics/btn129

Jombart, T., and Ahmed, I. (2011). adegenet 1.3-1: New tools for the analysis of genome-wide SNP data. Bioinformatics, 27(21), 3070–3071. https://doi.org/10.1093/bioinformatics/btr521

Katoh, M., and Katoh, M. (2004). Identification and characterization of human FCHSD1 and FCHSD2 genes in silico. International Journal of Molecular Medicine, 13(5), 749–754. https://doi.org/10.3892/ijmm.13.5.749

Kemp, B. M., Judd, K., Monroe, C., Eerkens, J. W., Hilldorfer, L., Cordray, C., Schad, R., Reams, E., Ortman, S. G., and Kohler, T. A. (2017). Prehistoric mitochondrial DNA of domesticate animals supports a 13th century exodus from the northern US southwest. PLoS ONE, 12(7). https://doi.org/10.1371/journal.pone.0178882

Kemp, B. M., Monroe, C., Judd, K. G., Reams, E., and Grier, C. (2014). Evaluation of methods that subdue the effects of polymerase chain reaction inhibitors in the study of ancient and degraded DNA. Journal of Archaeological Science, 42(1), 373–380. https://doi.org/10.1016/j.jas.2013.11.023

Kingsley, E. P., Manceau, M., Wiley, C. D., and Hoekstra, H. E. (2009). Melanism in Peromyscus is caused by independent mutations in Agouti. PLoS ONE, 4(7). https://doi.org/10.1371/journal.pone.0006435

Knaus, B. J., and Grünwald, N. J. (2017). vcfr: a package to manipulate and visualize variant call format data in R. Molecular Ecology Resources, 17(1), 44–53. https://doi.org/10.1111/1755-0998.12549

Kushlan, J. A., and Hancock, J. (2005). 14. The Herons: Ardeidea (Bird Families of the World). In Bird Families of the World (pp. xv–433). Oxford University Press.

Laaksonen, T., Sirkiä, P. M., Calhim, S., Brommer, J. E., Leskinen, P. K., Primmer, C. R., Adamík, P., Artemyev, A. v., Belskii, E., Both, C., Bureš, S., Burgess, M. D., Doligez, B., Forsman, J. T., Grinkov, V., Hoffmann, U., Ivankina, E., Král, M., Krams, I., … Sokolov, L. (2015). Sympatric divergence and clinal variation in multiple coloration traits of Ficedula flycatchers. Journal of Evolutionary Biology, 28(4), 779–790. https://doi.org/10.1111/jeb.12604

Lamason, R. L., Manzoor-Ali, P. K., Mohideen, Mest, J. R., and Wong, A. C. (2005). SLC24A5, a Putative Cation Exchanger, Affects Pigmentation in Zebrafish and Humans. Sceince, 310, 1782–1786.

Li, H., and Durbin, R. (2009). Fast and accurate short read alignment with Burrows-Wheeler transform. Bioinformatics, 25(14), 1754–1760. https://doi.org/10.1093/bioinformatics/btp324

Li, H., Handsaker, B., Wysoker, A., Fennell, T., Ruan, J., Homer, N., Marth, G., Abecasis, G., and Durbin, R. (2009). The sequence alignment/map format and SAMtools. Bioinformatics, 25(16), 2078–2079. https://doi.org/10.1093/bioinformatics/btp352

Lopes, R. J. J., Johnson, J. D. D., Toomey, M. B. B., Ferreira, M. S. S., Araujo, P. M. M., Melo-Ferreira, J., Andersson, L., Hill, G. E. E., Corbo, J. C. C., and Carneiro, M. (2016). Genetic basis for red coloration in birds. Current Biology, 26(11). https://doi.org/10.1016/j.cub.2016.03.076

Mackay, T. F. C. (2014). Epistasis and quantitative traits: Using model organisms to study gene-gene interactions. Nature Reviews Genetics, 15(1), 22–33. https://doi.org/10.1038/nrg3627

Manceau, M., Domingues, V. S., Linnen, C. R., Rosenblum, E. B., and Hoekstra, H. E. (2010). Convergence in pigmentation at multiple levels: Mutations, genes and function. Philosophical Transactions of the Royal Society B: Biological Sciences, 365(1552), 2439–2450. https://doi.org/10.1098/rstb.2010.0104

McKinnon, J. S., and Pierotti, M. E. R. (2010). Colour polymorphism and correlated characters: Genetic mechanisms and evolution. Molecular Ecology, 19(23), 5101–5125. https://doi.org/10.1111/j.1365-294X.2010.04846.x

Minvielle, F., Gourichon, D., Ito, S., Inoue-Murayama, M., and Riviè, S. (2007). Effects of the dominant lethal yellow mutation on reproduction, growth, feed consumption, body temperature, and body composition of the Japanese Quail. Poultry Science Association Inc., 86, 1646–1650.

Mock, D. W. (1980). White-dark polymorphism in herons. Proceedings of the First Welder Wildlife Foundation Symposium, 1, 145–161.

Mullen, L. M., and Hoekstra, H. E. (2008). Natural selection along an environmental gradient: A classic cline in mouse pigmentation. Evolution: International Journal of Organic Evolution, 62(7), 1555–1570. https://doi.org/10.1111/j.1558-5646.2008.00425.x

Mundy, N. I. (2005). A window on the genetics of evolution: MC1R and plumage colouration in birds. Proceedings of the Royal Society, 272(1573), 1633–1640.

Mundy, N. I., Badcock, N. S., Hart, T., Scribner, K., Janssen, K., and Nadeau, N. J. (2004). Conserved Genetic Basis of a Quantitative Plumage Trait Involved in Mate Choice. Science, 303(5665). https://doi.org/10.1126/science.1093834

Murphy, W. L., and Nanan, W. (1987). First confirmed record of Western Reef-Heron (Egretta gularis) for South America. American Birds, 41, 392–394.

Nadeau, N. J., Minvielle, F., Ito, S., Inoue-Murayama, M., Gourichon, D., Follett, S. A., Burke, T., and Mundy, N. I. (2008). Characterization of Japanese quail yellow as a genomic

deletion upstream of the avian homolog of the mammalian ASIP (agouti) gene. Genetics, 178(2), 777–786. https://doi.org/10.1534/genetics.107.077073

Nadeau, N. J., Mundy, N. I., Gourichon, D., and Minvielle, F. (2007). Association of a single-nucleotide substitution in TYRP1 with roux in Japanese quail (Coturnix japonica). Animal Genetics, 38(6), 609–613. https://doi.org/10.1111/j.1365-2052.2007.01667.x

Olaso, E., Lin, H. C., Wang, L. H., and Friedman, S. L. (2011). Impaired dermal wound healing in discoidin domain receptor 2-deficient mice associated with defective extracellular matrix remodeling. Fibrogenesis and Tissue Repair, 4(1). https://doi.org/10.1186/1755-1536-4-5

Orteu, A., and Jiggins, C. D. (2020). The genomics of coloration provides insights into adaptive evolution. In Nature Reviews Genetics (Vol. 21, Issue 8). https://doi.org/10.1038/s41576-020-0234-z

Park, M. N., Choi, J. A., Lee, K. T., Lee, H. J., Choi, B. H., Kim, H., Kim, T. H., Cho, S., and Lee, T. (2013). Genome-wide association study of chicken plumage pigmentation. Asian-Australasian Journal of Animal Sciences, 26(11), 1523–1528. https://doi.org/10.5713/ajas.2013.13413

Picard ToolKit (3.0.0). (2018). Broad Institute. broadinstitute.github.io/picard/

Plotly Technologies Inc. (2015). Collaborative Data Science. Plotly Technologies Inc. https://plot.ly

Poelstra, J. W., Vijay, N., Bossu, C. M., Lantz, H., Ryll, B., Müller, I., Baglione, V., Unneberg, P., Wikelski, M., Grabherr, M. G., Wolf, J. B. W., Muller, I., Baglione, V., Unneberg, P., Wikelski, M., Grabherr, M. G., Wolf, J. B. W., Müller, I., Baglione, V., … Wolf, J. B. W. (2014). The genomic landscape underlying phenotypic integrity in the face of gene flow in crows. Science, 344(6190), 1410–1414. https://doi.org/10.1126/science.1253226

Poelstra, J. W., Vijay, N., Hoeppner, M. P., and Wolf, J. B. W. (2015). Transcriptomics of colour patterning and coloration shifts in crows. Molecular Ecology, 24(18), 4617–4628. https://doi.org/10.1111/mec.13353

Pritchard, J. K., Stephens, M., and Donnelly, P. (2000). Inference of population structure using multilocus genotype data. Genetics, 155(2), 945–959. https://doi.org/10.1111/j.1471-8286.2007.01758.x

Prum, R. O., Berv, J. S., Dornburg, A., Field, D. J., Townsend, J. P., Lemmon, E. M., and Lemmon, A. R. (2015). A comprehensive phylogeny of birds (Aves) using targeted next-generation DNA sequencing. Nature, 526(7574), 569–573. https://doi.org/10.1038/nature15697

Purcell, S., Neale, B., Todd-Brown, K., Thomas, L., Ferreira M. A. R., Bender, D., Maller, J., Sklar, P., de Bakker, P. I. W., Daly, M. J., and Sham, P. C. (2007). Plink: A tool set for whole-genome association and population-based linkage analyses. The American Journal of Human Genetics, 81(3), 559–575. https://doi.org/10.1086/519795

Qu, W., Liang, N., Wu, Z., Zhao, Y., and Chu, D. (2020). Minimum sample size for invasion genomics: Empirical investigation in an invasive whitefly. Ecology and Evolution, 10(1), 38-49. https://doi.org/10.1002/ece3.5677

R Core Team. (2022). R: A language and environment for statistical computing. In R: A language and environment for statistical computing. R Foundation for Statistical Computing, Vienna, Austria. URL http://www. R-project. org (4.2.2). R Foundation for Statistical Computing. https://www.r-project.org/.

Rammal, H., Saby, C., Magnien, K., Van-Gulick, L., Garnotel, R., Buache, E., el Btaouri, H., Jeannesson, P., and Morjani, H. (2016). Discoidin domain receptors: Potential actors and targets in cancer. In Frontiers in Pharmacology (Vol. 7, Issue MAR). Frontiers Media S.A. https://doi.org/10.3389/fphar.2016.00055

Rankin, K. J., McLean, C. A., Kemp, D. J., and Stuart-Fox, D. (2016). The genetic basis of discrete and quantitative colour variation in the polymorphic lizard, Ctenophorus decresii. BMC Evolutionary Biology, 16(1), 1–14. https://doi.org/10.1186/s12862-016-0757-2

Recher, H. F. (1972). Colour dimorphism and the ecology of herons. Ibis, 114(4), 552–555. https://doi.org/10.1111/j.1474-919X.1972.tb00859.x

Rogers, A. R., Iltis, D., Wooding, S. (2004) Genetic variation at the MC1R locus and the time since loss of human body hair. Current Anthropology, 45(1), 105-108

Rosenblum, E. B., Hoekstra, H. E., and Nachman, M. W. (2004). Adaptive reptile color variation and the evolution of the MC1R gene. Evolution, 58(8). https://doi.org/10.1111/j.0014-3820.2004.tb00462.x

Roulin, A. (2004). The evolution, maintenance and adaptive function of genetic colour polymorphism in birds. Biological Reviews of the Cambridge Philosophical Society, 79(4), 815–848. http://www.ncbi.nlm.nih.gov/pubmed/15682872

Roulin, A., Emaresi, G., Bize, P., Gasparini, J., Piault, R., and Ducrest, A. L. (2011). Pale and dark reddish melanic tawny owls differentially regulate the level of blood circulating POMC prohormone in relation to environmental conditions. Oecologia, 166(4), 913–921. https://doi.org/10.1007/s00442-011-1955-7

RStudio Team. (2020). RStudio: Integrated Development for R. RStudio, PBC. http://www.rstudio.com/

Salzer, U., Kostan, J., and Djinović-Carugo, K. (2017). Deciphering the BAR code of membrane modulators. Cellular and Molecular Life Sciences, 74(13), 2413–2438. https://doi.org/10.1007/s00018-017-2478-0

San-Jose, L. M., and Roulin, A. (2017). Genomics of coloration in natural animal populations. Philosophical Transactions of the Royal Society B: Biological Sciences, 372(1724). https://doi.org/10.1098/rstb.2016.0337

Sato, S., Otake, T., Suzuki, C., Saburi, J., and Kobayashi, E. (2007). Mapping of the Recessive White Locus and Analysis of the Tyrosinase Gene in Chickens. Poultry Science Association Inc., 86, 2126–2133.

Shahrokhi, G., and Patten, M. A. (2022). Linking plumage dimorphism and environmental stress. Journal of Zoology, 1–9. https://doi.org/10.1111/jzo.12972

Sheldon, F. H., Mccracken, K. G., and Stuebing, K. D. (1995). Phylogenetic Relationships of the Zigzag Heron (Zebrilus undulatus) and White-Crested Bittern (Tigriornis leucolophus) Estimated by DNA-DNA Hybridization. 112(3), 672–679.

Sibley, C. G., and Ahlquist, J. E. (1990). Phylogeny and Classification of the Birds. In Phylogeny and Classification of the Birds. Yale University Press. https://doi.org/10.2307/j.ctt1xp3v3r

Sinervo, B., and Svensson, E. (2002). Correlational selection and the evolution of genomic architecture. In Heredity (Vol. 89, Issue 5, pp. 329–338). https://doi.org/10.1038/sj.hdy.6800148

Song, G., Yu, L., Gao, B., Zhang, R., Qu, Y., Lambert, D. M., Li, S., Zhou, T., and Lei, F. (2013). Gene flow maintains genetic diversity and colonization potential in recently range-expanded populations of an oriental bird, the light-vented bulbul (pycnonotus sinensis, aves: Pycnonotidae). Diversity and Distributions, 19(10), 1248–1262. https://doi.org/10.1111/ddi.12067

Theron, E., Hawkins, K., Bermingham, E., Ricklefs, R. E., and Mundy, N. I. (2001). The molecular basis of an avian plumage polymorphism in the wild: a melanocortin-1-receptor point mutation is perfectly associated with the melanic plumage morph of the bananaquit, Coereba flaveola. Current Biology, 11(8), 550–557. http://www.ncbi.nlm.nih.gov/pubmed/11369199

Turner, S. D. (2014). qqman: an R package for visualizing GWAS results using Q-Q and manhattan plots. Biorxiv, 14(005165). https://doi.org/10.1101/005165

Uy, J. A. C., Moyle, R. G., Filardi, C. E., and Cheviron, Z. A. (2009). Difference in plumage color used in species recognition between incipient species is linked to a single amino acid substitution in the melanocortin-1 receptor. American Naturalist, 174(2). https://doi.org/10.1086/600084

Vogel, W. (1999). Discoidin domain receptors: structural relations and functional implications. The FASEB Journal, 13(9001). https://doi.org/10.1096/fasebj.13.9001.s77

Wang, C. Z., Su, H. W., Hsu, Y. C., Shen, M. R., and Tang, M. J. (2006). A discoidin domain receptor 1/SHP-2 signaling complex inhibits α2β1-integrin-mediated signal transducers and activators of transcription 1/3 activation and cell migration. Molecular Biology of the Cell, 17(6), 2839–2852. https://doi.org/10.1091/mbc.E05-11-1068

Weir, B. S., and Cockerham, C. C. (1984). Estimating F-Statistics for the analysis of population structure. 38(6), 1358–1370.

Wickham, H., Averick, M., Bryan, J., Chang, W., McGowan, L., François, R., Grolemund, G., Hayes, A., Henry, L., Hester, J., Kuhn, M., Pedersen, T., Miller, E., Bache, S., Müller, K., Ooms, J., Robinson, D., Seidel, D., Spinu, V., … Yutani, H. (2019). Welcome to the Tidyverse. Journal of Open Source Software, 4(43), 1686. https://doi.org/10.21105/joss.01686

Wu, M. Y., Forcina, G., Low, G. W., Sadanandan, K. R., Gwee, C. Y., van Grouw, H., Wu, S., Edwards, S. V., Baldwin, M. W., and Rheindt, F. E. (2023). Historic samples reveal loss of wild genotype through domestic chicken introgression during the Anthropocene. PLoS Genetics, 19(1). https://doi.org/10.1371/journal.pgen.1010551

Wu, M. Y., Lau, C. J., Ng, E. Y. X., Baveja, P. Gwee, C. Y., Sadanandan, K., Ferasyi, T. R., Haminuddin, Ramadhan, R., Menner, J. K., and Rheindt F. E. (2022). Genomes From Historic DNA Unveil Massive Hidden Extinction and Terminal Endangerment in a Tropical Asian Songbird Radiation. Molecular Biology and Evolution, 39(9), msac189. https://doi.org/10.1093/molbev/msac189

Yan, W., Sheng, N., Seto, M., Morser, J., and Wu, Q. (1999). Corin, a mosaic transmembrane serine protease encoded by a novel cDNA from human heart. Journal of Biological Chemistry, 274(21), 14926–14935. https://doi.org/10.1074/jbc.274.21.14926

Yaswen, L., Diehl, N., Brennan, M. B., and Hochgeschwender, U. (1999). Obesity in the mouse model of pro-opiomelanocortin deficiency responds to peripheral melanocortin. Nature Medicine, 5(9), 1066–1070.

Zhai, X., Du, H., Shen, Y., Zhang, X., Chen, Z., Wang, Y., and Xu, Z. (2022). FCHSD2 is required for stereocilia maintenance in mouse cochlear hair cells. Journal of Cell Science, 135(16). https://doi.org/10.1242/jcs.259912

Zimmerman, D. A., Turner, D. A., and Pearson, D. J. (1996). Birds of Kenya and northern Tanzania. Princeton University Press. http://agris.fao.org/agris-search/search.do?recordID=US201300075290

Figures and Tables

Table 3. 1. Sample size, number of dark and white morph from five populations for Western Reef Heron (*Egretta gularis*) (WRH) and Dimorphic Egret (*Egretta dimorpha*) (DE). Three defined datasets for analyses with number of SNPs after the filtering for each dataset.

Species	Population	# Samples	# Dark morph	# White morph	Datasets	
Dimorphic Egret (*Egretta dimorpha*)	Madagascar	25	15	10	Dataset 1, Combined: 50 individuals 55,215 SNPs	Dataset 3, DE: 39 individuals 4,521,649 SNPs
	Seychelles	12	8	4		
	Tanzania	2	1	1		
Total Number		39	24	15		
Western Reef Heron (*Egretta gularis*)	São Tomé and Príncipe	7	5	3		Dataset 2, WRH: 11 individuals 6,414,649 SNPs
	Somalia	3	1	2		
Total Number		11	6	5		

Table 3. 2. Pairwise F_{ST} between the populations of Dataset 1 (combined dataset). The top table is key to the threshold of genetic differentiation between the populations. The populations with light blue color indicate the Western Reef Heron (*Egretta gularis*), and the light green color indicates the Dimorphic Egret *(Egretta dimorpha*) populations. (a) Genetic differentiation between the population of Western Reef Heron and Dimorphic Egret with consideration of individuals' plumage coloration. (b) Genetic differentiation between populations of Western Reef Heron and Dimorphic Egret not separated by color morphs.

F_{ST} < 0.05 no genetic differentiation	0.05 =< F_{ST} <= 0.15 Moderate genetic differentiation	F_{ST} > 0.15 High genetic differentiation

a.

	Dark – Somalia	White – Somalia	Dark – Sao Tome	White – Sao Tome	Dark - Madagascar	White - Madagascar	Dark - Seychelles	White - Seychelles	Dark - Tanzania	White - Tanzania
Dark – Somalia										
White – Somalia	0.00									
Dark – Sao Tome	0.06	0.06								
White – Sao Tome	0.04	0.07	0.00							
Dark – Madagascar	0.10	0.08	0.20	0.19						
White – Madagascar	0.15	0.10	0.22	0.21	0.00					
Dark – Seychelles	0.18	0.12	0.26	0.26	0.06	0.06				
White – Seychelles	0.19	0.13	0.27	0.28	0.05	0.06	- 0.12			
Dark – Tanzania	0.00	0.00	0.09	0.08	0.08	0.11	0.14	0.15		
White – Tanzania	0.00	0.00	0.08	0.05	0.07	0.09	0.11	0.13	0.00	

b.

	Somalia	São Tomé and Príncipe	Madagascar	Seychelles	Tanzania
Somalia					
São Tomé and Príncipe	0.09				
Madagascar	0.15	0.22			
Seychelles	0.22	0.28	0.05		
Tanzania	0.02	0.11	0.12	0.19	

Table 3. 3. Pairwise F_{ST} between populations of Dataset 2, Western Reef Heron (*Egretta gularis*). The top table is key to the threshold of genetic differentiation between the populations. (a) Genetic differentiation between the population of Western Reef Heron with consideration of individuals' plumage coloration (b) Genetic differentiation between populations of Western Reef Heron not separated by color morphs.

F_{ST} < 0.05 no genetic differentiation	0.05 =< F_{ST} <= 0.15 Moderate genetic differentiation	F_{ST} > 0.15 High genetic differentiation

a.

	Dark - Somalia	White - Somalia	Dark - São Tomé and Príncipe	White - São Tomé and Príncipe
Dark – Somalia				
White – Somalia	0.43			
Dark - São Tomé and Príncipe	0.53	- 0.04		
White - São Tomé and Príncipe	0.00	- 0.75	- 0.87	

b.

	Somalia	São Tomé and Príncipe
Somalia		
São Tomé and Príncipe	0.07	

Table 3. 4. Pairwise F_{ST} between populations of Dataset 3, Dimorphic Egret (*Egretta dimorpha*). The top table is key to the threshold of genetic differentiation between the populations. (a) Genetic differentiation between the population of Dimorphic Egret with consideration of individuals' plumage coloration (b) Genetic differentiation between populations of Dimorphic Egret not separated by color morphs.

F_{ST} < 0.05 no genetic differentiation	0.05 =< F_{ST} <= 0.15 Moderate genetic differentiation	F_{ST} > 0.15 High genetic differentiation

a.

	Dark - Madagascar	White - Madagascar	Dark - Seychelles	White - Seychelles	Dark - Tanzania	White - Tanzania
Dark – Madagascar						
White – Madagascar	- 0.01					
Dark – Seychelles	0.00	0.00				
White – Seychelles	0.01	- 0.02	0.00			
Dark – Tanzania	- 0.12	- 0.23	- 0.12	- 0.14		
White – Tanzania	- 0.43	- 0.48	- 0.42	- 0.41	0.00	

b.

	Madagascar	Seychelles	Tanzania
Madagascar			
Seychelles	0.00		
Tanzania	- 0.09	- 0.07	

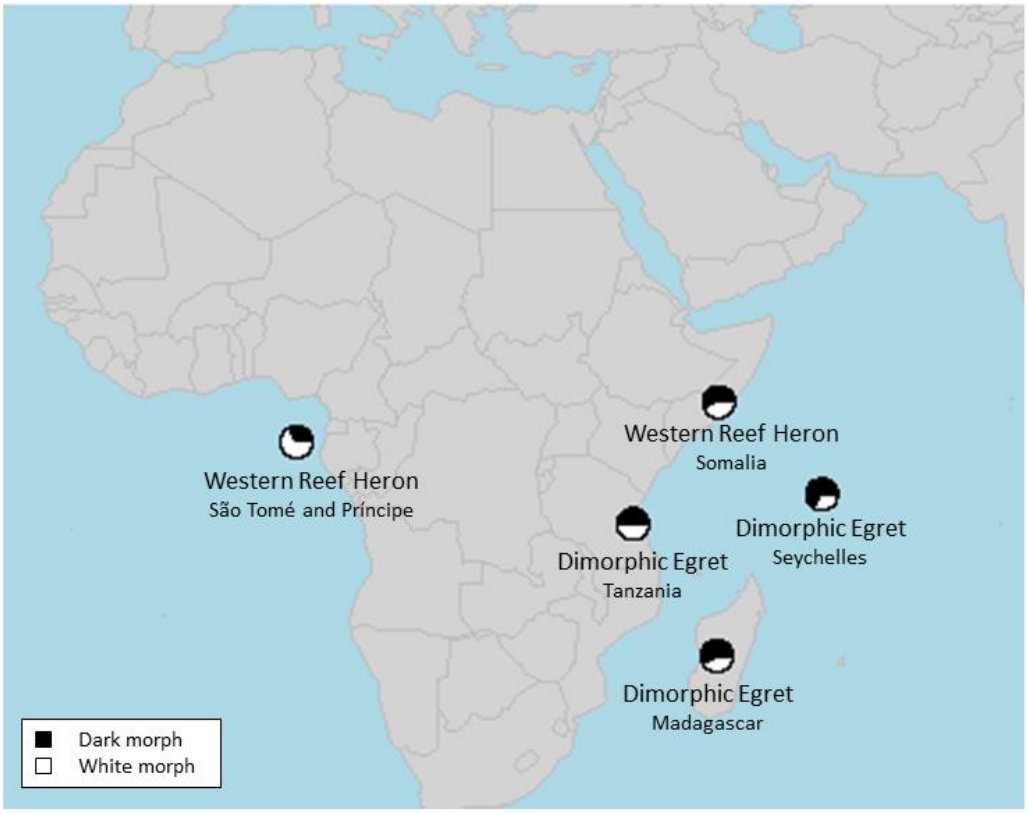

Figure 3. 1. Proportions of dark and white color morphs of Western Reef Heron (*Egretta gularis*) from two populations: São Tomé and Príncipe, Somalia, and Dimorphic Egret (*Egretta dimropha*) from three populations: Madagascar, Seychelles, and Tanzania

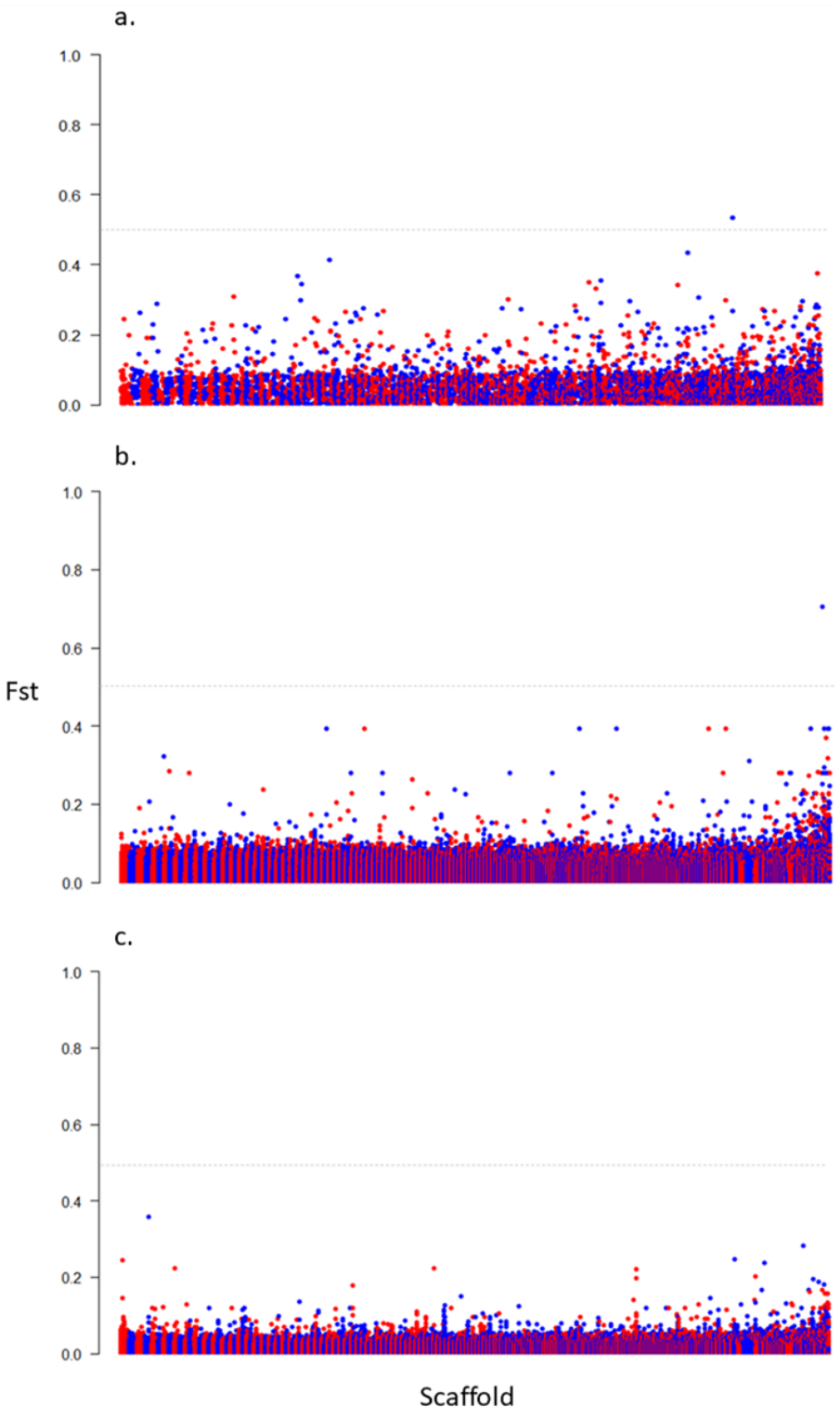

Figure 3. 2. Manhattan plots for (a) Dataset 1, combined; (b) Dataset 2, Western Reef Heron (*Egretta gularis*); and (c) Dataset 3, Dimorphic Egret (*Egretta dimorpha*). Gray line indicates genome-wide significance at F_{ST} 0.5. The locus with F_{ST} >0.5 on figure (a) is associated with FCHSD2 gene and on figure (b) is associated with DDR1 gene.

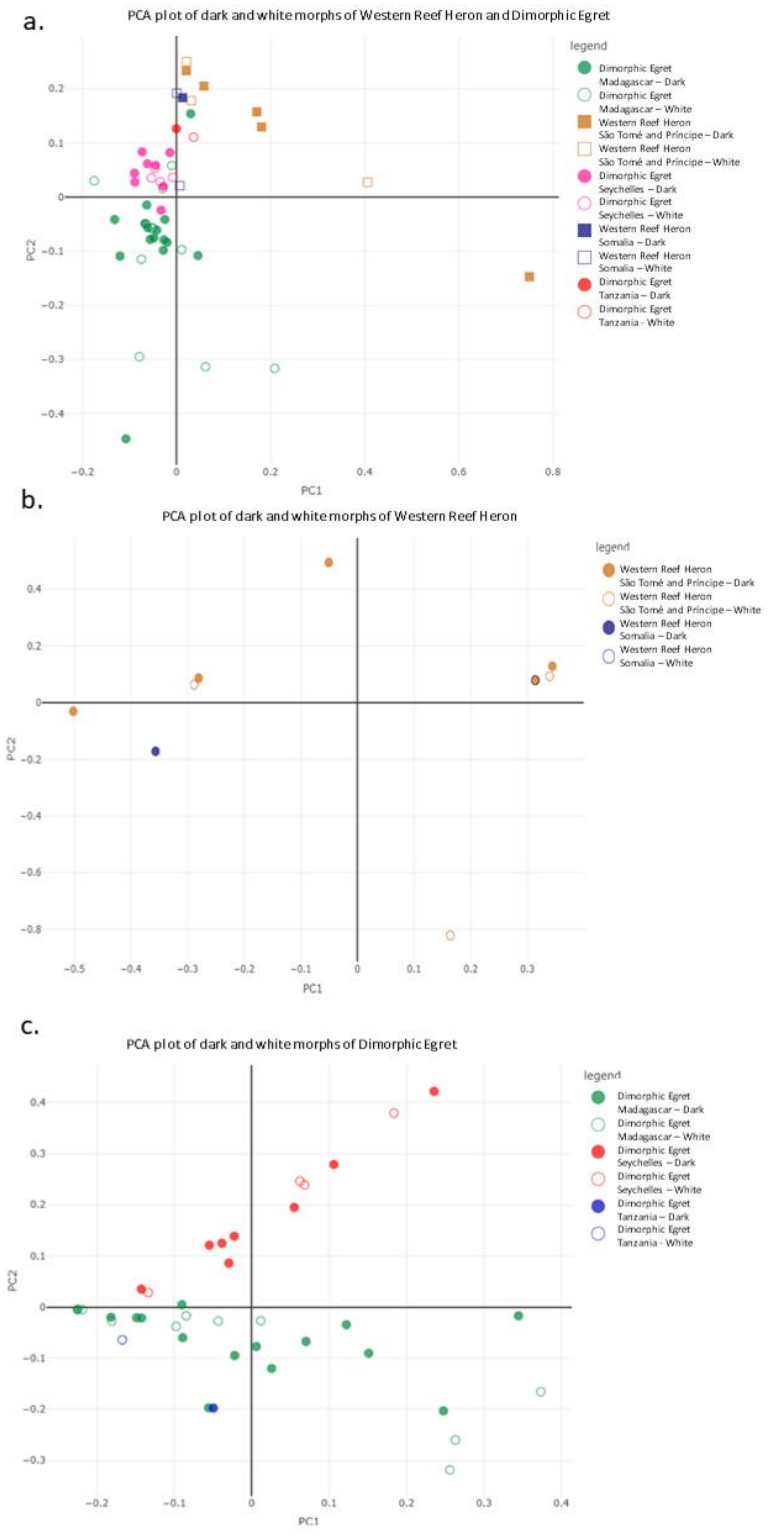

Figure 3. 3. PCA plots for (a) Dataset 1, combined; (b) Dataset 2, Western Reef Heron (*Egretta gularis*); and (c) Dataset 3, Dimorphic Egret (*Egretta dimorpha*), separated by color morphs and populations.

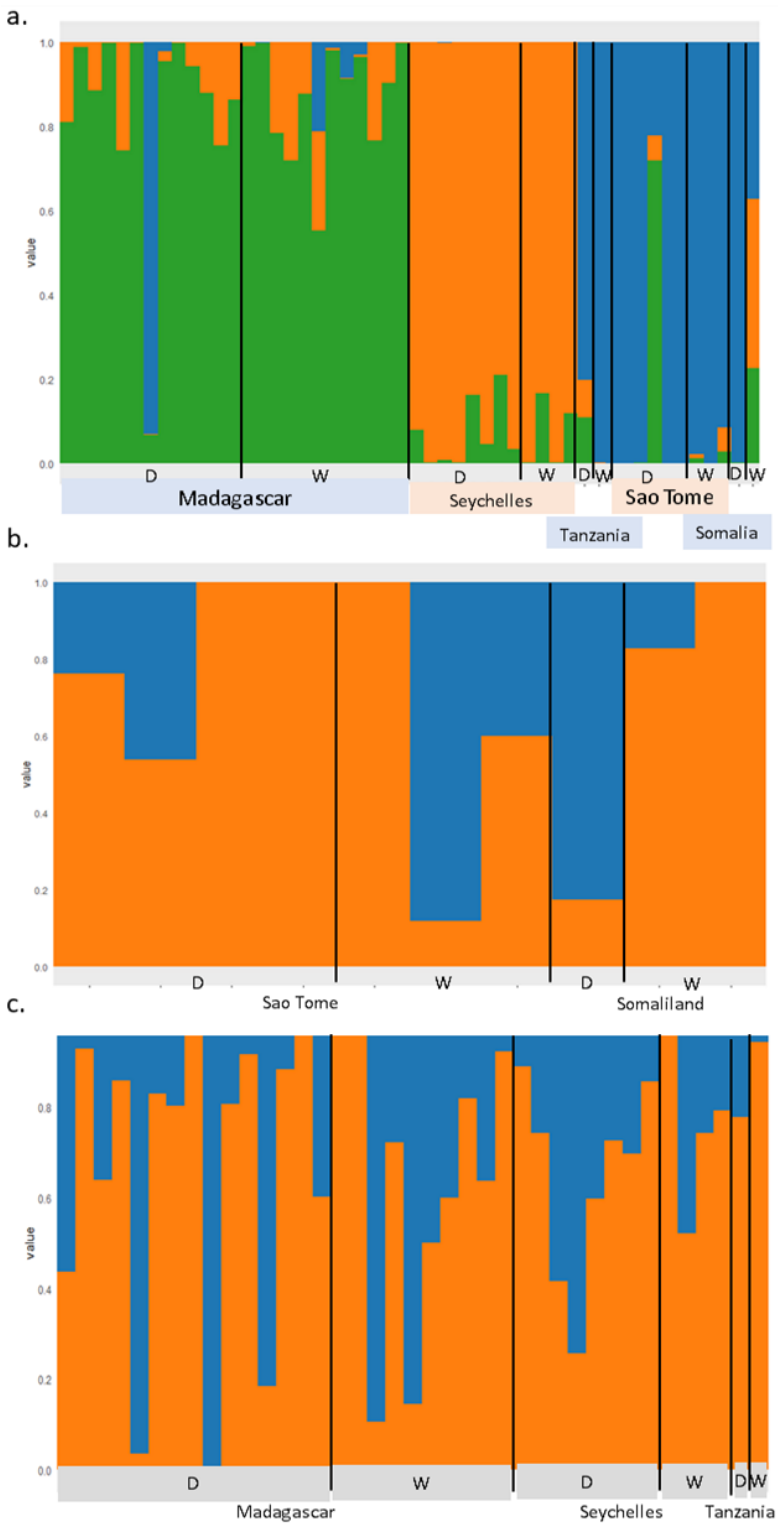

Figure 3. 4. STRUCTURE analysis of dark (D) and white (W) morphs of three datasets based on their optimal *K* values: (a) Dataset 1, combined (*K*=3); (b) Dataset 2, Western Reef Heron (*Egretta gularis*) (*K*=2); and (c) Dataset 3, Dimorphic Egret (*Egretta dimorpha*) (*K*=2).

Supplementary Materials

Table S 3. 1. Summary of information of Western Reef Heron (*Egretta gularis*) and Dimorphic Egret (*Egretta dimorpha*) toepad samples that used in this study from American Museum of Natural History specimens. Samples in grey shades have been excluded from statistical analyses.

Data Source	Species	Accession Number	Color morph	Country	Latitude	Longitude
American Museum of Natural History	*Egretta gularis*	AMNH529999	White	Somaliland	-11.4333333	43.45
		AMNH2702	Dark	Somaliland	-10.708381	46.613547
		AMNH530005	White	Somaliland	-0.11666666	6.65
		AMNH265989	Dark	Sao tome	-1.607453	7.432053
		AMNH268402	Dark	Sao tome	-0.33333333	6.7166666
		AMNH268410	White	Sao tome	-0.33333333	6.7333333
		AMNH265986	Dark	Sao tome	-0.38333333	6.6833333
		AMNH264839	Dark	Sao tome	-0.33333333	6.7333333
		AMNH268404	Dark	Sao tome	-0.31666666	6.7333333
		AMNH264842	White	Sao tome	-0.31666666	6.7333333
		AMNH264840	White	Sao tome	0.31666666	6.7333333
	Egretta dimorpha	AMNH410731	White	Madagascar	-12.2666666	49.383333
		AMNH410720	Dark	Madagascar	-23.5333333	43.733333
		AMNH410715	Dark	Madagascar	-13.2833333	48.383333
		AMNH52998	Dark	Madagascar	12.310831	49.306936
		AMNH410730	Dark	Madagascar	-13.25	48.316666
		AMNH529995	Dark	Madagascar	-23.0166666	43.533333
		AMNH410729	White	Madagascar	-17.4833333	49.466666
		AMNH410714	Dark	Madagascar	-22.8333333	47.266666
		AMNH529992	Dark	Madagascar	-13.3166666	48.166666
		AMNH410721	Dark	Madagascar	-19.65	44.966666
		AMNH410724	White	Madagascar	-24.314114	47.203208
		AMNH410783	White	Madagascar	-23.361556	43.668889
		AMNH410727	White	Madagascar	-17.6166666	48.466666
		AMNH410726	Dark	Madagascar	-16.1	45.333333
		AMNH410719	Dark	Madagascar	-23.55	43.75
		AMNH410728	Dark	Madagascar	-23.555478	43.757453
		AMNH529996	Dark	Madagascar	-12.30845	49.302436
		AMNH410717	Dark	Madagascar	-22.4666666	48.4666666
		AMNH52994	White	Madagascar	-13.327769	48.179492
		AMNH529993	White	Madagascar	-13.2666666	48°18'26.91"E
		AMNH410718	White	Madagascar	-23.35	43.666666
		AMNH410732	White	Madagascar	-12.275861	49.393964
		AMNH410725	White	Madagascar	-23.35	43.666666
		AMNH410723	Dark	Madagascar	-24.3	47.2
		AMNH529991	Dark	Madagascar	-13.31666666	48.1666666
		AMNH530001	White	Tanzania	-5.5	39.0666666
		AMNH530000	Dark	Tanzania	-6.65	39.216666
		AMNH529980	Dark	Seychelles	-9.3666666	46.333333
		AMNH793528	Dark	Seychelles	-9.3666666	46.333333
		AMNH529983	White	Seychelles	-9.3666666	46.333333

		AMNH529979	White	Seychelles	-9.3833333	46.316666
		AMNH529982	Dark	Seychelles	-9.3666666	46.333333
		AMNH529984	Dark	Seychelles	-9.3833333	46.333333
		AMNH529978	Dark	Seychelles	-9.3666666	46.333333
		AMNH829976	Dark	Seychelles	-9.379469	46.336936
		AMNH529989	Dark	Seychelles	-9.3666666	46.3166666
		AMNH529981	White	Seychelles	-9.3666666	46.316666
		AMNH529985	White	Seychelles	-9.3666666	46.333333
		AMNH529987	Dark	Seychelles	-9.3666666	46.316666
		AMNH529988	White	Seychelles	-9.3666666	46.3333333
		AMNH529977	White	Seychelles	-9.3833333	46.316666

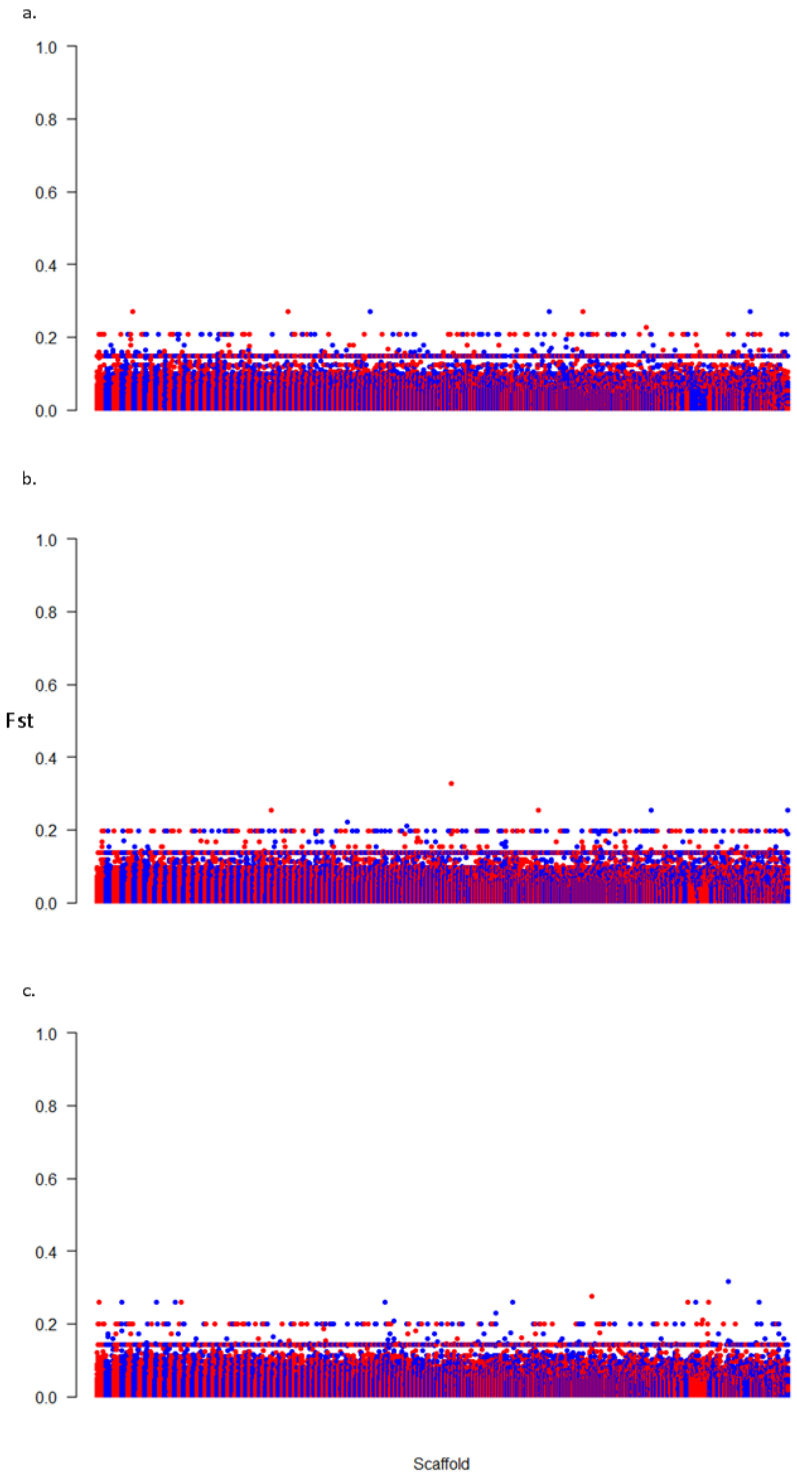

Figure S 3. 1. Manhattan plots for the three subsets of the combined dataset, with similar filtering to original dataset: (a) Split 1; (b) Split 2; and (c) Split 3.

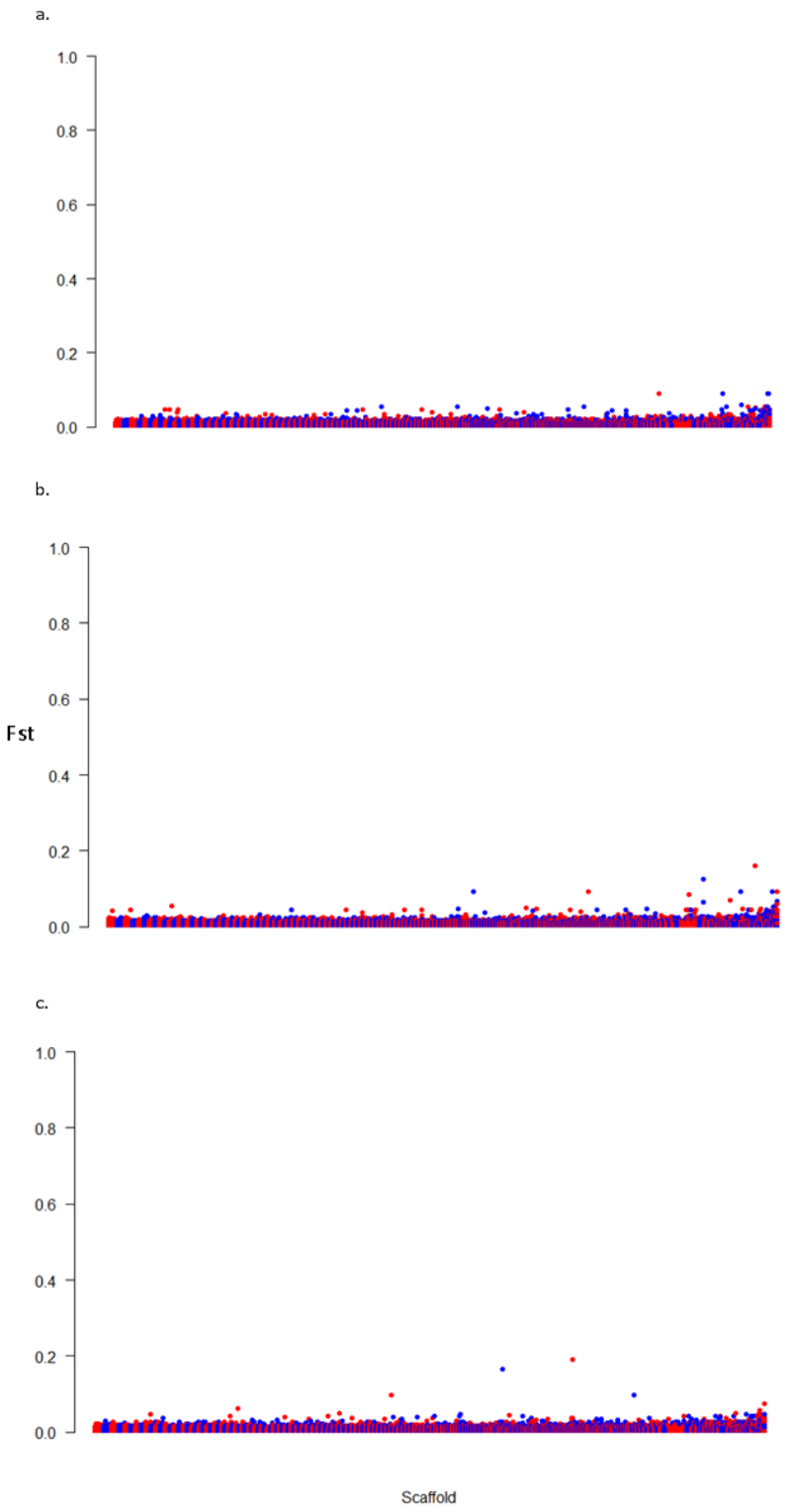

Figure S 3. 2. Manhattan plots for the three subsets of the combined dataset, with relaxed filtering: (a) Split 1; (b) Split 2; and (c) Split 3.

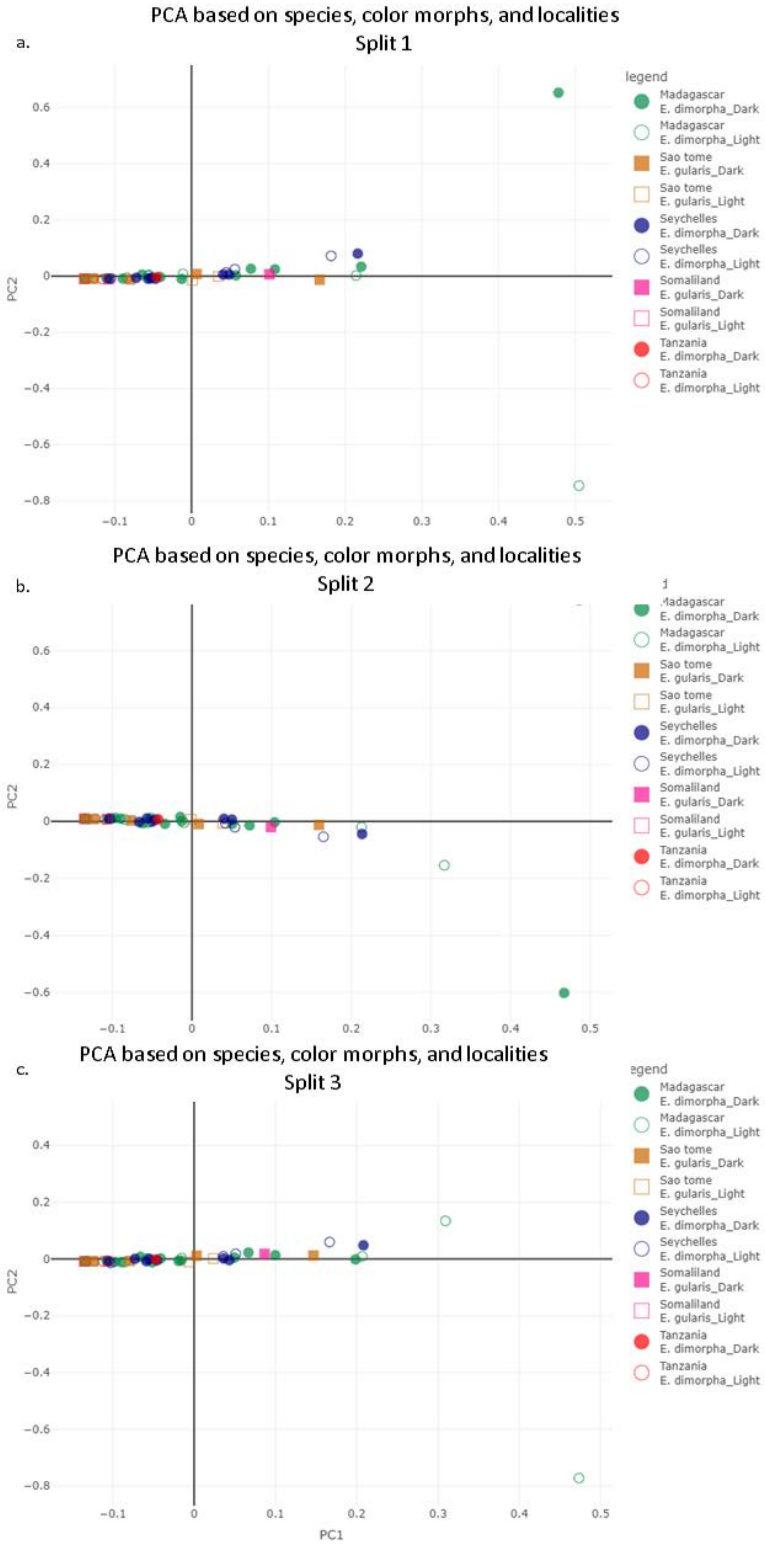

Figure S 3. 3. PCA plots for subsets of the combined dataset, with similar filtering, separated by color morphs and populations: (a) Split 1; (b) Split 2; and (c) Split 3.

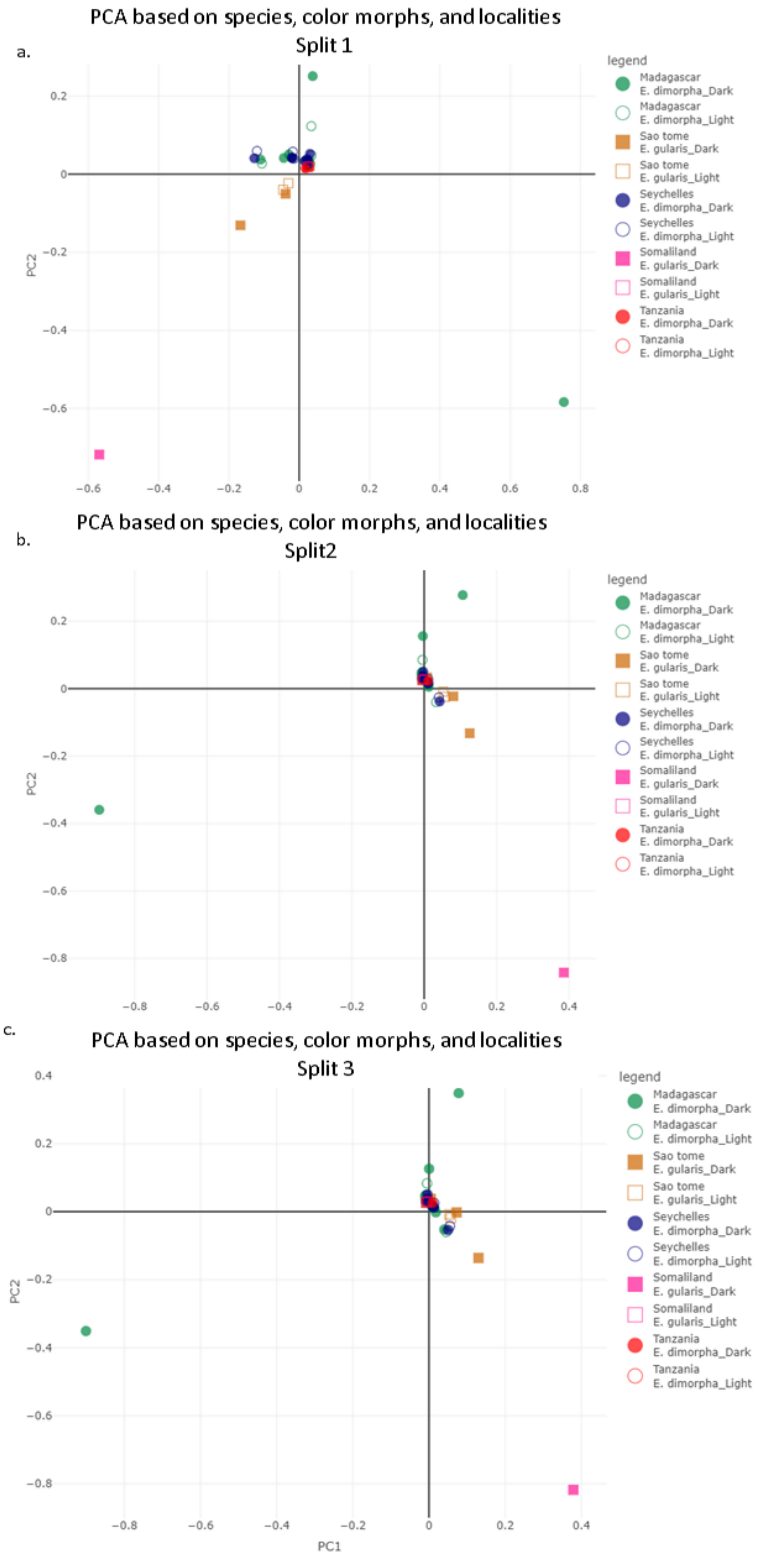

Figure S 3. 4. PCA plots for subsets of the combined dataset, with relaxed filtering, separated by color morphs and populations: (a) Split 1; (b) Split 2; and (c) Split 3.

Conclusion

In this study, I examined the evolutionary forces that maintain color polymorphism among herons within two dimorphic heron species, Western Reef Heron (*Egretta gularis*) and Dimorphic Egret (*Egretta dimorpha*). I used three different approaches, morphology, geographic distribution, and genomics, to address this question. Both morphs of both species live in the same region next to each other on the east and west coasts of Africa, with more distribution around the equator.

In the first part of the research, morphology, I examined the color variation among different body regions in unicolored individuals of both morphs. I found that the back feathers, followed by the breast, is more pigmented than the other body regions among the dark and whiter among the white morphs. Due to the birds' posture and foraging figure, the back and breast receive the highest incidence of UV radiation compared to the other parts, making them the two body regions with the most sun exposure. Among dark individuals, the melanin pigment, with the main responsibility of absorbing UV, is greater in the back and breast than in other parts of the body, to prevent the body from UV damage. On the other hand, these two body regions are whiter among white individuals, which would reflect sunlight more, helping the bird avoid UV stress. Therefore, UV resistance is a strong potential evolutionary mechanism that allows both morphs of the Western Reef Heron and Dimorphic Egret to live in the same region and in a high receiving dosage of sunlight.

I explored these questions further in my second chapter, on geographic distributions, in which I quantified and compared the ecological niches of morphs of Western Reef Heron and Dimorphic Egret. Based on Gloger's rule, we would expect to see that the ecological niches of dark and white morphs have different ecological niches. In contrast, I found that the ecological niches

between both species' dark and white morphs are identical. Since the dark and white morphs live next to each other in most parts of the distribution of both species, the evolutionary forces that shape their distribution do not align with what Gloger has suggested. The finding of this chapter, together with my results from the finding of the previous chapter, suggest that the evolutionary mechanism that maintains dimorphism in Wester Reef Heron and Dimorphic Egret and shapes the distribution of color morphs is UV resistance, which evolved via different mechanisms in different color morphs.

In my third chapter, on genomics, I compared whole genomes of the color morphs of each species to detect genes related to plumage coloration and dimorphism. The comparison did not indicate any highly significant related gene for the coloration between the morphs. This surprising finding suggests potentially high gene flow between the color morphs individuals, or that plumage coloration trait is polygenic. The gene flow is possible since the dark and white individuals live nearby and have similar ecological niches. However, my findings in Chapter 1 potentially support considering the plumage coloration among these species as a polygenic trait. More than one gene may be responsible for plumage coloration, which may affect the level of whiteness and darkness in different body parts of an individual. To address the ambiguity regarding which scenario applies to the Western Reef Heron and Dimorphic Egret, it is necessary to gather additional samples of both morphs from different populations.

In conclusion, the story of color for the Western Reef Heron and Dimorphic Egret suggests the high effectiveness of the UV resistance mechanism in shaping coloration, maintaining dimorphism, and distribution of morphs. To build upon these findings and confirm which of the two hypotheses regarding the relationship between genomic and coloration is true, additional samples from each color morph and different populations are required. I also suggest expanding

this research to include the study of the behavior and physiology of color morphs in both species, which could provide new insights into Herons, in which many species exhibit color polymorphism. Broader investigations across this group of birds might yield a better understanding of how evolutionary forces shape physiology, morphology, distribution, and lifestyle of dimorph species.